AD 269 883

TRANSIENT HEAT AND MOISTURE TRANSFER TO SKIN THROUGH THERMALLY IRRADIATED CLOTH

Technical Report No. 8

from

Fuels Research Laboratory
Massachusetts Institute of Technology
Cambridge, Massachusetts

H. C. Hottel
G. C. Williams
G. H. Miedel
N. Y. Chen
W. P. Jensen

December 26, 1961

Project Nos. 7-12-01-002C
and 7-99-01-001
Contract No. DA 19-129-QM-1592
Quartermaster Research and Engineering Command
United States Army

MIT Project
DSR 8556

AD ______________ Accession No. ______________
Fuels Research Lab., Massachusetts Institute of Technology, Cambridge, Massachusetts
TRANSIENT HEAT AND MOISTURE TRANSFER TO SKIN THROUGH THERMALLY IRRADIATED CLOTH - H.C.Hottel, G.C.Williams, G.H.Miedel, H.Y.Chen, W.P.Jensen

Technical Report No. 8, 26 Dec 61, 139pp - illus-tables (Contract No. DA19-129-QM-1592) Proj. 7-12-01-002C, Proj. 7-99-01-001, Unclassified Report

Methods are presented to model the temperature response of skin covered by dry or moist cloth and exposed to high-intensity thermal irradiation 1) experimentally using a copper-air skin simulant; 2) theoretically by finite-difference solution of the partial differential equations for heat and moisture transfer. Moisture transport is assumed to be due to water vapor diffusion only, neglecting bulk flow. The dry (opaque or diathermanous) cloth case is solved generally; the moist cloth system involves hygroscopic equilibrium of cloth and requires computer calculation of each specific case. The theoretical solution permits estimates of skin temperature response and inspection of influences of system parameters and time-variant irradiation of intensity as encountered in a nuclear explosion.

UNCLASSIFIED

1. Skin Simulants
2. Burn Protection
3. Heat and Moisture Transfer
4. Thermal Radiation
5. Finite Difference Methods
6. Contract DA19-129-QM-1592

AD ______________ Accession No. ______________
Fuels Research Lab., Massachusetts Institute of Technology, Cambridge, Massachusetts
TRANSIENT HEAT AND MOISTURE TRANSFER TO SKIN THROUGH THERMALLY IRRADIATED CLOTH - H.C.Hottel, G.C.Williams, G.H.Miedel, H.Y.Chen, W.P.Jensen

Technical Report No. 8, 26 Dec 61, 139pp - illus-tables (Contract No. DA19-129-QM-1592) Proj. 7-12-01-002C, Proj. 7-99-01-001, Unclassified Report

Methods are presented to model the temperature response of skin covered by dry or moist cloth and exposed to high-intensity thermal irradiation 1) experimentally using a copper-air skin simulant; 2) theoretically by finite-difference solution of the partial differential equations for heat and moisture transfer. Moisture transport is assumed to be due to water vapor diffusion only, neglecting bulk flow. The dry (opaque or diathermanous) cloth case is solved generally; the moist cloth system involves hygroscopic equilibrium of cloth and requires computer calculation of each specific case. The theoretical solution permits estimates of skin temperature response and inspection of influences of system parameters and time-variant irradiation of intensity as encountered in a nuclear explosion.

UNCLASSIFIED

1. Skin Simulants
2. Burn Protection
3. Heat and Moisture Transfer
4. Thermal Radiation
5. Finite Difference Methods
6. Contract DA19-129-QM-1592

AD ______________ Accession No. ______________
Fuels Research Lab., Massachusetts Institute of Technology, Cambridge, Massachusetts
TRANSIENT HEAT AND MOISTURE TRANSFER TO SKIN THROUGH THERMALLY IRRADIATED CLOTH - H.C.Hottel, G.C.Williams, G.H.Miedel, H.Y.Chen, W.P.Jensen

Technical Report No. 8, 26 Dec 61, 139pp - illus-tables (Contract No. DA19-129-QM-1592) Proj. 7-12-01-002C, Proj. 7-99-01-001, Unclassified Report

Methods are presented to model the temperature response of skin covered by dry or moist cloth and exposed to high-intensity thermal irradiation 1) experimentally using a copper-air skin simulant; 2) theoretically by finite-difference solution of the partial differential equations for heat and moisture transfer. Moisture transport is assumed to be due to water vapor diffusion only, neglecting bulk flow. The dry (opaque or diathermanous) cloth case is solved generally; the moist cloth system involves hygroscopic equilibrium of cloth and requires computer calculation of each specific case. The theoretical solution permits estimates of skin temperature response and inspection of influences of system parameters and time-variant irradiation of intensity as encountered in a nuclear explosion.

UNCLASSIFIED

1. Skin Simulants
2. Burn Protection
3. Heat and Moisture Transfer
4. Thermal Radiation
5. Finite Difference Methods
6. Contract DA19-129-QM-1592

AD ______________ Accession No. ______________
Fuels Research Lab., Massachusetts Institute of Technology, Cambridge, Massachusetts
TRANSIENT HEAT AND MOISTURE TRANSFER TO SKIN THROUGH THERMALLY IRRADIATED CLOTH - H.C.Hottel, G.C.Williams, G.H.Miedel, H.Y.Chen, W.P.Jensen

Technical Report No. 8, 26 Dec 61, 139pp - illus-tables (Contract No. DA19-129-QM-1592) Proj. 7-12-01-002C, Proj. 7-99-01-001, Unclassified Report

Methods are presented to model the temperature response of skin covered by dry or moist cloth and exposed to high-intensity thermal irradiation 1) experimentally using a copper-air skin simulant; 2) theoretically by finite-difference solution of the partial differential equations for heat and moisture transfer. Moisture transport is assumed to be due to water vapor diffusion only, neglecting bulk flow. The dry (opaque or diathermanous) cloth case is solved generally; the moist cloth system involves hygroscopic equilibrium of cloth and requires computer calculation of each specific case. The theoretical solution permits estimates of skin temperature response and inspection of influences of system parameters and time-variant irradiation of intensity as encountered in a nuclear explosion.

UNCLASSIFIED

1. Skin Simulants
2. Burn Protection
3. Heat and Moisture Transfer
4. Thermal Radiation
5. Finite Difference Methods
6. Contract DA19-129-QM-1592

TRANSIENT HEAT AND MOISTURE TRANSFER TO SKIN THROUGH THERMALLY IRRADIATED CLOTH

Technical Report No. 8

from

Fuels Research Laboratory
Massachusetts Institute of Technology
Cambridge, Massachusetts

H. C. Hottel
G. C. Williams
G. H. Miedel
N. Y. Chen
W. P. Jensen

December 26, 1961

Project Nos. 7-12-01-002C
and 7-99-01-001
Contract No. DA 19-129-QM-1592
Quartermaster Research and Engineering Command
United States Army

MIT Project
DSR 8556

TABLE OF CONTENTS

LIST OF FIGURES

LIST OF TABLES

FOREWORD

This report was prepared by the Fuels Research Laboratory of the Massachusetts Institute of Technology under Contract No. DA-19-129-QM-1592, Project Nos. 7-12-01-002C and 7-99-01-001, Quartermaster Research and Engineering Command, United States Army. The work was administered under the direction of the Pioneering Division, Headquarters, Quartermaster Research and Engineering Command, United States Army.

This report covers work conducted from December 1960 to October 1961. It incorporates a review of the underlying work done under the associated contract No. DA-19-129-QM-454.

The authors gratefully acknowledge the important contribution of Professor P. L. Thibault Brian, Chemical Engineering Department, Massachusetts Institute of Technology, to the theoretical analysis, and also the stimulating discussions with Mr. Cristobal Bonifaz, research assistant, on the mathematical side of the project. The computations were carried out on the IBM 709 digital computer of the MIT Computation Center. Finally, the careful preparation of the text and graphs by Miss Sally Drew is much appreciated.

ABSTRACT

A study has been made of the action of cloth in protecting skin from thermal injury resulting from exposure to high-intensity thermal radiation. Methods have been developed to obtain temperature-time-depth data for a system simulating skin covered by a layer of dry or moist cloth. Experimentally this has been accomplished by the use of a copper-air simulant which accepts heat at the same rate as human skin but develops a proportionally stretched temperature profile.

The analysis of the moist cloth-skin simulant system involves some simplifying assumptions regarding the mode of moisture transport. It is applicable to low- and medium-intensity exposures constant or variable in time. The solution is not general but requires new computer calculations for every specific case. The model yields reasonable estimates of the skin temperature response; due to the uncertainty of a number of physical parameters there is a margin of tolerance which could be narrowed by further experiments combined with further calculations. The description of the intermediate role of moisture flow as contributing to the heat transport may still require refinement; however, there is as yet no simple way to evaluate the b.l. of water vapor through the pores of a fabric.

The current method facilitates the inspection of the influences on temperature distribution in the skin of various system properties and the surrounding conditions.

The skin enthalpy rise above a critical temperature level, a feasible basis for correlating burn data, has been found to be very sensitive to slight variations in the temperature response and deserves further testing.

Besides an account of recent research, this project incorporates a review of the experimental work done earlier and of the mathematical models with the methods for their solution.

I. INTRODUCTION

Although thermal injury to skin has been an important medical problem for many years, quantitative studies on the relation between the temperature history and the production of cutaneous damage did not begin until the forties by Mantz and Henriques (5, 15, 16, 17). The importance of knowing the temperature history of skin during its exposure to thermal energy was pointed out by these authors. However, the problem of measuring the temperature rise in skin remains unsolved. The difficulty lies in the fact that the epidermis of the skin where the temperature history is essential to the analysis is only 80μ thick, and measurement of the temperature profile in such a thin layer is still beyond presently known techniques. In previous studies, (3) we have developed skin simulants made of copper and air with a stretch factor (depth magnification) 28.4 times that of skin. Thus the temperature profile in a skin layer 100μ thick can be measured accurately by means of the simulant over a distance of 2.84 mm.

The simulant has been used in evaluating the energy transport processes in a cloth-air gap-skin system by exposing the test assembly to high intensity solar radiation. Experimental temperature-time-depth data were thus obtained on the simulant. This paper presents the results of these experiments and the mathematical models proposed to describe the energy transport process in such systems. The presentation is divided into two parts. The first part deals with the dry cloth-skin system in which the heat transfer by conduction and radiation through the cloth layer is considered; the second part deals with the moist cloth-skin system in which in addition to conduction and radiation, diffusion of the moisture in the cloth layer also contributes importantly to the heat transfer from the cloth to the skin.

II. EXPERIMENTAL

A. SKIN SIMULANT

The principal interest in the present experiments was the temperature-time-depth variation in the skin simulant. No attempt was made to measure the temperature in any part of the cloth. In previous studies (5, 12) it was concluded that the complexity of the cloth structure made it impossible to

identify the cloth "surfaces" unambiguously. Consequently, little significance could be ascribed to experimentally measured cloth temperatures.

A soldered fin-type skin simulant (skin simulant #10) (3, 5) was used in all "in-contact" runs. It consisted of sixteen fins, with twelve mutually parallel and four perpendicular to the twelve to block the exposed air space and help to maintain more nearly isotherms in the individual fins of the main simulant. The fins were copper sheets, each 3.175 cm. and 7.95 cm. x 0.0102 cm. thick, bent into shallow channels as shown in Figure 1.5. The four guard fins were bent to a 3-inch radius arc in a specially machined die. In order to make simulants of this type symmetrical, six channels face one way and six the opposite way, i.e., all the flange toes faced toward the center of the simulant. The fins were soldered to a top sheet of copper having dimensions of 4.37 x 3.61 cm. x 0.0102 cm. thick, Five 0.0025 cm. diameter constantan wires were soldered onto the central copper fin, forming the hot junctions of the thermocouples. The five wires were led out from the bottom and soldered to heavier constantan leads (#24 B. and S. gage). A common copper lead wire was soldered to the copper sheet. The cold junction for the thermocouples consisted of several massive copper blocks, one for each constantan lead and another for the copper lead wire. The junctions were located inside the constant temperature box, where connections to the temperature recorder were made. A cylindrical simulant as shown in Figure 1.6 was also used in several experiments in which the cloth sample was set 0.038 cm. from the top surface of the simulant.

B. CLOTH SAMPLES

A series of six "standard" 9-ounce cotton sateen and 9-ounce Olive Green uniform cloths supplied by the Quartermaster Research and Development Command at Natick, Massachusetts, were used in the present investigation.

The optical properties of the cloths (5, 6) have been determined by the Naval Material Laboratory covering the wave-length range from 0.40 to 2.7 microns. These data have been integrated over the solar spectrum; the results are listed in Table 1.1.

Wooden embroidery rings 5-inches in diameter were used to hold the cloth samples. All cloth samples were oven dried at 105°C for 24 hours and then

cooled and conditioned in desiccators containing one of three items: (1) indicating silica gel, (2) saturated sodium nitrate solution (65-66% relative humidity at 15-30°C), and (3) saturated ammonium chloride solution (79.5% relative humidity at 20-30°C).

Table 1.1

OPTICAL PROPERTIES OF CLOTHS (INTEGRATED VALUE OVER SOLAR SPECTRUM)

Code No.	Designated Color	Reflectance	Absorptance	Transmittance*
QM-4	White with CMC	0.67	0.19	0.14
QM-5-65	Light gray with CMC	0.56	0.37	0.07
QM-6-40	Medium gray with CMC	0.50	0.47	0.03
QM-7-22	Dark gray with CMC	0.22	0.78	0
QM-8-12	Black with CMC	0.11	0.89	0
QM-9-7	Deep black with CMC	0.09	0.91	0
QM-3	Olive green 107	0.18	0.79	0.03

C. SOLAR FURNACE

The MIT Solar Furnace (5, 9, 10, 11) was used as the source of high intensity radiation. Intensity up to 6 cal/cm^2-sec. over a 5 cm^2 target area was obtainable with a clear sky.

D. TEMPERATURE MEASUREMENT

A four channel 150-1500 series Sanborn recorder equipped with "low-level" preamplifiers was used to record the outputs of thermocouples. The recorder has a maximum sensitivity of 100μv per cm (or approximately 2.5°C for copper-constantan thermocouples). The time constant is 0.03 sec.

---

* Since the cloths were made from the same white 9 oz. cotton sateen stock, and it is unlikely that a simple dyeing process would change the geometry of the fibers, it is reasonable to assume that the cloth construction provides complete geometrical blockage of the incident light, and that the transmittance depends on the degree of opacity of the individual cloth fibers. These transmittance values should therefore be regarded not as due to direct transmittance through holes but to diathermancy of the cloths.

III. PROCEDURE

Cloth samples were prepared several days in advance and kept in their respective desiccators until testing time. Then the sample was quickly transferred from the desiccator to a constant humidity box attached on the solar furnace. The constant humidity box was kept under the same condition as the desiccator. Constant temperature was maintained in the box with an air blower and a thermoregulator. After the skin simulant was placed behind the sample, the box was closed and the air blower was allowed to continue blowing for 10-15 minutes to insure constant temperature and relative humidity in the box. The air blower was stopped during the exposure of the sample to the radiation. The sample was exposed for one to 30 seconds to the high intensity radiation ranging from 0.3 to 6.0 cal/cm^2-sec. The length of the exposure was controlled by a timing device which opened and closed the diaphragm shutter. The intensity of radiation was regulated by partially blocking off the primary mirrors of the solar furnace.

IV. EXPERIMENTAL RESULTS

Experimental data obtained on six kinds of dry cloth are presented in the following figures in which the normalized temperature rise is plotted against the exposure time in seconds on logarithmic papers with the three or four skin depths as the parameters: Figure 1.7 combines the result on three opaque cloths (deco black, black, and dark gray); Figure 1.8 shows the result on the medium gray cloth; Figure 1.9 shows the result on the light gray cloth; and Figure 1.10 shows the result on the white cloth.

The experiments on moist cloth over skin were designed to study the effect of the radiation intensity on the coupling effect of moisture transfer on heat transfer. Two types of cloths, one black and one white were used.

The effect of moisture transfer on heat transfer can be illustrated by the following figures, in which the normalized temperature rise of the first thermocouple in the skin simulant is plotted against the exposure time, with intensity as the parameter. Figure 1.11 shows the result on the opaque cloth and Fig. 1.12 shows the result on the white cloth. The complete data may be found in reference (5).

V. THEORETICAL - DRY CLOTH OVER SKIN SIMULANT SYSTEM

A. THE MATHEMATICAL MODEL

The general assumptions made in the analysis are as follows. The system under consideration is sketched below:

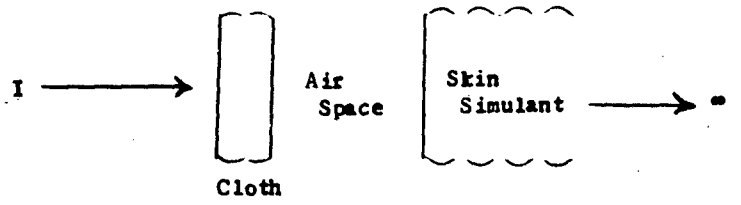

Figure 1.1

DRY CLOTH-AIR GAP-SKIN SIMULANT SYSTEM

1. Heat flow is unidirectional, occurring in the x-direction, from the cloth through the air space into the skin simulant. The surface of the cloth is irradiated by square wave radiation. It will be shown later that the general solution can be applied to radiation of any pulse form.

2. The cloth layer is considered to be a homogeneous solid. For cloths which show no measurable transmittance (e.g., deep black, black, and dark gray of the 9 oz. "standard" cotton sateen), radiant energy is absorbed at the surface of the cloth. For diathermanous cloths, the radiant energy is assumed to penetrate into the interior of the cloth layer in accordance with the Beer-Lambert law:

$$I_x = I_o \exp(-\gamma x_c)$$

where I_x = intensity of radiation at a plane distant x_c cm from the irradiated surface.

I_o = intensity of radiation entering the cloth layer, or $I_o = I(1 - r)$, cal/cm^2-sec.

I = incident intensity of radiation.

γ = extinction coefficient, cm^{-1}, a characteristic constant of the cloth for the particular source of radiation in question.

If the measured "transmittance" of a diathermanous cloth of thickness L cm is τ, then $\exp(-\gamma L) = \tau/(1-r)$, where r is the reflectance of the cloth.

The solution is applied specifically to the 9 oz. "standard" cotton sateen; it could be equally well be applied to either diathermanous or direct-transmitting cloths.

3. The physical properties of the cloth layer remain constant throughout the exposure.

4. Any effects due to moisture and/or chemical reaction are negligible.

5. Heat losses from the front surface of the cloth layer by convection and re-radiation are characterized by a single overall heat transfer coefficient U_o.

6. Heat transfer from the cloth layer through the air gap to the simulant is similarly characterized by an overall heat transfer coefficient U_i.

7. The skin simulant is considered to be a homogeneous opaque solid of infinite extent in its x-direction.

The validity of these assumptions must first be checked against experimental data obtained from an equivalent inanimate system. Furthermore it should be born in mind that such an analysis will be of value only if the temperature history data can in combination with some postulated mechanism of burning correlate the in vivo results.

The basic equations for the cloth layer are:

1. Opaque cloth

$$\frac{\partial T}{\partial \theta} = \left(\frac{k}{C\rho}\right)_c \frac{\partial^2 T}{\partial x_c^2} \qquad (1.1)$$

2. Diathermanous cloth

$$\frac{\partial T}{\partial \theta} = \left(\frac{k}{C\rho}\right)_c \frac{\partial^2 T}{\partial x_c^2} - \frac{I_o}{C\rho_c} \frac{\partial \exp(-\gamma x_c)}{\partial x_c} \qquad (1.2)$$

The equation for the skin is

$$\frac{\partial T}{\partial \theta} = \left(\frac{k}{C\rho}\right)_s \frac{\partial^2 T}{\partial x_s^2} \qquad (1.3)$$

The surface boundary equations are:

1. For opaque cloth

(a) Front surface

$$I_o - U_o(T_{x_c=0} - T_{surr}) = -k_c \frac{\partial T}{\partial x_c}\Big]_{x_c=0} \tag{1.4}$$

(b) Back surface and skin surface

$$-k_c \frac{\partial T}{\partial x_c}\Big]_{x_c=L_c} = U_i(T_{x_c=L_c} - T_{x_s=0}) = -k_s \frac{\partial T}{\partial x_s}\Big]_{x_s=0} \tag{1.5}$$

2. For diathermanous cloth

(a) Front surface

$$k_c \frac{\partial T}{\partial x_c}\Big]_{x_c=0} = U_o(T_{x_c=0} - T_{surr}) \tag{1.6}$$

(b) Back surface and skin surface

$$\begin{aligned} -k_c \frac{\partial T}{\partial x_c}\Big]_{x_c=L_c} + I_o \exp(-\gamma L_c) &= U_i(T_{x_c=L_c} - T_{x_s=0}) \\ + I_o \exp(-\gamma L_c) &= -k_s \frac{\partial T}{\partial x_s}\Big]_{x_s=0} \end{aligned} \tag{1.7}$$

These equations are solved by a finite-difference approximation method which gives temperature as a function of the following five independent variables; time, depth, U_i, U_o, and $\tilde{R}$, a property group. The solution is expressed as a relation among the following dimensionless groups.

1. Temperature group $\quad T^o = \dfrac{k_c T}{I_o L_c}$
2. Time group $\quad \theta_c^o = \left(\dfrac{k}{C\rho}\right)_c \dfrac{\theta}{L_c^2}$
3. Depth group $\quad x_c^o = \dfrac{x_c}{L_c}$
4. Surface heat losses group $\quad U_o^o = \dfrac{U_o L_c}{k_c}$

(1.8)

5. Air gap group $$U_i^o = \frac{U_o L_c}{k_c}$$

6. $\bar{R}$ group $$\sqrt{\frac{(kC\rho)_s}{(kC\rho)_c}} = \frac{\Delta X_c^o}{\Delta X_s^o}$$

Stated another way, the temperature-time-depth relation is a function of the three other groups.

The details of the solution are given in Appendix B.

B. GENERAL SOLUTION

The general solution consists of the temperature-time-depth relation as a function of the following parameters:

1. U_o^o the dimensionless surface heat loss group
2. U_i^o the dimensionless air gap group
3. $\bar{R}$ the physical property ratio group

For opaque cloth, only one set of solutions is needed; for diathermanous cloth, a technique which uses the weighted mean of three sets of solutions, each representing radiation absorption at a different plane in the system, gives results within 1 to 2% of those obtained by a more rigorous method.

These three sets of solutions are as follows:

1. The case of incident radiant energy absorbed at the exposed cloth surface,

2. The case of incident radiant energy absorbed at $X_c^o = 0.75$, and

3. The case of incident radiant energy absorbed at the surface of the skin simulant.

By taking advantage of the additive nature of the solutions, the temperature rise at any plane in any diathermanous-cloth problem can be obtained as the sum of the temperature rises due to assuming that the total energy absorption is lumped at three planes. The Beer-Lambert law is used to calculate absorption in the first half of the cloth, the second half, and the skin surface. These quantities are then treated as though lumped at the front surface of the cloth where $X_c^o = 0$, at the plane $X_c^o = 0.75$,

and at the skin surface, where $X_s^o = 0$.

1. Application to Other Types of Cloth Including those having Direct Transmittance

As a corollary to the above additive principle, these three curves can be weighted in any fashion according to known distribution rule of the incident radiation inside the cloth. For cloth having direct transmittance, an additional proportion of the Curve III solution is added. However, it must be noted that the solution is based on an opaque skin simulant, hence it is not applicable to diathermanous skin covered by a single open-weave cloth layer.

For cloths of different thicknesses and thermal conductivities, the general solutions are applicable. The only change is in the relationship between the actual temperature (^oC) - time (sec) - depth(cm) and their dimensionless groups. Thus doubling the thermal conductivity of the cloth doubles the T^o, θ_c^o, and X_s^o scales. Halving the thickness doubles the T^o and X_s^o scales, and quadruples the θ_c^o scale.

The general solutions also allow the prediction of the T^o, θ^o, X_s^o data at the skin surface, and other depths where experimental data are not available.

The following examples illustrate the effects of diathermancy, thickness, thermal conductivity of the cloth, and the size of air gap and surface heat losses on the $T^o - \theta_c^o - X_s^o$ relationship in the skin. The solutions are shown in the following figures.

Figures 1.13, 1.14 show ΔT^o versus $\Delta\theta_c^o$ at $X_s^o = 0$, and $X_s^o = 0.05$, 0.45 respectively. The solutions are plotted on Cartesian scale to demonstrate the effect of diathermancy on the time lag between the initiation of the exposure and the rise in temperature in the skin. These figures are self-explanatory.

Figure 1.15 illustrates the effect of doubling the value of k_c on the $T^o - \theta_c^o - X_s^o$ relationship. Curves to the right are calculated for white (W4) cloth, which is highly diathermanous, the curves to the left for opaque cloth. The different part k_c plays in these two types of cloth is interesting.

Figure 1.16 illustrates the effect of doubling the thickness for the same two types of cloth. It is seen that the variation in thickness has a much greater effect than thermal conductivity variation on the $T^o - \theta_c^o - X_s^o$ relationship.

Figure 1.17 illustrates the relative importance of U_i^o and U_o^o on the $T^o - \theta_c^o - X_s^o$; it is seen that, as expected, U_i^o is important at relatively small θ_c^o and U_o^o becomes important at long θ_c^o values.

2. Application to Relaxation Period.

Taking advantage again of the additive nature of the solution, the $T^o - \theta_c^o - X_s^o$ relationship during the relaxation time, i.e., after the termination of the radiant source, can be obtained from the general solution by adding at the termination time to the general solution a negative radiation of the same intensity.

Figures 1.18, 1.19 show the temperature-time curves at two depth planes with radiation terminated at various dimensionless times, in the case of diathermanous white cloth and black opaque cloth, respectively. These figures are self-explanatory, and it is interesting to note the time when various depths of skin reach their maximum temperatures.

3. Application to Non-Square Wave Radiant Source.

Even though the general solutions are based on a radiant source of uniform intensity, solutions to radiant sources of any shape or duration can be obtained from these general solutions. An example is shown in Figure 1.20. The pulse shape and duration is that of a 1.46 Megaton nuclear explosion (2, 3, 5). The procedure is illustrated by the sketch at the lower right corner of Figure 1.26. Radiation of uniform intensity is added to the solution in a step-wise fashion until it reaches the maximum intensity, then negative radiation is added to the solution in the same way, (shown as double cross-hatched area) and net radiation received by the system is shown as the cross-hatched area. The dimensionless temperature rise group expressed in terms of the maximum intensity, I_{max}, is plotted against dimensionless time, $\Delta\theta_c^o$, for various depths in skin as shown in Figure 1.26.

In Figure 1.27, the temperature history at a dimensionless skin depth of 0.05 for the nuclear explosion is compared with that of square wave

radiation of the same energy, delivered in 4.5 and 1 dimensionless time units.

It is to be noted that the theoretical solution is solved by dividing the cloth into 6 increments and the modulus, $\Delta X_c^{o2}/\Delta\vartheta_c^o$, is chosen as 2; thus each time increment represents 0.0139 dimensionless time units which in turn is equal to about 0.034 sec. for the 9 oz cotton sateen. If the non-uniform pulse is to be delivered in a very short time, say 0.1 sec, the present general solution would only give a very crude approximation of the pulse shape (i.e., in three time increments). But the situation can be easily improved by increasing the modulus or by decreasing the size of each increment.

C. DISCUSSION OF RESULTS

1. Properties of the Cloth and Skin Simulant

For the optical properties of the cotton sateen cloth the values listed in Table 1.1 have been used in the evaluation of experiments as well as in the calculations.

Literature values for the specific heat of cotton fabrics vary between 0.32 (7) and 0.35 cal/gm°C, (2). A value of 0.34 cal/gm°C was used in the calculations.

In determining the heat conductivity of cloth by the conventional steady-state method, it is difficult to assign a proper effective thickness to the cloth in a situation involving both radiation and conductive heat transfer. A similar problem is posed by the measurement of density. These difficulties are avoided by combining the thickness term with both the density and thermal conductivity. For the former, a value of $(\rho L)_c = 0.0273 \pm 2\%$ gm/cm^2 was measured by a method described in (4). The group $(k/L)_c$ has to be estimated and improved by a trial-and-error method also explained in (4), which uses an adjustment of theoretical to experimental temperature responses. This method should give a better approximation of k_c for our purposes than the steady-state method. However, it presupposes correct values of the heat transfer coefficients U_o and U_i, which are not known precisely. Therefore the influence of a possible error in k_c will have to be tested (see V, C, 2).

The value of $(k/L)_c$ for the 9 oz standard cotton sateen was determined to be around 3.76×10^{-3} cal/cm sec°C. If L_c is taken as 0.043 cm (measured

with a micrometer), then the above value corresponds to $k_c = 1.62 \times 10^{-4}$ cal/cm sec°C, which is close to the value $k_c = 1.5 \times 10^{-4}$ cal/cm sec°C indicated by other literature.

For the skin simulant (no. 10) used in the experiments the values $k_s = 1.035 \times 10^{-3}$ cal/cm sec°C and $(kC\rho)_s = 8.65 \times 10^{-4}$ cal²/cm⁴sec°C² were measured. These differ slightly from the properties of average white skin agreed upon at an AFSWP conference (1), which are $k_s = 1.065 \times 10^{-3}$ cal/cm sec°C and $(kC\rho)_s = 8.5 \times 10^{-4}$ cal²/cm⁴sec°C².

2. Comparison of the Theoretical Analysis with the Experimental Data on the Dry Cloth - Air Gap - Skin Simulant System

Using the physical properties mentioned above, the experimental data (Figures 1.7 - 1.10) are transformed into their dimensionless form and replotted in Figures 1.20 - 1.23, for comparison with two sets of theoretical results. The dotted lines are based on $U_o^o = 0.1$ and $U_i^o = 2.0$ (corresponding to a surface heat transfer coefficient $U_o = 3.76 \times 10^{-4}$ cal/cm²sec°C and an air gap of width 0.008 cm with an air conductivity of 0.6×10^{-4} cal/cm sec°C). The solid lines represent $U_o^o = 0.2$ and $U_i^o = 5.0$.

The theoretical solution can be expected to be influenced by the heat transfer coefficients, the thermal conductivity of cloth, the transmittance and residual moisture of cloth.

Figures 1.20 - 1.23 show that the effect of the temperature rise in the skin simulant of changing the assumed values of U_o^o and U_i^o decreases with rising diathermancy, as can be expected from the fact that the contribution of conduction to the heat transfer through the cloth diminishes.

For the diathermanous cloth, the agreement with the range of the two sets of calculations is quite good. The values for the opaque cloth, however, are better approximated by the solid curves than the dotted ones at short exposure times. The apparent necessity of assigning higher values to the heat transfer coefficients than those representing a stagnant air layer and natural convection at the front surface (case of $U_o^o = 0.1$ and $U_i^o = 2.0$) (McAdams, 14), may be explained by the fact that under rapid transient heating the transient heat transfer coefficients can be considerably higher than the values obtained under steady-state conditions (8, 13, 18). In addition,

movement of air in the pores of the cloth under a high temperature gradient may also contribute to the effective heat transfer coefficient.

Further possible influences are shown by Figures 1.20 - 1.24. Assumption of a small transmittance of the opaque cloth (although not revealed by spectrometer measurements) may raise the temperature response of the skin simulant considerably at low exposure times (Figure 1.20). A similar effect can be caused by a low residual moisture content of the "dry" cloth, whose desorption, migration and subsequent condensation on the surface of the relatively cool skin simulant will contribute to the energy transport. Figure 1.24 illustrates the variation due to 1.8% residual moisture content, calculated according to the moist cloth theory.

Last, the effect of a variation in the thermal conductivity of the cloth has been studied. In Figure 1.25 $(k/L)_c$ is raised by 30% over the value previously used. Here the dimensionless heat transfer coefficients are left constant (at 0.1 and 2.0), which implies that their dimensional equivalents U_o and U_i, too, are increased by 30% over their original values for natural convection and a stagnant air gap. This latter fact alone accounts for a rise in temperature. Thus if there is a contribution on $(k/L)_c$ to the temperature rise at all it must be rather small.

To reveal the influence of $(k/L)_c$ further, some experiments have been carried out with a cylindrical skin simulant placed at a distance of 0.038 cm behind the cloth. These tests clearly indicate that the heat transfer through the stagnant air space in our system is much higher than can be predicted by an increased thermal conductivity in conjunction with the stagnant-air value of U_i.

Summarizing, it may be said that while slight effects may be due to transmittance and residual moisture in the dry cloth as well as its thermal conductivity, they appear unlikely. The major influence on the theoretical temperature response of the system is most probably effected by the choice of proper heat transfer coefficients. It seems necessary to base the theoretical solution on values of U_o and U_i higher than those related to steady-state natural convection and a stagnant air space. A rigorous confirmation of this would require further experimental investigation.

VI. THEORETICAL - MOIST CLOTH OVER SKIN SIMULANT SYSTEM

A. THE MATHEMATICAL MODEL

Based on the assumption that a linear relationship exists between the physical properties of the cloth fibers and that of water, an attempt was made to correlate the moist cloth data with the theoretical solution for the dry cloth-skin system using the calculated "pseudo" physical properties. The calculated theoretical temperature history was for lower than the experimental data. This suggested that the moisture in the cloth vaporized when exposed to high intensity radiation with part of the water vapor penetrating through the air gap and condensing on the cold skin simulant surface, thus resulting in a high temperature rise. A successful mathematical model must, therefore include the effect of moisture transport on the heat transfer process. Our proposed model assumes the following:

1. Mass transfer of moisture is caused by the molecular diffusion and bulk flow of vapor through the gas voids surrounding the cloth fibers, but not by liquid diffusion on the surface of or through pores in the cloth fibers.

2. The local moisture content (called "regain" in textile technology) of the cloth is at all times in equilibrium with the partial preassure of water vapor at the temperature of the local gas in the voids, i.e., the rate of equilibration is much faster than the vapor diffusion process.

3. Sensible heat transfer in the vapor phase is negligible compared with the heat conduction through the cloth and with the heat effects of adsorption and desorption of water on the cloth fiber.

4. The volume of air flowing through the cloth is negligible compared with that of the water vapor due to desorption and adsorption of water to and from the cloth fiber, i.e., air can be considered as a stagnent layer through which water vapor diffuses.

5. Other assumptions are the same as those for the dry cloth problem. An energy balance around a differential element of the cloth layer gives:

$$k_c \frac{\partial^2 T}{\partial x^2} = \rho_o (1 - f) C_c \frac{\partial T}{\partial \theta} + \lambda \rho_o (1 - f) \frac{\partial M}{\partial \theta} \qquad (2.1)$$

or

$$\frac{\partial T}{\partial \theta} = \left(\frac{k}{C\rho}\right)_c \frac{\partial^2 T}{\partial x^2} - \frac{\lambda}{C_c} \frac{\partial M}{\partial \theta} \qquad (2.1a)$$

where $\rho_c = \rho_o(1 - f)$ = bulk density of cloth, and the continuity equation for water can be written as:

$$-\frac{\partial}{\partial x}\left[-\frac{gD}{(1 - y_1)} \frac{\partial y_1}{\partial x}\right] = \frac{\rho_c}{f M_1} \frac{\partial M}{\partial \theta} + \tilde{\rho} \frac{\partial y_1}{\partial \theta} \qquad (2.2)$$

Since the bulk flow due to a total pressure gradient is neglected in this model, the total pressure is assumed to be constant at 1 atm., and the mole fraction of water vapor, y_1 can be replaced by the fractional partial pressure p/π. Equation (2.2) can be written as:

$$\frac{\rho}{\pi} \frac{\partial p}{\partial \theta} = D'' \frac{\partial^2 p}{\partial x^2} - \frac{\rho_c}{f} \frac{\partial M}{\partial \theta} \qquad (2.2a)$$

where

$$D'' = \frac{g\mathcal{D}\bar{M}}{\left(1 - \frac{p_a y_1}{\pi}\right) RT}$$

ρ = mass density of the gas phase, $\mu gm/cm^3$

A third relationship can be obtained from assumption (2), thus

$$M = \mathcal{F}(T, p)$$

and

$$\frac{\partial M}{\partial \theta} = \left(\frac{\partial M}{\partial T}\right)_p \frac{\partial T}{\partial \theta} + \left(\frac{\partial M}{\partial p}\right)_T \frac{\partial p}{\partial \theta} \qquad (2.3)$$

Substituting (2.3) into (2.1a) and (2.2a), eliminating $\partial p/\partial \theta$ from the two equations and making the assumption that $\frac{\rho_c}{f}\left(\frac{\partial M}{\partial p}\right)_T >> \frac{\rho}{\pi}$, we obtain,

$$\frac{\partial T}{\partial \theta} = \left(\frac{k}{C\rho}\right)_c \frac{\partial^2 T}{\partial x^2} - \left[\frac{fD''\lambda}{C_c \rho_c}\right] \frac{\partial^2 p}{\partial x^2} \qquad (2.4)$$

and

$$\frac{\partial p}{\partial \theta} = \left[\frac{fD''\left(1 + \frac{\lambda}{C_c}\left(\frac{\partial M}{\partial T}\right)_p\right)}{\rho_c\left(\frac{\partial M}{\partial p}\right)_T}\right]\frac{\partial^2 p}{\partial x^2} - \left[\frac{\alpha_c\left(\frac{\partial M}{\partial T}\right)_p}{\left(\frac{\partial M}{\partial p}\right)_T}\right]\frac{\partial^2 T}{\partial x^2} \qquad (2.5)$$

Equations (2.4) and (2.5) represent the two equations describing the heat and mass transfer in the cloth layer.

For the skin simulant, we have,

$$\frac{\partial T}{\partial \theta} = \left(\frac{k}{C\rho}\right)_s \frac{\partial^2 T}{\partial x_s^2} \qquad (2.4a)$$

where the subscript s denotes skin simulant.

The boundary conditions are:

(1) At the front surface of the cloth:

(a) $$K_o(p_{x_c=0} - p_{surr}) = fD'' \frac{\partial p}{\partial x_c}\Big]_{x_c=0} \qquad (2.6)$$

(b) $$I_o - U_o(T_{x_c=0} - T_{surr}) = -k_c \frac{\partial T}{\partial x_c}\Big]_{x_c=0} \qquad (2.7)$$

(2) In the air gap between the cloth and the skin simulant, neglecting the heat capacity of the air:

(a) Material balance:

$$K_i(p_{x_c=L_c} - p_{x_s=0}) = -fD'' \frac{\partial p}{\partial x_c}\Big]_{x_c=L_c} \qquad (2.8)$$

(b) Energy balance:

$$\begin{aligned} -k_c \frac{\partial T}{\partial x_c}\Big]_{x_c=L_c} - K_i(p_{x_c=L_c} - p_{x_s=0}) &= U_i(T_{x_c=L_c} - T_{x_s=0}) - K_i(p_{x_c=L_c} - p_{x_s=0}) \\ &= -k_s \frac{\partial T}{\partial x_s}\Big]_{x_s=0} \end{aligned} \qquad (2.9)$$

B. METHOD OF SOLUTION

1. Dimensionless Formulation of the Basic Equations

Unlike the case of the dry cloth-skin system, the moist-cloth problem does not lend itself to a generalized solution in dimensionless form. Not only is its solution non-linear with respect to irradiation intensity, but a general formulation would also require analytical expression of the hygroscopic equilibrium behavior of the cloth, so far only available in tabulated form. To describe this equilibrium, as well as the water vapor pressure curve, a number of dimensionless parameters would have to be introduced besides those needed for the heat and mass transfer coefficients, diffusivity, and the surrounding conditions.

The solution method developed is therefore not general, but is specific with respect to water vapor as the vaporizable component, the initial moisture content, the initial temperature and the irradiation intensity; i.e., the functions relating vapor pressure and moisture content are dealt with in absolute terms. Nevertheless, the calculations are carried out in dimensionless form, which not only provides an organizational aid but also allows for examination of the degree of nonlinearity as exhibited by the results.

The transformation groups for time, space, temperature, pressure and the transfer and diffusion coefficients are listed below:

$T^o = \frac{Th_c}{I_o L_c}$ — dimensionless temperature group.

$X_c^o = \frac{x_c}{L_c}$ — dimensionless distance group, measured from the front surface of the cloth.

$X_s^o = \frac{x_s}{L_c} \cdot \frac{k_c}{k_s}$ — dimensionless skin-depth group.

$\theta_c^o = \left(\frac{k}{C\rho}\right)_c \cdot \frac{\Delta\theta_c}{L_c^2}$ — dimensionless time group.

$U_o^o = \frac{U_o L_c}{k_c}$ — surface convective and radiant heat losses group.

$$U_i^o = \frac{U_i I_c}{k_c}$$ convective heat transfer through air gap group.

$$\bar{K} = \sqrt{\frac{(kC\rho)_a}{(kC\rho)_c}} = \frac{\Delta X_c^o}{\Delta X_s^o}$$ property-ratio group.

$$P^o = \frac{P}{P^o} - \frac{P_{surr}}{P^o}$$ dimensionless partial water vapor pressure group. (P_o is a convenient base pressure value, taken to be 1000, p_{surr} the equilibrium partial pressure of water vapor at time zero.)

$$K_o^o = - \frac{\lambda K_o P_o}{I_o}$$ surface heat losses group due to moisture removal.

$$K_i^o = - \frac{\lambda K_i P_o}{I_o}$$ heat transfer group due to moisture transfer through the air gap.

$$D^o = - \frac{\lambda D'' P_o}{L_c I_o}$$ heat transfer group due to moisture diffusion.

Using the above transformations, the differential equations (2.4, 2.4a, 2.5) become:

(a) For the cloth layer:

$$\frac{\partial T^o}{\partial \theta^o} = \bar{A} \frac{\partial^2 T^o}{\partial X_c^{o2}} + \bar{B} \frac{\partial^2 P^o}{\partial X_c^{o2}} \qquad (2.4)'$$

$$\frac{\partial P^o}{\partial \theta^o} = \bar{C} \frac{\partial^2 T^o}{\partial X_c^{o2}} + \bar{D} \frac{\partial^2 P^o}{\partial X_c^{o2}} \qquad (2.5)'$$

where

$$\bar{A} = 1.$$

$$\bar{B} = fD^o$$

$$\bar{C} = - \frac{\left(\frac{\partial M}{\partial T}\right)_p \cdot I_o L_c}{\left(\frac{\partial M}{\partial p}\right)_T \cdot P_o k_c}$$

$$\bar{D} = + \frac{fD^o L_c C_c I_o}{k_c \lambda P_o} \left[\frac{1}{\left(\frac{\partial M}{\partial p}\right)_T} + \frac{\lambda \left(\frac{\partial M}{\partial T}\right)_p}{C_c \left(\frac{\partial M}{\partial p}\right)_T} \right]$$

(b) For the skin:

$$\frac{\partial T^o}{\partial \theta^o} = \frac{\partial^2 T^o}{\partial X_s^{o2}} \qquad (2.4a)'$$

The boundary conditions (2.6, ... 2.9) are transformed into:

(a) At the outer surface of the cloth:

$$\text{Mass flux: } P^o_{x_c^o = 0} = (f(D^o/K_o)) \cdot \left.\frac{\partial p^o}{\partial X_c^o}\right|_{x_c^o = 0} \qquad (2.6)'$$

$$\text{Energy flux: } 1 - U_o^o \cdot T^o_{x_c^o = 0} = \left.\frac{\partial T^o}{\partial X_c^o}\right|_{x_c^o = 0} \qquad (2.7)'$$

(b) In the air gap:

$$\text{Mass flux: } P^o_{x_c^o = 1} - P^o_{x_s^o = 0} = Xf(D^o/K_i)) \cdot \left.\frac{\partial P^o}{\partial X_c^o}\right|_{x_c^o = 1} \qquad (2.8)'$$

$$\text{Energy flux: } -\left.\frac{\partial T^o}{\partial X_c^o}\right|_{x_c^o = 1} + K_i(P^o_{x_c^o = 1} - P^o_{x_s^o = 0})$$

$$= U_i^o (T^o_{x_c^o=1} - T^o_{x_s^o=0}) + K_i(P^o_{x_c^o=1} - P^o_{x_s^o=0})$$

$$= -\left.\frac{\partial T^o}{\partial X_s^o}\right|_{x_s^o = 0}$$

2. Difference Equations and Solution Algorithm

(a) Finite difference notation

In order to solve the system (2.4', 2.4a', 2.5), it is rewritten in the form of finite-difference equations. The variables involved now are lumped quantities, their values being assigned to discrete points in space and time, separated by intervals ΔX_c^o (cloth), ΔX_s^o (skin) and $\Delta\theta^o$ (Figure 2.1). The subscripts j and n denote, respectively, a point in space and time. In particular, the subscript n denotes "present time"; n-1 refers to "past time",

and n+1 to "future time".

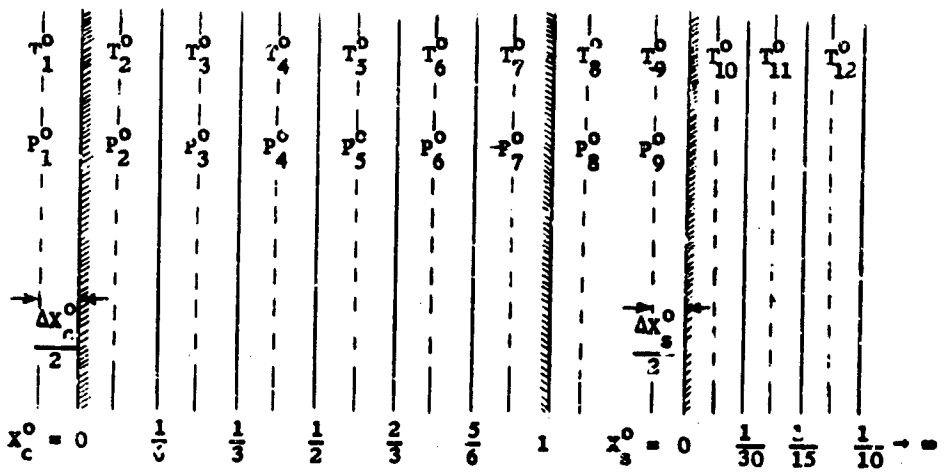

Figure 2.1

SLAB DIVISION FOR MOIST CLOTH-SKIN SIMULANT SYSTEM

The partial derivatives, e.g. of the temperature distribution, in finite difference notation take the following form:

$$\left.\frac{\partial^2 T^o}{\partial X_c^{o2}}\right|_{\substack{X_c^o = j\Delta X_c^o \\ \theta^o = n\Delta\theta^o}} = \frac{T^o_{j-1,n} - 2T^o_{j,n} + T^o_{j+1,n}}{(\Delta X_c^o)^2}$$

$$\text{abbr.: } \frac{\Delta^2 T_{j,n}}{(\Delta X_c^o)^2} \text{ or } T^o_{xxj,n} \qquad (2.10)$$

$$\left.\frac{\partial T^o}{\partial \theta^o}\right|_{\substack{X_c^o = j\Delta X_c^o \\ \theta^o = n\Delta\theta^o}} = \frac{T^o_{j,n+1} - T^o_{j,n}}{\Delta\theta^o}$$

$$\text{abbr.: } \frac{\Delta T^o_{j,n}}{\Delta\theta^o} \text{ or } T^o_{\theta j,n} \qquad (2.11)$$

Thus, the governing difference equations are (with the abbreviations introduced above):

(1) For the cloth layer:

$$\frac{\Delta T^o}{\Delta \theta^o} = \bar{A} \frac{\Delta^2 T^o}{(\Delta X_c^o)^2} + \bar{B} \frac{\Delta^2 P^o}{(\Delta X_c^o)^2} \qquad (2.4)''$$

$$\frac{\Delta P^o}{\Delta \theta^o} = \bar{C} \frac{\Delta^2 T^o}{(\Delta X_c^o)^2} + \bar{D} \frac{\Delta^2 P^o}{(\Delta X_c^o)^2} \qquad (2.5)''$$

(2) For the skin:

$$\frac{\Delta T^o}{\Delta \theta^o} = \bar{A} \frac{\Delta^2 T^o}{(\Delta X_s^o)^2} \qquad (2.4a)''$$

and the boundary conditions become:

(1) at the front surface of the cloth:

Mass flux: $$P^o_{x_c^o=0} = (f(D^o/K_o^o)) \cdot \frac{\Delta P^o}{\Delta X_c^o}\Big]_{X_c^o=0} \qquad (2.6)''$$

Heat flux: $$1 - U_o^o \cdot T^o_{x_c^o=0} = -\frac{\Delta T^o}{\Delta X_c^o}\Big]_{X_c^o=0} \qquad (2.7)''$$

(2) In the air gap.

Mass flux: $$P^o_{x_c^o=1} - P^o_{x_s^o=0} = -(f(D^o/K_i^o)) \cdot \frac{\Delta P^o}{\Delta X_c^o}\Big]_{X_c^o=1} \qquad (2.8)''$$

or, if one assumes condensation to take place to the plane 1/2 ΔX_s^o above the skin surface and accordingly reduces the diffusional resistance across the air gap ($1/K_i^o$) by that through half a skin increment:

$$P^o_{x_c^o=1} - P^o_{x_s^o=0} = -(f(D^o/K_i^{o'})) \cdot \frac{\Delta P^o}{\Delta X_c^o}\Big]_{X_c^o=1} \qquad (2.8a)''$$

where

$$\left.\begin{aligned} P^o_{x_c^o=1} &= \frac{P_7^o + P_8^o}{2} \\ P^o_{x_s^o} &= -\Delta x_s^o/2 = P_9^o \\ \frac{\Delta P^o}{\Delta X_c^o}\Big]_{X_c^o=1} &= \frac{P_7^o - P_8^o}{2} \end{aligned}\right\} \text{ in the 6-slice model of Figure 2.1.}$$

$$\text{Heat flux: } -\left.\frac{\Delta T^o}{\Delta X_c^o}\right]_{X_c^o=1} + K_i^{o'}\,(P^o_{x_c^o=1} - P^o_{x_s^o=0})$$

$$= U_i^o\,(T^o_{x_c^o=1} - T^o_{x_s^o=0}) + K_i^{o'}(P^o_{x_c^o=1} - P^o_{x_s^o=0})$$

$$= -\left.\frac{\Delta T^o}{\Delta X_s^o}\right]_{X_s^o=0} \qquad (2.9)''$$

(b) Backward difference method

In solving difference equations the structure of the computing algorithm as well as the stability and accuracy of the solution depend on the choice of subscripts assigned to each of the derivatives. For example, in the case of the heat conduction equation,

$$\frac{\partial^2 T^o}{\partial X^{o2}} = \frac{\partial T^o}{\partial \theta^o}$$

taking the second derivative in space at present time results in the "explicit" formulation:

$$\frac{T^o_{j-1,n} - 2T^o_{j,n} + T^o_{j+1,n}}{(\Delta X^o)^2} = \frac{T^o_{j,n+1} - T^o_{j,n}}{\Delta\theta^o}$$

which at each point (j,n) contains only one unknown, since the distribution of T^o at time n is known.

If instead one chooses to take the second derivative at future time, one arrives at the so-called "backward difference" equation:

$$\frac{T^o_{j-1,n+1} - 2T^o_{j,n+1} + T^o_{j+1,n+1}}{(\Delta X^o)^2} = \frac{T^o_{j,n+1} - T^o_{j,n}}{\Delta\theta^o}$$

which at each point (j,n+1) presents the three unknowns $T_{j-1,n+1}$, $T_{j,n+1}$, $T_{j+1,n+1}$ and is also called "implicit".

Besides these methods, there are others involving both present and future time values in the evaluation of the next distribution (18). The formulation mentioned first is explicit in that the single unknown quantity

at each point (j,n) is readily obtainable. However, this method is known to possess a restriction on the solution stability. The second, backward difference formulation with three unknowns at (j,n) requires setting up a system of as many simultaneous equations as there are space points. Since the equations deal with subsequent space points, the unknowns appear in advancing positions and thus form a tridiagonal set of equations which can be solved by recursion after application of the boundary conditions. This procedure entails more computational work than the explicit method, but in the case of the heat conduction equation it is known to produce an unconditionally stable solution. A backward difference method was chosen, too, to solve the problem presented by equations (2.4", 2.4a", 2.5"). An investigation of the stability of the particular algorithm used has been carried out and is described in chapter VI, B, 5.

Whenever one of the equations is used to calculate implicitly the distribution of either variable at future time (subscript n+1), the distribution of the other variable is its last known distribution. Furthermore, the two equations are used alternatingly in a pair of time steps, such that in the first step one first solves for T, then for P, and in the second step, first for P, then for T.

a. Solve (2.4)" and (2.4a)" for $T^o_{j,n+1}$ for all j; $T^o_{j,n}$ and $P^o_{j,n}$ known

b. Solve (2.5)" for $P^o_{j,n+1}$ for all j; $T^o_{j,n+1}$ and $P^o_{j,n}$ known

c. Solve (2.5)" for $P^o_{j,n+2}$ for all j; $T^o_{j,n+1}$ and $P^o_{j,n+1}$ known

d. Solve (2.4)" and 2.4a)" for $T^o_{j,n+2}$ for all j; $T^o_{j,n+1}$ and $P^o_{j,n+2}$ known

(2.12)

then replace n by n+2.

Details of the computing algorithm are described in Appendix C.

The main difference in solving for the temperature or pressure distribution is that the coefficients $\bar{C}$ and $\bar{D}$ in equation (2.5)', are dependent on temperature and pressure. Their present time values are determined at each time step preceding the solution of the equation set. This is done by means of a double interpolation (with entries T and p) of tabulated values

for $(\partial M/\partial T)_p$ and $(\partial p/\partial T)_M$, which are based on equilibrium data for moist cloth obtained by Urquhart and Williams (22).

3. Remarks on the Boundary Conditions and Variable Water Vapor Diffusivity

(a) Moisture condensation of the skin surface

The boundary condition (2.8)" relates the mass transfer at the inner cloth surface to the vapor diffusion through the air gap. In it, $P^o_{x^o_s=0}$ is the water vapor pressure at the skin surface, or, more precisely, the saturated vapor pressure at the temperature of the skin surface, since the skin is taken to have no absorptivity for moisture. In calculating the pressure distribution, the above relation is used first, implying the assumption that there is condensed moisture on the skin. If this assumption is incorrect, (as revealed by a test of the pressure gradient at the air gap and a record of the moisture condensed), the pressure calculation is repeated once, with a simpler boundary condition stating that the moisture flux through the inner cloth surface is zero:

$$P^o_7 = P^o_8 \text{ (in the 6-slice model of Figure 2.1)}$$

A distinction has to be made in this context between the phases b and c of the alternating scheme (2.12), although both phases apply the same basic equations.

In phase b, the skin surface temperature at "future time" $T^o_{x^o_s=0,\ n+1}$ is known and thus also $P^o_{x^o_s=,n+1}$. In phase c, when n+2 means future time, this is not true. The "present time" value $T^o_{x^o_s=0,n+1}$ is therefore chosen as a trial value. If the ensuing calculation of temperatures in phase d does not confirm it closely enough, an improved value for the skin surface temperature is chosen and phases c and d are repeated until convergence is achieved.

(b) Treatment of dry cloth slices

At sufficiently high irradiation intensity, the evaporation of water and the moisture flow to the cooler interior of the system will eventually cause parts of the cloth to become dry, starting from the outer surface. A slice of the cloth is called dry when either its temperature rises above some fixed level (i.e., 180°C) or the relative humidity in it drops below a minimum (5%). The dry slices are now excluded from the pressure calculation based on the moisture equilibrium relationship. If, however, the equation

for the temperature calculation (2.4)" is to remain unaltered, some meaningful, if very low, pressure values must be assigned to the "dry" slices. The storage capacity of these slices for moisture can be considered negligible as long as they stay "dry". Therefore at these points the pressure values should not contribute to the temperature response as expressed by equations (2.4)"; the second derivative of pressure may be considered to be zero, which turns these equations into pure heat conduction equations. In other words, the pressure profile is to have a linear section, which is equivalent to stating that the values in question are only determined by the diffusion from the known vapor pressure in the first moist slice to the outside surface.

If m is the number of dry cloth slices, then P_1^o and P_{m+2}^o are related by a modification of the boundary condition (2.6)" which takes into account the lengthened path of diffusion to the boundary:

$$K_o^o \cdot P^o_{x_c^o=0} = fD^o \cdot \frac{\Delta P^o}{\Delta X_c^o}\Bigg]_{X_c^o=0}$$

No dry slices:

$$P_1^o = P_2^o \cdot \frac{2fD^o - K_o^o \cdot \Delta X_c^o}{2fD^o + K_o^o \cdot \Delta X_c^o} \qquad (2.6)"$$

m slices dry:

$$P_1^o = P_2^o \cdot \frac{2fD^o - K_o^o \cdot \Delta X_c^o}{2fD^o + (2m+1)K_o^o \cdot \Delta X_c^o} \qquad (2.6)"'$$

(See Figure 2.2 below)

Accordingly, the pressures in the "dry" part of the cloth are found by interpolation.

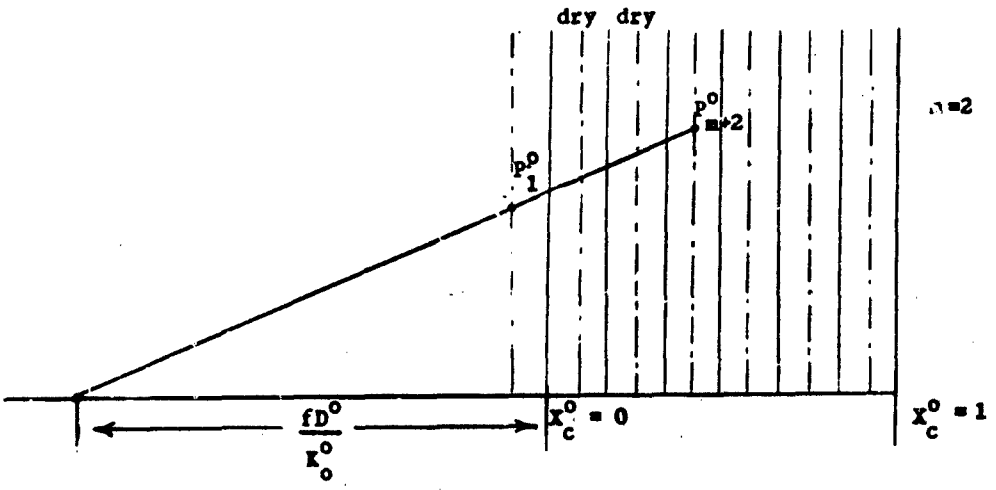

Figure 2.2

(c) The diffusivity of water vapor through air is given as a function of temperature:

$$\mathcal{D} = 0.22 \left(\frac{T}{273}\right)^{3/2}$$

The effective coefficient of diffusion D" can be calculated from $\mathcal{D}$ using an average temperature (e.g., 50°C):

$$D'' = \frac{g \mathcal{D} \bar{M}}{(1 - \frac{p_{av}}{\pi}) RT} \qquad (2.13)$$

where g is the tortuosity factor.

The program allows for the use of either a fixed value of D" or a variable one, to be determined from the local vapor pressure and temperature at each cloth slice and at each time step.

4. Summary of the Computer Program

(a) Input

The program requires four groups of input data. The first type of data describes the moisture-temperature-water vapor pressure relationship for the

moist cloth. The functions

$$(\frac{\partial M}{\partial p})_T = f(T,p)$$

and

$$(\frac{\partial p}{\partial T})_M = f(T,p)$$

form tables with entries T and p. Their values are also listed in Table G.2. They are based on original data obtained by Urquhart and Williams, (22), which are compiled in (5).

The second group of data contains constants describing the properties of the physical system:

U_c^o

U_i^o

$fD^o \cdot I_{omax}$

$K_i^o \cdot I_{omax}$

$K_o^o \cdot I_{omax}$

$(L/k)_c$

$(\lambda/k)_c$

$(L^2C_p/k)_c$

T_{crit}

$(kC_p)_c$

The third group comprises constants referring to the properties of the mathematical model:

A tolerance for the trial value of the skin surfact temperature rise

$M_A = (\Delta X_c^o)^2/\Delta\theta^o$

ΔX_c^o

ΔX_s^o

The number of double time steps

An indicator for constant or variable water vapor diffusivity

The number of single time steps between printouts

The number of cloth slices

A time mark for optional change of M_A

An alternate value for M_A

Last, a number of parameters define "experimental" conditions, namely the surrounding temperature and relative humidity, the irradiation intensity, its duration and pulse shape:

p_{surr}

T_{surr}

An indicator for the type of irradiation pulse shape

I_{max}

The pulse width

The trapezoidal pulse shape parameter

(b) Output

The results of computations are presented as:

The dimensionless temperature distribution in and at the cloth and skin simulant

The dimensionless pressure distribution in and at the cloth

as functions of dimensionless time.

As a by-product, the values of the variable coefficients in equation (2.5)' are given as well as measures for the moisture loss due to evaporation at the cloth surface and condensation on the skin simulant.

A record of the number of cloth slices having dried out is kept, and optionally the value of the maximum critical enthalpy assumed by the skin is indicated.

(c) Program description

A common experience with any complete description of a sizeable computer program is that it tends to become as involved as the program itself appears at first glance. It is hoped, however, that the computing process is explained sufficiently by the description of the algorithm which forms the basic part

of the program (Appendix C) along with diagrams showing the flow of control through its main portions, a commentary on the purpose of the subroutines used and the program listings, all of which are included in Appendix E. The program in form of symbolic and binary cards may be obtained upon request from the files of the Fuels Research Laboratory, Chemical Engineering Department, Massachusetts Institute of Technology, Cambridge 39, Massachusetts.

5. Stability

A main distinction between the formulation of a differential equation in analytical or finite-difference terms arises from the fact that the latter formulation may be satisfied not only by one true solution but also by a number of so-called extraneous solutions contributing to the total calculated function. If these are not to disturb the solution of the problem, the condition to be imposed on them is that their amplitudes decay with time, i.e., that values of an extraneous solution u at a space point i at successive time steps n and n+1 have an amplitude ratio or growth factor $\xi \leq 1$.

$$\xi = \frac{u_{i,n+1}}{u_{i,n}} \leq 1$$

This is the condition of stability of the solution process.

Whether a finite-difference method has the property of (unconditional or conditional) stability is determined by the structure of the particular computing algorithm chosen (see VI, B, 2), in conjunction with the coefficients of the differential equations. An investigation of the stability problem associated with the alternating explicit-implicit scheme used for the moist cloth-skin simulant system follows below *. It results in a simple criterion for stability which is dependent only on the four coefficients of the equation system.

In the derivations below, a nomenclature exclusive to this chapter is used; T, P and the coefficients $\bar{A}$, $\bar{B}$, $\bar{C}$, $\bar{D}$ only retain their meaning. The superscripts denoting "dimensionless" are dropped, and for the derivatives, the abbreviations (2.10, 2.11) of chapter VI, B, 2 are used.

---

* This study was done with the kind assistance of Professor P. L. Thibault Brian, Department of Chemical Engineering, M.I.T.

Temporarily, the system is assumed to be linear, i.e., to possess constant coefficients $\bar{A}$, $\bar{B}$, $\bar{C}$, $\bar{D}$. The equations in question are

$$T_\theta = \bar{A}T_{xx} + \bar{B}P_{xx} \tag{3.1}$$

$$P_\theta = \bar{C}T_{xx} + \bar{D}P_{xx} \tag{3.2}$$

Assuming T and P to consist of separable functions,

$$T_{(x,\theta)} = r_{(x)} \cdot f_{(\theta)} \tag{3.3}$$

$$P_{(x,\theta)} = s_{(x)} \cdot g_{(\theta)} \tag{3.4}$$

the system becomes:

$$\bar{A}f \cdot (r''/r) + \bar{B}g \cdot (s''/r) = f' \tag{3.5}$$

$$\bar{C}f \cdot (r''/s) + \bar{D}g \cdot (s''/s) = g' \tag{3.6}$$

If the variables are truly separated, then the functions

$$(r''/r),\ (r''/s),\ (s''/r),\ \text{and}\ (s''/s)$$

must be independent of x.

Setting $(r''/r) = -\omega^2 = \lambda$ we find

$$r_{(x)} = s_{(x)} = e^{i\omega x} \tag{3.7}$$

We now solve for $f_{(\theta)}$ and $g_{(\theta)}$.

$$\bar{A}\lambda f_{(\theta)} + \bar{B}\lambda g_{(\theta)} = f'_{(\theta)} \tag{3.8}$$

$$\bar{C}\lambda f_{(\theta)} + \bar{D}\lambda g_{(\theta)} = g'_{(\theta)} \tag{3.9}$$

From (3.10)

$$g_{(\theta)} = \frac{f'_{(\theta)} - \bar{A}\lambda f_{(\theta)}}{\bar{B}\lambda}$$

$$g'_{(\theta)} = \frac{f''_{(\theta)} - \bar{A}\lambda f'_{(\theta)}}{\bar{B}\lambda} \tag{3.10}$$

Substituting into (3.9) we find:

$$f''_{(\theta)} - (\overline{A} + \overline{D})\lambda f'_{(\theta)} + (\overline{AD} - \overline{BC})\lambda^2 f_{(\theta)} = 0$$

Therefore,

$$f_{(\theta)} = c_1 e^{\mu_1 \theta} + c_2 e^{\mu_2 \theta}$$

with

$$\begin{pmatrix} \mu_1 \\ \mu_2 \end{pmatrix} = (-\omega^2)\left\{ \frac{\overline{A} + \overline{D}}{2} \pm \sqrt{\left(\frac{\overline{A} + \overline{D}}{2}\right)^2 - (\overline{AD} - \overline{BC})} \right\}$$

Analogously, the solution for $g_{(\theta)}$ is,

$$g_{(\theta)} = c_3 e^{\mu_1 \theta} + c_4 e^{\mu_2 \theta}$$

The total solution then is,

$$T_{(x,\theta)} = \sum_k (c_1 e^{\mu_1 \theta} + c_2 e^{\mu_2 \theta})(c_5 \cos \omega_k x + c_6 \sin \omega_k x) \quad (3.12)$$

$$P_{(x,\theta)} = \sum_k (c_3 e^{\mu_1 \theta} + c_4 e^{\mu_2 \theta})(c_5 \cos \omega_k x + c_6 \sin \omega_k x) \quad (3.13)$$

T and P are wave functions in distance, Their "growth" with time depends on the four coefficients as follows:

if $\overline{AD} > \overline{BC}$	T and P decay with time
if $\overline{AD} = \overline{BC}$	T and P are independent of time
if $\overline{AD} < \overline{BC}$	T and P increase with time

Since only the first case is physically meaningful, a finite-difference procedure to solve for T and P must also provide solutions that decay with time.

We define

$$T_{j,n} = T_{(x=j\cdot\Delta x,\ \theta=n\cdot\Delta\theta)}$$

$$P_{j,n} = P_{(x=j\cdot\Delta x,\ \theta=n\cdot\Delta\theta)}$$

$$r_j = e^{im j\Delta x}$$

In the finite-difference notation, we introduce as usual,

$$r'' = r_{j-1} - 2r_j + r_{j+1}$$

It follows, for the functions introduced in (3.5, 3.6)

$$(r''/r) = \frac{e^{i\omega(j-1)\Delta x} - 2e^{i\omega j\Delta x} + e^{i\omega(j+1)\Delta x}}{e^{i\omega j\Delta x}}$$

$$(r''/r) = e^{-i\omega\Delta x} - 2 + e^{i\omega\Delta x} = -4\sin^2(\omega\Delta x/2) \qquad (3.14)$$

and likewise,

$$(r''/r),\ (r''/s),\ (s''/r),\ (s''/s) = -4\sin^2(\omega\Delta x/2)$$

Introducing the abbreviations,

$$\alpha = -4\overline{A}\,\frac{\Delta\theta}{(\Delta x)^2}\cdot\sin^2(\omega\Delta x/2)$$

$$\beta = -4\overline{B}\,\frac{\Delta\theta}{(\Delta x)^2}\cdot\sin^2(\omega\Delta x/2)$$

$$\gamma = -4\overline{C}\,\frac{\Delta\theta}{(\Delta x)^2}\cdot\sin^2(\omega\Delta x)$$

$$\delta = -4\overline{D}\,\frac{\Delta\theta}{(\Delta x)^2}\cdot\sin^2(\omega\Delta x)$$

we rewrite the equation system in the sequence to be used for its solution (see VI, B, 2):

$$-\alpha f_{n+1} - \beta g_n = f_{n+1} - f_n \qquad (3.16a)$$

$$-\gamma f_{n+1} - \delta g_{n+1} = g_{n+1} - g_n \qquad (3.16b)$$

$$-\gamma f_{n+1} - \delta g_{n+2} = g_{n+2} - g_{n+1} \qquad (3.16c)$$

$$-\alpha f_{n+2} - \beta g_{n+2} = f_{n+2} - f_{n+1} \qquad (3.16d)$$

This represents a double time step scheme in the second half of which the sequence of operations is inverted (thus "alternating"). We are interested

in determining its behavior over one entire double time step, i.e., in finding a relation between f_{n+2} and f_n, and likewise between g_{n+2} and g_n.

From (3.16a) is extracted,

$$f_{n+1} = \frac{f_n - \beta g_n}{1 + \alpha} \tag{3.17}$$

Substituting this into (3.16b) yields,

$$g_{n+1} = \frac{-\gamma}{(1+\alpha)(1+\delta)} \cdot f_n + \frac{\gamma\beta + 1 + \alpha}{(1+\alpha)(1+\delta)} \cdot g_n \tag{3.18}$$

Substituting these two expressions into (3.16c) results in

$$-\gamma(2+\delta)f_n - (\delta+1)^2(\alpha+1)g_{n+2} + \left[\beta\gamma(2+\delta) + 1 + \alpha\right] g_n = 0 \tag{3.19}$$

and into (3.16d) in

$$(1+\alpha)^2 f_{n+2} - f_n + (1+\alpha)\beta g_{n+2} + \beta g_n = 0 \tag{3.20}$$

Having elimenated all functions values at time n+1, we now actually consider the double time step as one period, rewirting the last equations:

$$-\gamma(2+\delta)f_m - (\delta+1)^2(\alpha+1)g_{m+1} + \left[\beta\gamma(2+\delta) + 1 + \alpha\right] g_m = 0 \tag{3.19a}$$

$$(1+\alpha)^2 f_{m+1} - f_m + (1+\alpha)\beta g_{m+1} + \beta g_m = 0 \tag{3.20a}$$

Next a relation is to be found for the time behavior of one of the solutions, i.e., $g_{(\theta)}$, expressed as a growth factor

$$\zeta = g_{m+1}/g_m$$

Thus the functions f are to be eliminated first; this is done most easily by substituting f_m from (3.19a) into (3.20a), hereafter also f_{m+1} from the

same equation, having increased the index by 1. The result is,

$$\underbrace{(1+\alpha)^2(1+\delta)^2}_{\text{"a"}}\xi^2 - \underbrace{\left\{(1+\alpha)^2+\beta\gamma(2+\alpha)(2+\delta)+(1+\delta)^2\right\}}_{\text{"b"}}\xi + \underbrace{1}_{\text{"c"}} = 0 \qquad (3.21)$$

The stability condition is on the function g is

$$g_{n+1}/g_n \leq 1$$

It is not necessary to go through the same derivation to find a corresponding relation for the growth factors associated with the function f. Consider the double time step to go from n+1 to n+3, comprising the solution of equations (3.16c,d), i.e., n+1 to n+2, followed by that of equations (3.16a,b), i.e., n+2 to n+3.

$$\left.\begin{aligned} -\alpha f_{n+1} - \beta g_n &= f_{n+1} - f_n \\ -\gamma f_{n+1} - \delta g_{n+1} &= g_{n+1} - g_n \end{aligned}\right\} \text{original double step } n \to n+2$$

$$\left.\begin{aligned} -\gamma f_{n+1} - \delta g_{n+2} &= g_{n+2} - g_{n+1} \\ -\alpha f_{n+2} - \beta g_{n+2} &= f_{n+2} - f_{n+1} \\ -\alpha f_{n+3} - \beta g_{n+2} &= f_{n+3} - f_{n+2} \\ -\gamma f_{n+3} - \beta g_{n+2} &= g_{n+3} - g_{n+2} \end{aligned}\right\} \text{new double step } n+1 \to n+3 \qquad (2.12)$$

If for the moment we replace

T by P
P by T
α by δ^*
δ by α^*
β by γ^*
γ by β^*
f by g*
g by f*

then the system n+1 to n+3 is formally identical with the original one. Therefore we know from the foregoing discussion the quantities a*, b*, c* that will

be associated with the equation

$$a^* \frac{g^*_{m+2}}{g^*_m} + b^* \frac{g^*_{m+2}}{g^*_m} + c^* = 0 \qquad (3,21)$$

or because of the replacement definition

$$a^* \frac{f_{m+2}}{f_m} + b^* \frac{f_{m+2}}{f_m} + c^* = 0 \qquad (3,22a)$$

where a^*, b^*, c^* are expressed in terms of $\alpha^* \ldots \delta^*$. Resubstituting $\alpha^* = \delta$ etc., we obtain the terms in (3,20a) in terms of the original quantities $\alpha \ldots \delta$, only to find that they are identical with those in the growth factor relation (3,19) for g. This could be expected from the fact that the equation system and the algorithm for its solution are symmetric with respect to T and P (or f and g).

It remains to be seen under what conditions the stability criterion, identical for f and g, is satisfied, i.e.,

$$\xi \leq 1 \quad \text{where } a\xi^2 + b\xi \quad c = 0 \quad \text{from equation (3,21)}$$

This can be transformed as follows:

$$\xi_{\frac{1}{2}} = -(b/2a) \pm \frac{\sqrt{b^2 - 4ac}}{2a} \leq 1$$

resulting in

$$-c \leq a + b$$

Using these terms as expressed in (3,21) we have,

$$-1 \leq (1+\alpha)^2(1+\delta)^2 - (1+\alpha)^2 - \beta\gamma(2+\alpha)(2+\delta) - (1+\delta)^2$$

From this follows:

$$-1 \leq (1 + 2\alpha + \alpha^2)(1 + 2\delta + \delta^2) - (1 + 2\alpha + \alpha^2) - \beta\gamma(2 + \alpha)(2 + \delta) - (1 + 2\delta + \delta^2)$$

or

$$0 \leq (2\alpha + \alpha^2)(2\delta + \delta^2) - \beta\gamma(2 + \alpha)(2 + \delta)$$

which reduces to

$$\frac{\beta\gamma}{\alpha\delta} \leq 1$$

Thus the condition of stability is satisfied whenever $\overline{BC} / \overline{AD} \leq 1$.

So far, we have assumed the coefficients $\overline{A}$, $\overline{B}$, $\overline{C}$, and $\overline{D}$ to be constant. Since in fact $\overline{C}$ and $\overline{D}$ are evaluated anew at each time step by table interpolation, and $\overline{B}$ can be either variable or held constant, one would have to ascertain that their values always fulfill the stability condition. A special subroutine was therefore written into an intermediate version of the computer program to test the criterion, which indeed was never violated during computations.

6. Convergence

The question of convergence of the finite difference solution method bears upon two aspects of the problem:

(a) Ultimate uniqueness of the finite difference solution

(b) Expense of machine time versus accuracy

One is interested in determining the convergence of the finite-difference solution, when the difference net is refined, to the "true solution" that satisfies the finite difference system. (The true response of the physical system, as obtained experimentally, is valuable for comparison but not decisive for the consideration of convergence, since the mathematical abstraction implies simplifying assumptions). Unfortunately, no analytical solution of the system in question is available by which the accuracy of the calculated one could be determined. All one may ask for is ultimate convergence of the solution to a unique result, when finer steps in time and

space are taken. In the absence of general methods for establishing such behavior for coupled equations with coefficients depending on the response functions, a somewhat experimental approach was used to investigate it.

If one expresses the terms occurring in the finite difference equations in Taylor series forms, then the total truncation error for the two functions T^o and P^o comprises terms containing $\Delta\theta^o$, $(\Delta x_c^o)^2$ and $(\Delta x_s^o)^2$. It may be expected that the truncation error diminishes as these factors are reduced, as it does in simpler, linear systems so long as the condition for stability is obeyed. This latter requirement is in fact fulfilled by our system.

In order to observe convergence rather than prove it rigorously, calculations have been carried out to test the influence of different values of the intervals Δx_c^o, Δx_s^o and $\Delta\theta^o$. First, the resulting response curves are expected to appear in the same sequence as the respective values of $\Delta x_{c,s}^o$ and/or $\Delta\theta^o$. Second, the rate of change of these curves is expected to become smaller as successively smaller finite differences are used, i.e., they should converge against a final function. Figures 2.7a,b illustrate the results of these calculations, i.e., the temperature response of the skin obtained at constant irradiation intensities of $I_{omax} = 0.5$ and 1.0 cal/cm^{2}sec and dimensionless step widths,

$$\Delta x_c^o = 1/2,\ 1/6 \text{ and } 1/18,$$
$$\Delta x_s^o = 1/10,\ 1/30,\ 1/90 \text{ (resp.)}$$
$$\Delta\theta^o = 0.0031 \ldots 0.25$$

For comparison, the temperature responses of the cloth are also depicted for the case of $I_{omax} = 0.5$ cal/cm^{2}sec, (Figure 2.7c).

Inspection of the calculated results shows that the curves for the skin temperature lie in the expected order with respect to each other. (Note that the sequence may be ascending or descending as the truncation error may change its sign with time).

A similar behavior was observed for the cloth temperatures, at least over a time range until $\theta^o = 2.0$ (Figure 2.7c).

Furthermore, it appears that successive refinement of Δx_c^o, Δx_s^o and

$\Delta\theta^o$ results in a progressively smaller variation of the curves. For I_{omax} = 0.5 cal/cm^{2}sec the case of ΔX_c^o = 1/18 was not computed. At I_{omax} = 1.0 cal/cm^{2}sec however, the refinement of intervals in fact leads to convergence in that the response obtained with ΔX_c^o = 1/6 and $\Delta\theta^o$ = 0.00556 very precisely reproduces that obtained with ΔX_c^o = 1/18 and $\Delta\theta^o$ = 0.0031, within the low time range until θ^o = 1.0.

The agreement found from these trial calculations certainly has to be taken cum grano salis. In particular, the comparison with the case of finest step widths ha not been carried out over a very large range of time, first since this alone would have required excessive amounts of machine time, and second, because one can hardly expect a perfect reproduction over such a range from a system with slight built-in discontinuities, such as the effect of cloth slices drying out. (The approximative treatment of those cloth slices, which might introduce slight deviations, must make itself felt more strongly in the 18-slice model than with 2 or 6 slices, simply since the condition applies to a larger number of such slices as time goes on).

For practival purposes one has to make a comparison between the accuracy of the computed solution and the expense of machine time required to obtain it. The amount of comput.· time used per time step strongly depends on the fineness of the slices into which the continuum is conceptually divided, and on the length of time intervals, since the former affects the size of the equation system to be solved, while the latter is immediately related to the progression on the real time scale. The attempt at finding experimentally the degree to which a somewhat "unique" or final solution is gained by refining the space-time mesh leads one to believe that the 2-slice model does not provide sufficient accuracy, producing deviations of up to 10% from the 6-slice case. On the other hand, not much accuracy is gained by preferring 18-slices over 6. As far as computer time is concerned, this is a fortunate balance. The actual amounts of computer time required per second of real time are given in Appendix E.

7. Time-variant Irradiation Intensity

In the earlier studies of a mathematical model to describe the moist cloth-skin system the intensity of irradiation was assumed to be constant.

This represents in fact the case of the experiments carried out at MIT; here an exposure shutter was kept open for a certain time interval and then closed rapidly, thus forming a square wave of irradiation.

The situation is different in the case of a thermonuclear explosion, where the intensity of irradiation is time-variant, exhibiting a very pronounced peak value and a long decaying section. (An analytical expression for this intensity distribution was given by Batter, (23).

Thus the temperature-pressure-time response of the system will be quite different; in particular it may be expected that an irradiation of constant intensity much smaller than the peak intensity of a thermonuclear pulse will produce a given temperature rise in the skin. At constant irradiation, temperature rises monotonously and the moisture migrates to the cooler interior of the system, partly condensing on the skin surface, and although the moisture on the skin may later vaporize, there is no reversal of heat flow during irradiation. With an irradiation pulse of finite duration and energy, on the other hand, the temperature rise will eventually be followed by a decay, first in the cloth, later also on the skin surface and in the interior of the skin. Furthermore, it can be expected that there will be a reversal of the heat flow and with it will be associated a reversal of the moisture flow.

In order to show these differences between the responses to constant and time-variant irradiation as well as to allow a comparison of theoretical results with those obtained from experiments that actually involved a square wave, the mathematical method has been set up to accept a variable irradiation intensity as a boundary condition.

This facility allows for four cases of intensity distributions:

Step function
Square wave
Trapezoidal wave
Thermonuclear explosion pulse

It is introduced as follows:

The irradiation intensity affects only the heat boundary condition at the

outer cloth surface

$$I_o = U_o(T_{x_c=0} - T_{surr}) = -K_o \left.\frac{\partial T}{\partial X_c}\right]_{X_c=0} \qquad (2.7)$$

or in dimensionless finite-difference terms:

$$1 - U_o^o \cdot T^o_{x_c^o=0} = \left.\frac{\Delta T^o}{\Delta X_c^o}\right]_{X_c^o} \qquad (2.7)''$$

Note that elsewhere in the formulation of the dimensionless system I_o is used also, but merely as a reduction factor for dimensionless notation. If one still retains some characteristic value of intensity, such as the maximum of a pulse distribution, as a reference value, one is free to introduce into the boundary condition a term expressing the relative irradiation intensity $I_{o(\theta)}/I_{omax}$:

$$I_{o(\theta^o)}/I_{omax} - U_o^o \cdot T^o_{x_c^o=0} = \left.\frac{\Delta T^o}{\Delta X_c^o}\right]_{X_c^o = 0}$$

This value is computed at each time step, preceding the solution for the temperature distribution.

(a) Description of irradiation pulses

The maximum irradiation intensity is prescribed in absolute terms ($cal/cm^2 sec$). Since the program used a dimensionless time scale throughout, all characteristic extensions of pulses in time are prescribed in dimensionless terms, (Figure 2.3).

For the squarewave, one quantity θ^o_{char} suffices. The time scale of the trapezoidal pulse requires two quantities: θ^o_{er} defining the end of its first ramp, and θ^o_{char} the end of the pulse.

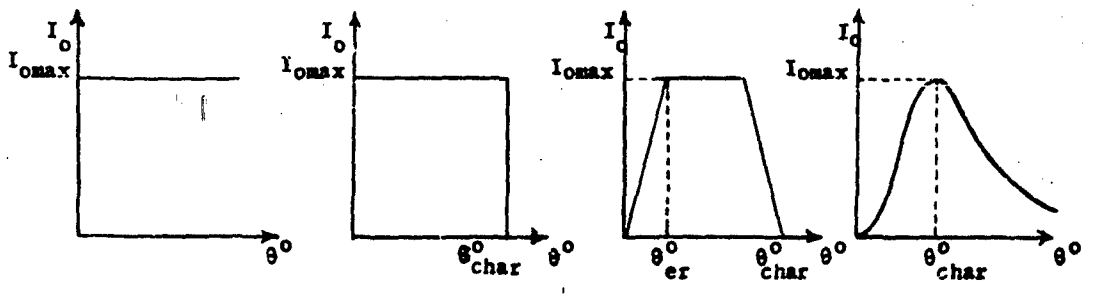

Figure 2.3

IRRADIATION PULSE SHAPES

The thermonuclear explosion pulse requires one characteristic value θ^o_{char}, locating the peak of the distribution, and a normalized shape function (20) indicated in Table 2.1 (see for example, Figure 2.20).

Table 2.1

THERMONUCLEAR PULSE INTENSITY DISTRIBUTION

Region θ^o/θ^o_{char}	Relative intensity $I_{o(\theta^o)}/I_{omax}$	Energy delivered at time θ^o (cal/cm^{2}sec)
0 - 0.3	$0.565(\theta^o/\theta^o_{char})$	$I_{omax} \cdot \theta^o_{char} \cdot 0.2825(\frac{\theta^o}{\theta^o_{char}})$
0.3 - 0.65	$1.72(\frac{\theta^o}{\theta^o_{char}}) - 0.347$	$I_{omax} \cdot \theta^o_{char}\left[0.0521 + 0.86(\frac{\theta^o}{\theta^o_{char}})^2 - 0.347(\frac{\theta^o}{\theta^o_{char}})\right]$
0.65 - 1.4	$1.0 - 1.42\left[(\frac{\theta^o}{\theta^o_{char}}) - 1.05\right]^2$	$I_{omax} \cdot \theta^o_{char}\left[-0.49 + (\frac{\theta^o}{\theta^o_{char}}) - 0.473(\frac{\theta^o}{\theta^o_{char}} - 1.05)^2\right]$
1.4 - 10.0	$1.434(\frac{\theta^o}{\theta^o_{char}})^{-1.64}$	$I_{omax} \cdot \theta^o_{char}\left[2.696 - 2.24(\frac{\theta^o}{\theta^o_{char}})^{-.64}\right]$

For comparison, the program verifies the areas of pulses, i.e., the radiation energies delivered.

(b) Remark on the square wave

In computing the response to a square wave input, a slight difficulty is sometimes encountered at the end of the pulse. The sudden termination of irradiation leaves in the above mentioned boundary condition only the term for the heat losses. Since a surface temperature value is taken to govern the outward heat flow during an entire time step, the size of time steps may have to be reduced at this point so as not to simulate too large a heat loss during the beginning of the relaxation period. At a later time, when the surface temperature has dropped, the original interval size can be resumed. The occurrence of this disturbing effect depends on whether a sufficiently high surface temperature has been reached at the end of the pulse. A convenient way of changing the time step size by altering the modulus $(\Delta X_c^o)^2/\Delta\theta^o$ is provided in the program.

The effect described does not occur in the cases of a trapezoidal or thermonuclear pulse shape, where the process is sufficiently smooth.

8. Burn Severity Correlation

Different ways of relating the temperature response of the irradiated cloth-skin system to the severity of a resulting burn have been dealt with in former studies, (3, 5). Among these, a correlation based on the concept of a critical base temperature and a constant skin enthalpy increase appeared most promising. It states that a burn of given severity is effected by a certain minimum value of that part of the skin enthalpy which lies above a critical temperature level, (see sketch below).

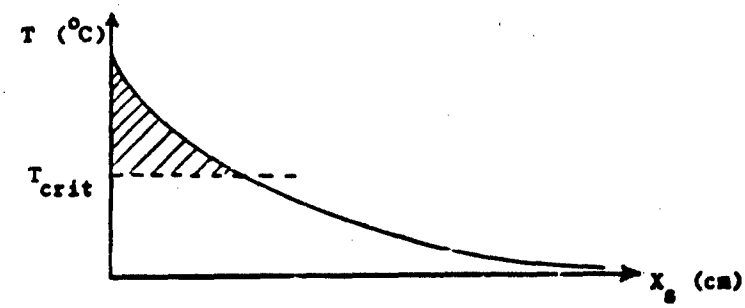

This criterion has been tested earlier in particular by comparing University of Rochester data on mild 2+ burns with the results of skin simulant experiments. Here the maximum of the critical enthalpy (i.e., the shaded area in the above plot) was taken to occur at the time at which the measured temperature closest to the skin simulant surface reached a maximum, (effected by a square wave of irradiation). Temperature distributions were plotted, extrapolated towards the skin simulant surface and their area above T_{crit} measured. A constant thermal energy increase of 0.89 - 0.93 cal/cm^2 above a critical temperature of 53°C was found to agree with most of the University of Rochester data.

The same procedure can be applied to temperature distributions obtained from theoretical calculations. It is more practical, however, to include this evaluation in the computing program, as the entire temperature history is available to it and in particular because this provides a more precise way of finding that distribution which yields the maximum value in time of the critical enthalpy:

$$(\rho C_p)_s \cdot \int_0^{X_s(T=T_{crit})} (T_{(X_s,\theta)} - T_{crit})\, dX_s = f(\theta) \qquad (4.1)$$

(When a pulse of irradiation is applied, the maximum value need not be associated with the maximum skin surface temperature, as the temperatures in the interior of the skin simulant may still continue to rise while the irradiation intensity and the skin simulant surface temperature begin to decrease).

The computer program described in this report is set up to calculate by means of a Simpson-rule integration the maximum critical enthalpy attained at any time during the process. The quantities $(\rho C_p)_s$ and T_{crit} are to be prescribed as input parameters.

The temperature distribution in the skin depends strongly on the assumptions made for the heat and mass transfer coefficients, which can only be defined within a certain tolerance. Since the burn correlation integral represents only the top part of the area under a temperature profile, it should be kept in mind that its value is influenced even more by the choice

of these coefficients. Nevertheless, with this restriction, it appears useful to obtain in this direct way the information regarding the burn correlation that the theoretical solution is able to supply. Moreover, the facility can be used to find the maximum total heat content of the skin simulant if the critical temperature is given the value of the surrounding temperature.

C. DISCUSSION OF RESULTS

Earlier studies (5) have shown that the theoretical solutions obtained for a system involving diathermanous cloth tend to agree better with experimental observations than those found for an opaque cloth layer. This is true for the case of dry cloth as well as for that of moist cloth, and may be explained by the direct admittance of part of the heat received, into the interior of the system. The purpose of extensive computer calculations devoted to the opaque cloth situation was fourfold:

First, the convergence of the numerical solution with refinement of the difference-net was tested. The results of these calculations are discussed in Chapter VI, B, 6.

Next, a number of computations was designed to show the influence of the transfer coefficients U_o, U_i, K_o, K_i and the water vapor diffusivity D'' on the theoretical response as well as its agreement with experimental results for constant irradiation levels I_o = 0.5 - 3.96 cal/cm^{2}sec, 30°C and 80% relative humidity.

A further aim was to investigate the type of response obtained under time-variant irradiation of various pulse shapes and equal total energy, at maximum intensity levels I_{omax} = 0.3 - 1.0 cal/cm^{2}sec, 30°C and 80% relative humidity, using one set of transfer coefficients.

A last group of calculations was carried out in order to test the agreement between a number of experimental results from square-wave, short exposure irradiation and the theoretical solutions obtained with identical irradiation, temperature and relative humidity conditions, (I_{omax} = 1.0, 1.4 and 2.6 cal/cm^{2}sec; 19°C; 65% relative humidity). The transfer coefficients

and the diffusivity were varied in these tests. Furthermore, some theoretical results for the diathermanous cloth case in comparison with experimental curves are presented.

1. Numerical Values used in the Computations

The values of the parameters used are summarized below. A complete reference, in particular on the estimation of the transfer coefficients, is given in (5).

(a) Properties of the cloth:

ρ_o = 1.57 gm/cm^3 for cellulose

$\rho_c L_c$ = 0.0273 gm/cm^2 for 8 oz. standard cotton sateen

L_c = 0.043 cm (measured)

f = $1 - (\rho_c/\rho_o)$ = 0.594

C_c = 0.34 cal/gm°C

k_c = $1.62 \cdot 10^{-4}$ cal/cm sec°C, based on $(L/k)_c$ = 266 cm^{2}sec°C/cal

D^* = 0.105 µgm/cm sec mm Hg at an average temperature of 50°C and with a tortuosity factor of g = 1/2.4 (see VI, B, 3)

(b) Properties of the skin simulant: see V, C, 1.

Transfer Coefficients:

The following estimates were used as a basis:

Surface heat transfer coefficient:

A dimensionless value U_o^o = 0.1 was used, corresponding to

U_o = $18.6 \cdot 10^{-3}$ cal/cm^{2}sec°C

Air gap heat transfer coefficient:

U_i^o = 5.0, corresponding to U_i = $3.76 \cdot 10^{-3}$ cal/cm^{2}sec°C

Surface moisture transfer coefficient:

K_o = 0.2µgm/cm^{2}sec mm Hg

Air gap moisture transfer coefficient (effective):

K_i = 14.4µgm/cm^{2}sec mm Hg

The variations applied to the transfer coefficients are discussed in the following sections.

Heat of desorption:

λ = 650 cal/gm H_2O

In all of the computations, the 6-slice model was used with a modulus $M_A = 5$ and a skin/cloth property ratio group $\tilde{R} = 5$.

2. Constant Irradiation - Influence of Transfer Coefficients and Diffusivity; Comparison with Experiments

The estimates of the parameters U_o, U_i, K_o, K_i and D^* have been established in (5). Considerable tolerance has to be allowed for these values, particularly regarding the effective water vapor diffusivity D^* and the mass transfer coefficients. D^* is subject to an uncertainty due to the tortuosity factor which may range between 1 and 0.2 or less. It also enters into the derivation of the mass transfer coefficient for the air gap. The theoretical results vary rather strongly with changes in the choice of all these parameters, especially at long exposure times.

In fact, once it has been shown that the experimental results can be reproduced closely by a calculation, the comparison between theoretical and experimental responses may be looked at as a method to find values of the coefficients rather than as a check on the validity of the analytic model.

The following discussion concerns calculations involving a surrounding temperature of 30°C and a relative humidity of 80%.

Figure 2.10 shows the dimensionless skin simulant temperature response at simulated depths $X_s^o = 0.05$ and 0.15 as a function of dimensionless time. At an irradiation intensity $I_o = 0.83$ cal/cm^{2}sec, the transfer coefficients are varied through the range:

$$U_o^o = 0.1 \ldots 0.025 \quad \text{or} \quad U_o = (3.76 \ldots 0.94)\cdot 10^{-4} \text{ cal/cm}^2\text{sec}$$

$$U_i^o = 5.0 \ldots 10.0 \quad \text{or} \quad U_i = (18.6 \ldots 37.2)\cdot 10^{-4} \text{ cal/cm}^2\text{sec}$$

$$K_o = 0.2 \ldots 0.05 \ \mu\text{gm/cm}^2\text{mm Hg}$$

$$K_i = 14.4 \ldots 3.6 \ \mu\text{gm/cm}^2\text{mm Hg}$$

The effective diffusion coefficient D^* is held at a constant value of $D^* = 0.105$ μgm/cm sec mm Hg (except where indicated to be variable). It is seen that K_o, K_i and U_i have the strongest influence, while the surface

heat transfer coefficient only affects the solution at longer exposure times.

Figures 2.11 and 2.12, based on Figure 2.10, present a comparison with the experimental response, determined also at I_o = 0.83 cal/cm^{2}sec. Two cases having different transfer coefficients are given. The experimental curves describe the temperature at simulated depths X_s^o = 0.028, 0.038 and 0.122 cm (thermocouple locations).

The theoretical curves referring to these same depth values have been obtained from cross-plots of the calculated data. It appears that a not too drastic alteration from the original estimates for the transfer coefficients (by factors 1/2 for U_i and 1/4 for U_o, K_o, and K_i) leads to quite good agreement with the measured temperatures.

Figure 2.13, also at I_o = 0.83 cal/cm^2, shows the variation introduced when variable diffusivity values D", based on equation (2.13), are used in the calculations instead of a fixed average value. This does not seem to improve the agreement in the above case; in other examples, however, which are discussed later (VI,C, 4) the refinement has indeed led to a better approximation, which means a different combination of transfer coefficients may be needed here for closer agreement.

In Figure 2.14 the influence of an increased value of U_i and decreased ones for U_o, K_o and K_i is shown again for an irradiation intensity I_o = 0.5 cal/cm^{2}sec.

Figures 2.15, 2.16, and 2.17 present a comparison with the experimental response at intensities 0.5, 1.26, and 3.96 cal/cm^{2}sec. The irregular appearance of the experimental curves at I_o = 1.26 stems from a partly scorched cloth layer. The cases of I_o = 0.5 and 1.26 show rather good agreement, with the theoretical curves being slightly too steep at longer times. At I_o = 3.96 the position of the calculated curves is high from the beginning. It appears that in all of these cases the application of a variable diffusivity (according to equation 2.13), with transfer coefficients in the range indicated on the figures, would have yielded a considerably better reproduction of the experimental response.

A comparison between the temperature responses of the moist and dry, opaque cloth systems is drawn in Figures 1.11 (experimental) and 2.18

(theoretical). The two figures are not precisely analogous in that they refer to slightly different skin simulant depths (x_s = 0.028 cm and to X_s^0 = 0.05 ≙ x_s = 0.014 cm). Yet they show that the theoretical response for the larger intensities lacks the pronounced change in slope occurring in the experimental moist cloth curves prior to their intersection with the curve for the dry cloth. In the logarithmic plots, too, this discrepancy is displayed by the slopes of the theoretical curves which are too steep at longer times.

The role of moisture in the system contributes greatly to the heat transport towards the skin simulant, but only initially. Eventually, the pressure gradients in the cloth reverse their direction (which can be read from the numerical results), leaving conduction as the only mode of heat transmission into the interior of the system. An inspection of the above figures suggests that this effect is not simulated strongly enough by the theory. The reason may be sought in the neglection of bulk flow of water vapor, in our model, but it is also possible that refinement is needed for the treatment of completely dry parts of the cloth which so far involves the assumption of a partially linear pressure profile.

Deviations between theory and experiments as discussed above are less striking in the case of a diathermanous (moist or dry) cloth, for which an analogous comparison based on earlier studies (5) is given in Figures 1.12 and 2.19.

So far, the theoretical results have been judged by the response at small skin depths relatively close to each other (0.028 and 0.038 cm). At larger depths (0.122 cm) a deviation is common to most cases, which cannot be neglected. It may be accounted for by the fact that the value used exclusively for the skin/cloth property ratio $\tilde{R}\sqrt{(kC\rho)_s/(kC\rho)_c} = 5.0$ is the one based on the dry cloth system and need not hold exactly true for the moist cloth situation; this would distort the simulated skin depth scale. As yet the effect has not been tested.

The water vapor diffusivity D^* has not been given alternate (constant) values in the calculations, since it affects the results mainly in the short-time range, while the major deviations of the calculated responses still occur at longer times.

The preceding discussions concern only the predominant parameters among those not known precisely. Their influences at least can be established by the use of the computing program. The effects of further variations, e.g., of the tortuosity factor occurring both in D^* and K_i, of the cloth heat conductivity k_c and $\tilde{R}$, as well as the surrounding temperature and relative humidity can likewise be determined, requiring a large but not excessive amount of computer time. In order to define a narrower range for the first group of parameters (U_o, U_i, K_o, K_i, D^*) however, not only a considerable number of calculations would be needed but also a larger set of experiments repeated under each condition.

3. Time-Variant Irradiation - Influence of Pulse Shape

A set of calculations has been carried out in order to observe qualitatively the response variation with irradiation pulses of different shapes. In order to provide some common basis for comparison, the areas of the pulses (i.e., the total irradiation energies) are kept the same within each of two groups. The first group is based on the total energy delivered by a thermonuclear pulse distribution with peak intensity $I_{o\max} = 0.5$ cal/cm^{2}sec and peak time $\theta^\circ_{char} = 0.5$ until $\theta^\circ = 5.0$; this energy equals 0.545 cal/cm^{2}sec (its dimension stems from the use of a dimensionless time scale but absolute intensity). The second group uses a thermonuclear pulse with peak intensity $I_{o\max} = 1.0$ cal/cm^{2}sec as a basis, with an area of 1.09 cal/cm^{2}sec until $\theta^\circ = 5.0$.

Square and trapezoidal waves at different irradiation intensity levels and the thermonuclear pulse are used as input forms. The latter, for convenience, shall be referred to as the "true pulse". The other conditions assumed and common to all of these calculations are: surrounding temperature 30°C, relative humidity 80%, and transfer coefficients and constant water vapor diffusivity as stated in VI, C, 1.

The results of the first group of runs are shown in Figure 2.20. The four cases presented are the true pulse with peak at 0.5 cal/cm^{2}sec, a square wave distribution with intensity level $I_{o\max} = 0.5$ cal/cm^{2}sec, a square and trapezoidal wave both with $I_{o\max} = 0.3$ cal/cm^{2}sec; these distributions are indicated in the upper part of Figure 2.20. The lower part

of the graph shows the respective temperature responses of the skin simulant at simulated depths $X_s^o = 0.0167$ and 0.15. In order to permit a comparison, the temperatures are given in reduced, but not dimensionless form, i.e., as value of $T^o \cdot I_{omax}$ $(= \Delta T \cdot (k/L)_c)$.

It is not surprising that the square wave with $I_{omax} = 0.5$ cal/cm^{2}sec yields a higher temperature response than the true pulse of same intensity level. However, the latter response shows values still considerably lower than those produced by the square and trapezoidal waves at 60% of its peak intensity, (0.3 cal/cm^{2}sec) near the skin simulant surface as well as in its interior.

Figure 2.21 shows the results of the second group of calculations, comparing the true pulse function of maximum level 1.0 cal/cm^{2}sec with trapezoidal waves at $I_{omax} = 1.0$ and 0.6 cal/cm^{2}sec, a square wave with $I_{omax} = 0.6$ and 0.4 cal/cm^{2}sec, and the case of constant irradiation intensity 1.0 cal/cm^{2}sec. The temperature response $T^o \cdot I_{omax}$ is given for one depth value $X_s^o = 0.0167$. As in the first group, the square and trapezoidal waves not only at 0.6 but even at 0.4 cal/cm^{2}sec lead to much higher skin simulant temperatures than the true pulse. This can be attributed to the fact that the latter irradiation distribution yields a faster rise of the cloth surface temperature and of the water vapor pressure near the cloth surface than square and trapezoidal waves at lower intensity levels, thus increasing the heat and moisture losses at the system surface. Furthermore, the reversal of the pressure gradient in the cloth takes place at an earlier time with the true pulse so that during the section of decaying irradiation intensity the conductive heat transfer to the skin simulant is counteracted by the moisture transport directed outward.

In none of the cases described do the temperature gradients in cloth and skin reverse their direction, so that within the calculated time range the decay of temperatures in the skin simulant is only due to the mass transfer from its surface to the cloth. Naturally, the temperatures in its interior keep rising for some time while the surface temperature has begun to drop.

These conditions can be read clearly from the numerical results; they may only be stated here in passing since a complete representation of the

results would require too much space. Reference is made though to the logarithmic plots of the skin simulant temperature responses of all the cases, given for simulated depths up to $X_s^o = 0.95$ in Figures 3.8 through 3.16, Appendix F.

4. Time-Variant Irradiation - Comparison with Experiments

It is clear from previous discussions that a rather wide range of experiments is required to serve as a yardstick, if the capacity of the mathematical analysis to model our physical system is to be examined. The number of physical coefficients which are subject to an estimation only underlines this necessity. In the effort to come to a closer agreement between theoretical predictions and experimental evidence, the judgement of how well the model reproduces the situation and the "improvement" of those parameters are intertwined, thus making the judgment somewhat relative.

The examples for a theoretical approximation of the measured response described before have left some uncertainty regarding which of the five most important parameters are to be altered and to what degree. They applied to a constant irradiation input, i.e., to cases in which the entire precess develops in one direction. A more rigid test for the model may be formed by a pulse input, where the direction of events ultimately is reversed, even to the extent that part of the cloth layer will dry out first and later attain moisture again.

Some calculations serving such a test have been executed, with conditions matching those of experiments. All of them were done with a surrounding temperature of 19°C, and 65% relative humidity.

The first group of these computations applied to a square wave irradiation of intensity level 1.0 cal/cm^{2}sec and 4 seconds exposure time ($\theta^o_{char} = 1.62$). In the calculations presented by Figures 2.22 through 2.24, constant values $D' = 0.105$ µgm/cm sec mm Hg and $U_o^o = 0.1$ ($U_o = 3.76 \cdot 10^{-4}$ cal/cm^{2}sec°C) are used, while the other transfer coefficients are varied in the ranges:

$U_i^o = 2.5 - 10.0$ or $U_i = (9.3 - 37.2) \cdot 10^{-3}$ cal/cm^{2}sec°C

$K_o = 0.05 - 0.2$ µgm/cm^{2}sec mm Hg

$K_i' = 3.6 - 14.4$ µgm/cm^{2}sec mm Hg

(The combinations are indicated on the plots).

Neither the positions nor the shapes of the curves referring to 3 simulated skin depths appear quite satisfactory. Additional trial runs in the above range of parameter values (not presented here) have not yielded any better agreement. It is to be noted that the cloth is recorded by the program to become dry throughout after $\theta^o = 1.6$ (≈ 4 seconds, i.e., at the end of the pulse). In the cases quoted first, half of the cloth is dry already at $\theta^o \approx 0.95$. Obviously the test is hampered by the fact that 65% relative humidity may be low enough to produce a situation where the moist-cloth theory finally applies only to a very small section of the cloth, namely just the last slice out of six slices, while the dry part is manipulated according to the procedure described in V, B, 3.

It is suspected that the water vapor diffusivity must not be excluded from our parameter trial procedure. In fact, one calculation carried out with variable diffusivity (according to equation 2.13) and the "original" values for the transfer coefficients (VI, C, 1) yields much better agreement between theory and experiment, if not beyond the maximum of the temperature functions, (Figure 2.25). It seems that further improvement can be achieved by not too severe variations of the heat or mass transfer coefficients from their original estimated values, while using variable diffusivity.

Considering the required expense of machine time however, the effort had to be limited to a few trials.

The situation looks more favorable in a second pair of calculations involving a square wave of intensity $I_{omax} = 1.4$ cal/cm^{2}sec and two seconds exposure time.

In the case recorded in Figure 2.26, a constant diffusivity $D^* =$ 0.105 μgm/cm sec mm Hg is used, while Figure 2.27 depicts the response when D^* is variable. For U_o, U_i, K_o, K_1 the original estimates are used. Again it appears that the assumption of a fixed average diffusivity should not be made. As before, the cloth dries out rapidly while irradiated, until only two out of six slices are left moist (contrasted with one in the previous example, which may explain the discrepancy in agreement with the experiment there). In the subsequent relaxation period, the cloth becomes moist throughout, nourished from the condensed moisture on the skin simulant surface.

Thus considering the fact that the computation has to treat the system as a composite dry-moist system during almost the entire period, the results mentioned last could be considered remarkable. While the reversal of moisture flow can be detected readily from the numerical results, the temperature gradient in the cloth and skin simulant - except in the outermost half-slice of the cloth - does not change its direction, so that the only outward heat flow in the system interior during the relaxation period is constituted by the action of the moisture transport. This observation holds true for all pulse responses computed so far.

5. Remark on the Burn Severity Correlation

In the calculations discussed above, the integral (4.1) designed to serve as a basis for the correlation of burn severity has been evaluated. As expected, its maximum occurs at some time after the surface temperature of the skin simulant is highest. The results also show that the value of the integral varies more than do the temperatures obtained when transfer coefficients etc. are changed. For example, while the skin simulant temperatures at and near the surface vary by about 9% between the curves of Figures 2.22 and 2.24, the integral changes its value by about 24%. This indicates that a fairly high reliability of the calculated temperature profiles is required to define the critical skin enthalpy closely enough, if it is to be applied to a correlation with experimental burn data.

VII. SUMMARY AND CONCLUSIONS

The temperature response of a system composed of a skin simulant covered by dry or moist cloth and exposed to radiative heating has been studied experimentally and theoretically.

The mathematical analysis adequately describes the behavior of the dry cloth-skin simulant system. The response to constant or time-variant irradiation can be constructed on the basis of general solutions both for opaque and diathermanous cloth.

The theoretical model for the moist cloth-skin simulant system is based on molecular diffusion of water vapor as the only mode of moisture transfer, thus neglecting bulk flow of water vapor and other simplifying

assumptions. It is designed for an opaque cloth layer but could be altered to apply to diathermanous cloth as well by a method analogous to that developed for the dry cloth case. The theoretical formulation is not general but requires new computer calculations for any set of specific conditions. Either constant or time-variant irradiation intensities are acceptable as boundary conditions; the latter may be a square wave, trapezoidal wave or a thermonuclear explosion pulse distribution. It also takes into account the complete drying of part of the cloth layer which can always be expected in reality.

This model yields solutions which agree fairly well with experimental results both for constant and time-varying irradiation. Uncertainties are inherent mainly in the values of heat and mass transfer coefficients and the water vapor diffusivity. Both further experiments and calculations extending over a range of these parameters could serve to determine better estimates for their values and thus improve the capability of the computing system for predicting the system behavior more accurately.

With the above reservations the variation in the temperature responses to irradiation of different distribution forms can be established clearly. The model can serve as a tool for inspection of the influences caused not only by the transfer coefficients, but by other conditions such as the surrounding temperature, relative humidity and properties of the cloth. The numerical results permit the observation of phenomena which cannot be detected experimentally, such as the direction and rate of moisture flow and the process of drying out of the cloth.

The solution includes a measure for the "critical enthalpy" of the cloth, which can be related to the severity of burns. This criterion is most sensitive to slight variations of the theoretical temperature response and deserves further testing.

The study of the influences on the heat transfer by chemical reactions in the irradiated cloth, by the structure of the fabric and moisture-retaining additives still are open paths for further research into the protection from burns.

APPENDIX A

NOMENCLATURE

$\bar{A}$ Coefficient in partial differential equation

$\bar{B}$ Coefficient in partial differential equation

C Mass heat capacity, cal/μgm°C

$\bar{C}$ Coefficient in partial differential equation

D Diffusion coefficient = $\mathscr{D}_\rho$ gm mol/cm sec

D' Average diffusion coefficient = $D/(1-y_{av})$ gm mol/cm sec

D" Corrected mass diffusion coefficient through cloth = $gD'\bar{M}/\pi$ μgm/cm sec mm Hg

$\mathscr{D}$ Diffusivity, cm^2/sec

$\bar{D}$ Coefficient in partial differential equation

f Volume fraction of voids in cloth, dimensionless

g Tortuosity factor for the diffusion through cloth

I Intensity of incident radiation, cal/cm^2sec

I_o Intensity of unreflected radiation, cal/cm^2sec; constant, unless specified as time-variant

I_{omax} Characteristic intensity level of unreflected radiation, cal/cm^2sec; (used whenever I_o specified as time-variant)

I_x Intensity of radiation at depth x, cal/cm^2sec

k Thermal conductivity, cal/cm sec°C

K Mass (moisture) transfer coefficients, $\mu gm/cm^2sec°C$

L Thickness, cm

M Moisture content of cloth, wt. H_2O/100 wt. dry cloth

$\bar{M}$ Molecular weight

M_A Modulus

p	Partial pressure, mm Hg
P_o	Base pressure used in connection with dimensionless transformation, mm Hg
P^o	Dimensionless partial pressure
R	Universal gas constant, cm^3 mm Hg/g mol ^oK
$\tilde{R}$	Property ratio = $\Delta X_c^o / \Delta X_s^o = \sqrt{(kC\rho)_s/(kC\rho)_c}$
t	Time, sec
T	Temperature, ^oC except when specified as ^oK
T_o	Base temperature, ^oC
u	Function
U	Overall heat transfer coefficient, cal/cm^2sec ^oC
w_j	Right hand sides of tridiagonal equation system for finite difference solution
x	Distance or depth, cm
X^o	Dimensionless depth
y	Mole fraction, dimensionless

Greek:

α_c	Thermal diffusivity of cloth
β_j	Lefthand side coefficients of tridiagonal equation system for finite difference solution
γ	Extinction coefficient, cm^{-1}
Δ	Finite increment
φ_j	Right hand sides of tridiagonal equation system for finite difference solution
θ	Exposure or irradiation time, sec
λ	Heat of desorption, cal/μgm (numerically negative)
π	Total pressure, mm Hg

u_j Left hand side coefficients of bidiagonal equation system for finite difference solution

ρ Mass density, $\mu gm/cm^3$

ρ_o Mass density of cellulose or solid, gm/cm^3

$\tilde{\rho}$ Molal density, gm mol/cm^3

$\sum$ Summation

τ Transmittance

ϕ Function

Subscripts:

c Cloth

char Characteristic abscissa in irradiation pulse

cond Moisture condensation

crit Critical value (temperature)

er Characteristic abscissa in trapezoidal irradiation pulse

evap Moisture evaporation

i Air gap between cloth and skin simulant except when used to denote i components

j Depth planes

n Time increments

o Cloth surface unless specified otherwise

s Skin simulant

surr Surroundings

A, B, ... Depth planes

first subscript : space

second subscript : time

Superscripts:

o Dimensionless groups

APPENDIX B

METHOD OF SOLUTION - DRY CLOTH OVER SKIN SIMULANT SYSTEM

A. OPAQUE CLOTH

With the dimensional transformations (1.8) introduced in the main section and with the finite-difference notations:

$$\left.\frac{\partial^2 T^o}{\partial X_c^{o2}}\right|_{\substack{X_c^o = j\cdot\Delta X_c^o \\ \theta^o = n\Delta\theta^o}} \approx \frac{T^o_{j-1,n} - 2T^o_{j,n} + T^o_{j+1,n}}{(\Delta X_c^o)^2} = \frac{\Delta^2 T^o}{(\Delta X_c^o)^2}$$

$$\left.\frac{\partial T^o}{\partial \theta^o}\right|_{\substack{X_c^o = j\cdot\Delta X_c^o \\ \theta^o = n\Delta\theta^o}} \approx \frac{T^o_{j,n+1} - T^o_{j,n}}{\Delta\theta^o}$$

the problem of the opaque-cloth-skin system (equations 1.1 - 1.3) can be stated in dimensionless terms as follows:

1. Basic Equations:

(a) For the cloth layer:

$$\frac{\Delta T^o}{\Delta \theta_c^o} = \frac{\Delta^2 T^o}{(\Delta X_c^o)^2} \qquad (1.1)'$$

(b) For the skin simulant:

$$\frac{\Delta T^o}{\Delta \theta_s^o} = \frac{\Delta^2 T^o}{(\Delta X_s^o)^2} \qquad (1.3)'$$

where $\Delta\theta_c^o = \Delta\theta_s^o = \Delta\theta^o$ if the modulus $(\Delta X^o)^2/\Delta\theta^o$ is taken to be the same in both the cloth and skin simulant, which implies that the ratio of space intervals becomes:

$$\frac{\Delta X_c^o}{\Delta X_s^o} = \sqrt{\frac{(kC\rho)_s}{(kC\rho)_c}} = R \qquad (1.9)$$

2. Boundary Conditions:

(a) At the outer surface of the cloth:

$$\left.\frac{\Delta T^o}{\Delta X_c^o}\right|_{X_c^o=0} = -\frac{(1/U_o^o) - (T^o_{X_c^o=0} - T^o_{surr})}{(1/U_o^o)} \qquad (1.4)'$$

(b) At the inner surface of the cloth and the skin surface:

$$-\left.\frac{\Delta T^o}{\Delta X_c^o}\right|_{X_c^o=1} = \frac{T^o_{X_c^o=1} - T^o_{X_s^o=0}}{(1/U_i)} = -\left.\frac{\Delta T^o}{\Delta X_s^o}\right|_{X_s^o=0} \qquad (1.5)'$$

3. Numerical Solution - Modified Schmidt Technique

Cloth and skin simulant are divided into slices of width ΔX_c^o and ΔX_s^o, respectively. The reference planes for temperature are located at the center of the slices and also half a slice beyond the surfaces of the cloth and skin simulant (see Figure 1.2). This convention is known to produce a better approximation to the true solution than taking the surfaces as reference planes (14, 19, 20). A scheme having two cloth slices is used below for demonstration.

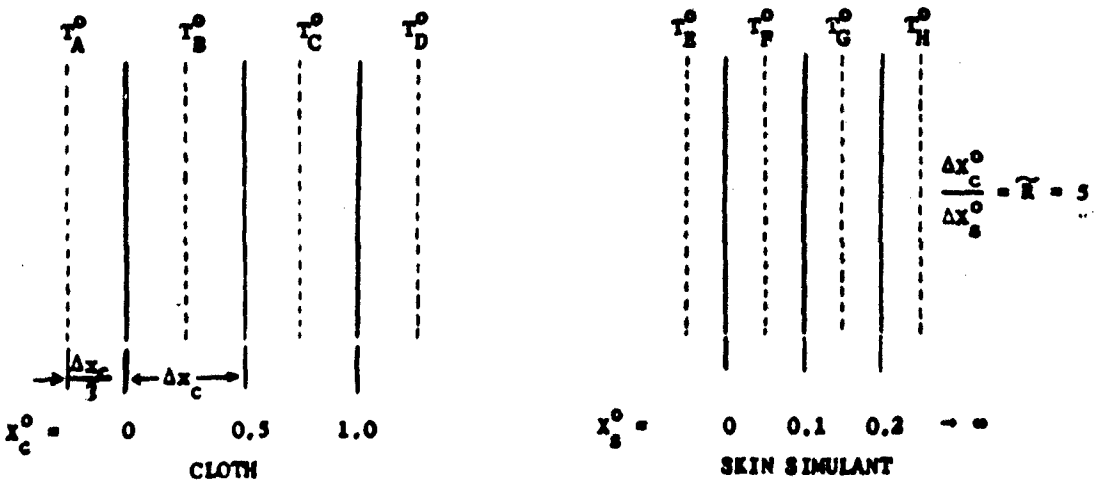

Figure 1.2

The calculation of a temperature distribution starts with the temperature value at plane A, for which the boundary condition (1.4)' can be written as:

$$T_{A,n+1} = \frac{(1/U_o^o) - T_{B,n}^o}{(1/U_o^o) + (\Delta X_c^o/2)} \cdot \Delta X_c^o + T_{B,n}^o \quad \text{(n initially zero)} \qquad (1.4)''$$

where $(T_A^o + T_B^o)/2 = T_{x_c^o=0}^o$ and $T_{surr}^o = 0$. This relation is illustrated by Figure 1.3.

Next, the temperature values inside the cloth are computed according to equation (1)' , which may be written as:

$$(T_{C,n}^o - T_{B,n}^o) - (T_{B,n}^o - T_{A,n}^o) = \frac{(\Delta X_c^o)^2}{\Delta\theta^o} \cdot (T_{B,n+1}^o - T_{B,n}^o)$$

This relation can be simplified considerably if the modulus $(\Delta X_c^o)/\Delta\theta^o$ is taken to be 2, as proposed by Schmidt:

$$T_{B,n+1}^o = \frac{T_{A,n}^o + T_{C,n}^o}{2}$$

or generally,

$$T_{j,n+1}^o = \frac{T_{j-1,n}^o + T_{j+1,n}^o}{2}$$

where j may denote any slice within the cloth. In particular, this formulation allows for a graphical interpretation of the process, (Figure 1.3).

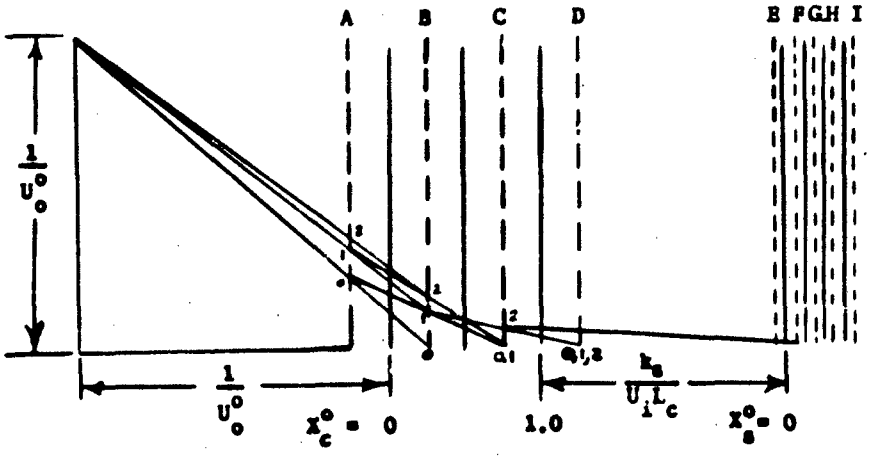

Figure 1.3

At the planes above the inner cloth surface and the skin surface (D and E for the 2-slice model) the temperatures at time n+1 are obtained by means of the boundary condition (1.5)', which in reordered form yields:

$$T^{o}_{D,n+1} = \frac{(T^{o}_{C,n} - T^{o}_{F,n})\ \frac{1}{U^{o}_{i}} + \frac{\Delta X^{o}_{s} - \Delta X^{o}_{c}}{2}}{\frac{1}{U^{o}_{i}} + \frac{\Delta X^{o}_{s} + \Delta X^{o}_{c}}{2}} + T^{o}_{F,n}$$

and similarly (1.5)"

$$T^{o}_{E,n+1} = \frac{(T^{o}_{C,n} - T^{o}_{F,n})\ \Delta X^{o}_{s}}{\frac{1}{U^{o}_{i}} + \frac{\Delta X^{o}_{c}}{2} + \frac{\Delta X^{o}_{s}}{2}} + T^{o}_{F,n}$$

These relations can also be verified graphically if the planes $X^{o}_{c} = 1$ and $X^{o}_{s} = 0$ are separated by a distance $1/U^{o}_{i}$ (Figure 1.4); the temperature distribution throughout the system can then be drawn continuously.

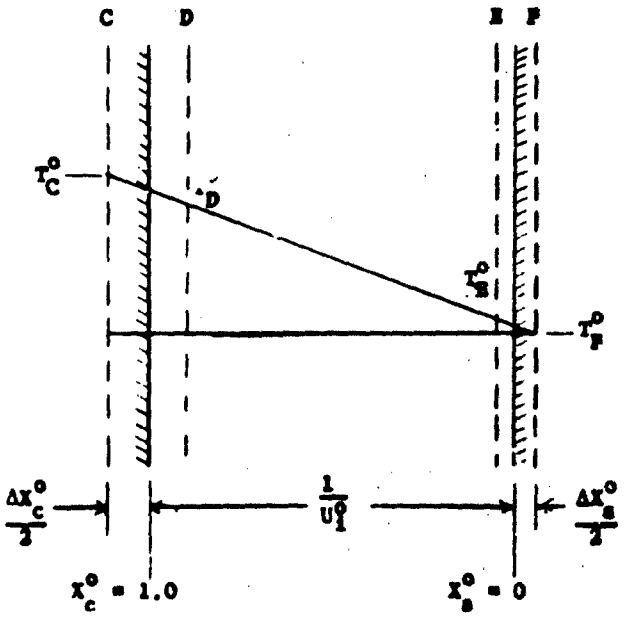

Figure 1.4

The conduction of heat into the interior of the skin is governed by equation (1.3)'. Using the modulus $(\Delta X_s^o)^2/\Delta\theta^o = 2$ for the skin simulant, the same simple formulation is obtained as for the cloth equation:

$$T^o_{j,n+1} = \frac{T^o_{j-1,n} + T^o_{j+1,n}}{2} \qquad (1.3)''$$

It is to be noted here that the method outlined above is a modification of the one originally proposed by Schmidt (19, 20). In applying the boundary condition (1.4), Schmidt's method properly states that at time o, $T_{x_c^o=0} = T^o_{surr} = 0$ at the outer cloth surface. However, in the next step, the calculation of $T^o_{B,1}$, all the space between the planes A and B is implicitly assumed to have the heat capacity of cloth. In the modified technique described, this error is partly compensated for by the assumption (in boundary condition 1.4") of $T^o_{B,o} = T^o_{surr} = 0$ at time 0 and the neglection of heat capacity in the half-slice from the surface to plane B, which leads to a closer approximation to the true solution.

4. Stability and Accuracy

It is known for this particular type of computing algorithm that the solution is both stable and convergent with refinement of the intervals if the modulus is larger than or equal to 2, (18).

Comparitive solutions using the 2- and 6-slice models and a modulus M = 2 (in order to retain the simplicity of the computing scheme) have shown that the accuracy is improved only in the low-time range ($\theta^o \leq 1$, corresponding approximately to $\theta^o \leq 2.5$ sec of real time) by the finer mesh. Therefore the calculations are best started using the 6-slice model and then continued with the 2-slice model.

Further details of the method are described in (4).

B. DIATHERMANOUS CLOTH

1. Basic Equations

The basic equations governing the case of diathermanous cloth can be transformed into the following dimensionless and finite-difference form:

(a) For the cloth layer:

$$\frac{\Delta T^o}{\Delta \theta_c^o} = \frac{\Delta^2 T^o}{(\Delta X_c^o)^2} - \frac{\Delta(e^{-\gamma L_c X_c^o})}{\Delta X_c^o} \qquad (1.2)'$$

(b) For the skin simulant:

(identical with the opaque cloth case)

$$\frac{\Delta T^o}{\Delta \theta_s^o} = \frac{\Delta^2 T^o}{(\Delta X_c^o)^2} \qquad (1.3)'$$

again with $\Delta\theta_c^o = \Delta\theta_s^o = \Delta\theta^o$ and $\Delta X_c^o/\Delta X_s^o = \overline{K}$. Thus the only new term introduced is a heat source $-\frac{\Delta(e^{-\gamma L_c X_c^o})}{\Delta X_c^o}$ at each cloth increment.

In using the finite-difference model, it is assumed that the amount of radiant energy absorbed in the center of each slice of the cloth is distributed according to the Beer-Lambert law. Inspection of this distribution shows this to be justified for cloth of high diathermancy, where the radiant energy decreases nearly linearly across the cloth. With a cloth of low diathermancy, however, the decay of intensity is much stronger near the exposed surface of the cloth. Therefore a better assumption is that the fraction of incident radiation absorbed by the first cloth slice is absorbed at the front surface (analogous to the opaque cloth case).

The boundary condition at the front surface thus appears different according to either assumption.

2. Boundary Condition at the Front Cloth Surface

(a) High diathermancy

$$\left.\frac{\Delta T^o}{\Delta X_c^o}\right]_{X_c^o=0} = U_o^o(T_{x_c^o=0}^o - T_{surr}^o) \qquad (1.6a)'$$

(b) Low diathermancy

$$\left.\frac{\Delta T^o}{\Delta X_c^o}\right]_{X_c^o=0} = -\frac{\frac{1}{U_o^o}(\Delta e^{-\gamma L_c X_c^o}) - (T_{x_c^o=0}^o - T_{surr}^o)}{\frac{1}{U_o^o}} \qquad (1.6b)'$$

Also for low diathermancy, the radiation term disappears from the equation for the first increment:

$$\left.\frac{\Delta T^o}{\Delta \theta^o}\right]_{X_c^o=0} = \frac{\Delta^2 T^o}{(\Delta X_c^o)^2} \qquad (1.2a)'$$

3. Boundary Conditions in the Air Gap

(a) Between the back surface of the cloth and the air gap:

$$-\left.\frac{\Delta T^o}{\Delta X_c^o}\right]_{X_c^o=1} = \frac{T^o_{x_c^o=1} - T^o_{x_s^o=0}}{\frac{1}{U_i^o}} \qquad (1.7a)'$$

(b) Between the air gap and the skin simulant:

$$\left.\frac{\Delta T^o}{\Delta X_s^o}\right]_{X_s^o=0} = -\frac{\frac{1}{U_i^o}(e^{-\gamma L_c}) - (T^o_{x_s^o=0} - T^o_{x_c^o=1})}{\frac{1}{U_i^o}} \qquad (1.7b)'$$

The evaluation of this problem follows the same path as that of the opaque case, except that the independent variable $\frac{\Delta(e^{-\gamma L_c X_c^o})}{\Delta X_c^o}$ has to be evaluated for each cloth increment.

As a consequence, the solution will be specific with respect to the value γL_c.

4. Simplified General Solution for Diathermanous Cloth

Since the system is linear, however, it is in fact possible to arrive at a generalized solution eliminating the need to calculate anew for different diathermancies.

The response to any one intensity can be considered to be the weighted sum of a number of solutions, in each of which a unit of radiant energy is assumed to be absorbed in one particular cloth increment only. The weighting factors to be applied then are the fractions of the incident radiation that are associated with each increment by the given distribution, i.e., $\Delta(e^{-\gamma L_c X_c^o})_j$.

Thus as many basic solutions are required as there are planes in

which absorption is assumed, (which needs not coincide with the number of conceptual slices in the cloth). In particular, a method was proposed in which absorption is taken to occur at three locations only, resulting in three basic curves or solutions:

Curve I represents the case of absorption of a unit of radiant energy at the exposed surface of the cloth, which is equivalent to the opaque cloth solution.

Curve II represents the case of unit absorption at $X_c^o = 0.75$, and

Curve III represents that of absorption at the surface of the skin simulant. For this method, the equations in dinite difference form become:

Curve I: identical with opaque cloth case.

Curve II:

1. For the cloth layer:

(a) Any increment other than that associated with $X_c^o = 0.75$

$$\frac{\Delta T^o}{\Delta \theta^o} = \frac{\Delta^2 T^o}{(\Delta X_c^o)^2} \qquad (1.2a)'$$

(b) The cloth increment whose centerline is at $X_c^o = 0.75$

$$\frac{\Delta T^o}{\Delta \theta^o} = \frac{\Delta^2 T^o}{(\Delta X_c^o)^2} + \frac{1}{\Delta X_c^o} \qquad (1.2b)'$$

2. For the skin simulant:

$$\frac{\Delta T^o}{\Delta \theta^o} = \frac{\Delta^2 T^o}{(\Delta X_s^o)^2} \qquad (1.3)'$$

3. Boundary conditions at the front surface of the cloth:

$$\left.\frac{\Delta T^o}{\Delta X_c^o}\right|_{X_c^o=0} = U_o^o \left(T^o_{X_c^o=0} - T^o_{surr}\right) \qquad (1.6a)'$$

4. Boundary conditions in the air gap:

$$-\frac{\Delta T^o}{\Delta X_c^o}\Bigg]_{X_c^o=1} = U_i^o \left(T^o_{x_c^o=1} - T^o_{x_s^o=0}\right) \qquad (1.7a)'$$

$$= \frac{\Delta T^o}{\Delta X_s^o}\Bigg]_{X_s^o=0} \qquad (1.7b)'$$

Curve III:

1. For all increments of the cloth layer:

$$\frac{\Delta T^o}{\Delta \theta^o} = \frac{\Delta^2 T^o}{(\Delta X_c^o)^2} \qquad (1.2a)'$$

2. For the skin simulant:

$$\frac{\Delta T^o}{\Delta \theta^o} = \frac{\Delta^2 T^o}{(\Delta X_s^o)^2} \qquad (1.3)'$$

3. Boundary condition at the front surface of the cloth:

$$\frac{\Delta T^o}{\Delta X_c^o}\Bigg]_{X_c^o=0} = U_o^o\left(T^o_{x_c^o=0} - T^o_{surr}\right) \qquad (1.6a)'$$

4. Boundary conditions at the air gap:

(a) Between the back surface of the cloth and the air gap:

$$-\frac{\Delta T^o}{\Delta X_c^o}\Bigg]_{X_c^o=1} = U_i^o \left(T^o_{x_c^o=1} - T^o_{x_s^o=0}\right) \qquad (1.7a)'$$

(b) Between the air gap and the surface of the skin simulant:

$$-\frac{\Delta T^o}{\Delta X_s^o}\Bigg]_{X_s^o=0} = \frac{\frac{1}{U_i^o}\left(T^o_{x_s^o=0} - T^o_{x_c^o=1}\right)}{\frac{1}{U_i^o}} \qquad (1.7b)'$$

The total response resulting from any particular diathermancy can be obtained from contributions of the three curves by applying to them a weighting factor according to the fractions of radiant energy absorbed at the three discrete locations:

$$T^{o}_{\gamma L} = \left[e^{-\gamma L_c X^{o}_c}\right]^{X^{o}_c = \infty}_{X^{o}_c = 0.5} \cdot T^{o}_{I} + \left[e^{-\gamma L_c X^{o}_c}\right]^{X^{o}_c = 0.5}_{X^{o}_c = 1.0} \cdot T^{o}_{II}$$

$$+ \left[e^{-\gamma L_c X^{o}_c}\right]^{X^{o}_c = 1.0}_{X^{o}_c = \infty} \cdot T^{o}_{III} \qquad (1.9)$$

A solution in which radiant energy is assumed to be absorbed in each cloth slice (according to equation 2') can be expected to be more accurate, than the scheme described above. Calculations of such a solution for the 6-slice model, however, have shown that the gain in accuracy is in fact small and would not justify the increase in computing effort over that required by the general three-curve solution method.

APPENDIX C

SOLUTION ALGORITHM - MOIST CLOTH - SKIN SIMULANT SYSTEM

In the following description the cloth is assumed to be conceptually divided into six slices of width ΔX_c^o and the skin is assumed to have an infinite number of slices ΔX_s^o (Figure 2.1).

The T^o- and P^o values associated with these are taken at their mid-points. Points 1, 8 and 9 are located above the cloth and skin surfaces at distances $\Delta X_c^o/2$ and $\Delta X_s^o/2$, respectively.

With the derivatives written out and the unknowns separated to the left hand sides, the equations governing the four phases of the alternating solution scheme are:

$$\bar{A}\, T^o_{j-1,n+1} - (2\bar{A} + M_A)T^o_{j,n+1} + \bar{A}\, T^o_{j+1,n+1} =$$

$$- \bar{B}(P^o_{j-1,n} - 2P^o_{j,n} + P^o_{j+1,n}) - M_A \cdot T^o_{j,n} \qquad (2.14)$$

$$\bar{D}\, P^o_{j-1,n+1} - (2\bar{D} + M_A)\, P^o_{j,n+1} + \bar{D}\, P^o_{j+1,n+1} =$$

$$- \bar{C}(T^o_{j-1,n+1} - 2T^o_{j,n+1} + T^o_{j+1,n+1}) - M_A P^o_{j,n} \qquad (2.15)$$

$$\bar{D}\, P^o_{j-1,n+2} - (2\bar{D} + M_A)P^o_{j,n+2} + \bar{D}P^o_{j+1,n+2} =$$

$$- \bar{C}(T^o_{j-1,n+1} - 2T^o_{j,n+1} + T^o_{j+1,n+1}) - M_A P^o_{j,n+1} \qquad (2.16)$$

$$\bar{A}\, T^o_{j-1,n+2} - (2\bar{A} + M_A)T^o_{j,n+2} + \bar{A}T^o_{j+1,n+2} =$$

$$- \bar{B}(P^o_{j-1,n+2} - 2P^o_{j,n+2} + P^o_{j+1,n+2}) - M_A \cdot T^o_{j,n+1} \qquad (2.17)$$

$$\bar{A} = 1$$

Both skin and cloth are treated in the same calculating system, such that equations (2.15) and (2.16) are only evaluated for points j in the cloth. Whenever in equations (2.14) and 2.17) j denotes a point in the skin, the pressure term is dropped and the space interval ΔX_c^o replaced by ΔX_s^o.

As an example, the first phase of the alternating solution scheme shall be described. Equation 2.14 is applied to the entire set of points in the cloth, which is verified identically by lines 2 ... 6 of the system Figure 2.5. At the cloth and skin surfaces, the boundary conditions are to be taken into account. Thus as j = 1, the unknown $T^o_{1,n+1}$ is temporarily substituted by means of $T^o_{2,n+1}$ and the boundary condition 2.7"

$$1 - U_o^o \, (T^o_{X_c^o=0}) = \left.\frac{\Delta T^o}{\Delta X_c^o}\right|_{X_c^o=0}$$

equivalent to

$$T^o_{1,n+1} = \frac{2\Delta X_c^o}{2 + U_o^o \Delta X_c^o} + \frac{U_o^o \Delta X_c^o - 2}{U_o^o \Delta X_c^o + 2} \cdot T^o_{2,n+1} \qquad (2.7a)"$$

which modifies both the left and right hand sides of the first equation (line 0 → line 1 in Figure 2.5).

The temperatures $T^o_{7,n+1}$ ... $T^o_{10,n+1}$ near the surfaces confining the air gap are related through boundary condition (2.9)", which can be written as,

$$T^o_{8,n+1} = \frac{(T_{7,n+1} - T_{10,n+1})\left[\frac{1}{U_i^o} + \frac{\Delta X_s^o - \Delta X_c^o}{2}\right] + \frac{\Delta X_c^o \, \Delta X_s^o}{2} K_i' \left[\frac{P_7^o + P_8^o}{2} - P_9^o\right]}{\frac{1}{U_i^o} + \frac{\Delta X_s^o + \Delta X_c^o}{2}} \qquad (2.9a)"$$

as well as

$$T^o_{9,n+1} = \frac{(T_{7,n+1} - T_{10,n+1})\Delta X_s^o + \left[\frac{\Delta X_c^o \, \Delta X_s^o}{2} + \frac{\Delta X_s^o}{U_i^o}\right] K_i' \left[\frac{P_7^o + P_8^o}{2} + P_9^o\right]}{\frac{1}{U_i^o} + \frac{\Delta X_s^o + \Delta X_c^o}{2}} + T_{10,n+1} \qquad (2.9b)"$$

After reordering, these relations match the general scheme applied in the

system (Figure 2.5) and form lines 7 and 8.

Last, equation (2.4a)" is applied to all of the points in the skin, which is considered semi-infinite. At the start, i.e., at time zero, the equations are written down for a small, arbitrary number of points in the skin, since initially $T^c_{skin} = 0$. In this way, a tridiagonal system of equations is formed. The expressions for all of the coefficients appearing in the middle diagonal and for the right hand sides are listed in Figure 2.5.

Next, the system is solved by successive elimination. Dividing the first equation by a factor $v_1 = \beta_1$ and adding to the second equation, one obtains:

$$\underbrace{-(\beta_2 - (1/v_1))}_{v_2} \cdot T^o_{3,n+1} + T^o_{4,n+1}$$

$$= -((w_1/v_1) + \varphi_2) = -w_2$$

Dividing this by $v_2 = (\beta_2 - 1/v_1)$ and adding to the third yields,

$$\underbrace{-(\beta_3 - 1/v_2)}_{v_3} \cdot T^o_{4,n+1} + T^o_{5,n+1}$$

$$\cdot \cdot ((w_2/v_2) + \varphi_3) = -w_3$$

etc.

This elimination scheme, carried throughout the system, results in a bidiagonal set of equations (Figure 2.6), the coefficients and right hand sides of which follow the relations:

$$v_1 = \beta_1$$

$$v_i = \beta_{i-1}/v_{i-1}, \; i = 2 \ldots 6, 9 \ldots$$

$$w_1 = \varphi_1$$

$$w_i = w_{i-1}/v_{i-1}, \; i = 2 \ldots 6, 9 \ldots$$

Equations (2.9a)" and (2.9b)" are brought to match the bidiagonal pattern

by means of a linear combination of the 6th, 7th, and 8th lines, resulting in

$$v_7 = \frac{(v_6 Q - 1)(1 - S) + (1 - Q)}{v_6 S(1 - Q)}$$

$$v_8 = \frac{v_6 v_7 S - 1}{v_6 v_7 (S - 1)}$$

$$w_7 = \frac{w_6(Q - S) + v_6\left[(1 - S)QH - (1 - Q)SR\right]}{v_6 S(1 - Q)}$$

$$w_8 = \frac{w_6 + v_6 SR\left[\frac{P_7^o + P_8^o}{2} - P_9^o\right] + w_7/v_7}{v_6(S - 1)}$$

where

$$Q = \frac{(2/U_i^o) + \Delta X_s^o + \Delta X_c^o}{(2/U_i^o) + \Delta X_s^o - \Delta X_c^o}$$

$$S = \frac{(1/U_i^o) + (\Delta X_c^o + \Delta X_s^o)/2}{\Delta X_s^o}$$

$$QH = \frac{\Delta X_c^o \Delta X_s^o}{(2/U_i^o) + \Delta X_s^o - \Delta X_c^o} \cdot K_i^o$$

$$SR = (\Delta X_c^o/2 + 1/U_i^o) K_i^o$$

The bidiagonal system is solved by backward substitution, yielding the future time temperature values $T^o_{j,n+1}$. Starting with the last equation, in the interior of the skin, we get

$$T^o_{M+1,n+1} = T^o_{M+2,n+1} + w_M/v_M$$

$$T^o_{M,n+1} = T^o_{M+1,n+1} + w_{M-1}/v_{M-1}$$

$$\vdots \qquad \vdots \qquad \vdots$$

$$T^o_{j,n+1} = T^o_{j+1,n+1} + w_{j-1}/v_{j-1}$$

until $j = 2$. $T^{o}_{j,n+1}$ results from the boundary condition (2.7)". At the point M+2 in the skin simulant, the temperature is zero. After each time step, the number of points M and thus the size of the equation system is increased by one, accounting for the propagation of the temperature profile into the skin simulant.

The three remaining phases of the alternating scheme (2.12), namely those based on equations (2.15 - 2.17), in principle follow the same path as outlined above. In treating the implicit evaluation of future time pressures, the elimination of $P^{o}_{1,n+1}$ is done by means of the boundary condition (2.8)". The boundary condition (2.9)" for the pressure in the air gap enters into the 7th equation of the tridiagonal system, which has a constant size corresponding to the number of cloth slices.

APPENDIX D

MASS AND HEAT BALANCE - MOIST CLOTH - SKIN SIMULANT SYSTEM

A means of testing the internal consistency of the computation is provided by the indication of the (cumulative) amounts of moisture lost due to evaporation at the front surface of the cloth and condensation at the skin simulant surface.

A mass balance can be set up as follows:

$$M_{evaporation} + M_{condensation} + M_{cloth,\ final} = M_{cloth,\ initial}$$

From equation (2.6)" follows:

$$M_{evap} = K_o \Delta\theta \sum_n \left[\frac{p_1 + p_2}{2}\right]$$

The sum of the surface pressure values, taken over all n past time steps, is recorded as

$$\text{"SURF LOSS"} = \sum_n \left[\frac{p_1^o + p_2^o}{2}\right]$$

with $\Delta\theta = \Delta\theta^o \cdot (L^2\rho C/k)_c$ .n: $M_A = (\Delta x_c^o)^2/\Delta\theta^o$, the surface loss of moisture is

$$M_{evap} = P_o K_o \cdot \frac{M_A}{(\Delta x_c^o)^2} \cdot (L^2\rho C/k)_c \cdot (\text{SURF LOSS})\ (\mu gm H_2O/cm^2) \qquad (5.1a)$$

The moisture flux through the inner cloth surface is given by:

$$\text{moisture flux}_{(air\ gap)} = K_i' \cdot \left[\frac{p_7 + p_8}{2} - p_9\right] \qquad (5.2)$$

(taking the 6-slice model as an example)

The program evaluates

$$\text{"COND"} = \sum \left[\frac{p_7^o + p_8^o}{2} - p_9^o\right]$$

Thus the total amount of moisture condensed is given by

$$M_{cond} = P_o K_i' \cdot \frac{M_A}{(\Delta X_c^o)^2} \cdot (L^2 \rho C/k)_c \cdot (COND) \quad (\mu gm H_2O/cm^2) \qquad (5.2a)$$

The remaining moisture content of the cloth is constructed as

$$M_{cloth,\ final} = \rho_c L_c \sum_{i=1}^{I} M_{(T_i, P_i)} \quad (\mu gm H_2O/cm^2) \qquad (5.3)$$

(i counting the number of cloth slices)

A heat balance may also be established; however, the integrals required (over the surface temperature gradients and over the enthalpy fluxes due to moisture evaporation) are not evaluated by the program and would have to be calculated from the printed results.

APPENDIX B

COMPUTER PROGRAM DESCRIPTION

A. FUNCTION OF MAIN- AND SUBPROGRAMS

The MAIN-program and subroutines are written in FORTRAN - and FAP-language and can be run at any IBM 709 - installation (16K or 32K) under FMS control. The explicit subroutines are:

SUBP
DOUBIN
DTAB, TAB
PULSE
TARA
CHANGE
F2PM

All other subroutines are FMS 709 library programs.

1. MAIN Program

The flow of control is shown in Figure 2.7.

Any number of data sets can be handled in one run.

First, the equilibrium data for cloth are read in, to be used for all data sets.

Next, a set of data is read. The calculation starts with the determination of the relative irradiation intensity followed by phase (a) of the alternating scheme (2.12), which establishes the distribution of temperatures. Based on the new temperature values, the variable coefficients C and D of equation (2.5)' are found by interpolation of the tabulated data.

Hereafter, phase (b) is solved for the pressure profile, assuming that the boundary condition (2.6)' is valid, which implies condensation of moisture on the skin surface. A test for this condition follows. If it shows no condensation, the pressure calculation is repeated assuming

this subroutine determines the relative irradiation intensity $I_{o(\theta^o)}/I_{omax}$ and records it.

5. PARA

The input parameters pertaining to irradiation intensity and pulse shape are interpreted and printed in dimensionless and absolute terms.

6. ERG

This subroutine computes, at the end of a run, the total irradiation energy received in the cases of a step function or a thermonuclear pulse, (equations of Table 2.1).

7. CHANGE

With CALL CHANGE(1), the purpose of this subprogram is threefold:

1. To record the number of dry cloth slices.

2. Optional: to determine the maximum of the heat content of the skin above a given critical temperature level, attained at any time (equation 4.1).

3. Optional: to vary the size of time steps at prescribed dimensionless times by means of altering the modulus M_A. Any number of such changes is possible. The use of this procedure lies in the facility to reduce the time step size near the end of a square wave of irradiation, and to increase it at a later time again. - Any new value for M_A must be a multiple of the original one. The functions 2 and 3 are only activated by special data cards.

B. MACHINE TIME CONSUMPTION

The amount of machine time used per time step depends mainly on the number of cloth slices, since the determination of pressure profiles requires most of the work. The approximate expense of computer time is given below:

No. of Cloth Slices	Machine Time / Double Time Step (Sec.)
2	> 2
6	2 - 2.6
18	4 - 5

Using the 6-slice model with a modulus $M_A = 5.0$, a double time step is $2\Delta\theta^\circ = 0.0111$, which corresponds to $2\Delta\theta = 0.0272$ sec (with $\theta/\theta^\circ = (L^2\rho C/k)_c = 2.45$). The ratio of the machine time scale to the real time scale is,

$$\frac{\text{machine time}}{\text{real time}} \approx 70 - 95$$

in other words, a second of real time requires 1.2 - 1.6 minutes of computer time.

Table E.1

COMPUTER PROGRAM LISTING MOIST CLOTH - SKIN SIMULANT SYSTEM

```
C     TRANSIENT HEAT AND MOISTURE TRANSFER TO SKIN                       MAI[illegible]
C     THROUGH THERMALLY IRRADIATED CLOTH.                                 [illegible]
C     709-VERSION FOR VARIABLE IRRADIATION INTENSITY.                     [illegible]
C     SUBROUTINES ARE, SUMP, DOUBIN,DTAB,TAB,PARA,PULSE,ERG,CHANGE.       [illegible]
C     FURTHER SUBROUTINES ON FORTRAN MONITOR SYSTEM LIBRARY TAPE.         [illegible]
C     AUGUST 1961. G.MIEDEL.                                              MA[illegible]005
C     ALTERNATE IMPLICIT T AND P SOLUTION                                 MA[illegible]006
 900  DIMENSION ALPH(1000),AA(18),T(1000),TA(1000),P(21),PA(21),          MAIN0007
     1BETA(1000),CMC(18),CMD(18),COFC(18),COFD(18),GAM(18),GAMA(19),      MAIN0008
     2DELT(19),CC(18),DVP(18),F(3),TB(3),                                 MAIN0009
     3[illegible](13),TEMP(10),PRES(10,12),DPT(10,12),OMP(10,12)          MAIN0010
 901  COMMON TEMP,PRES,DPT,OMP,T,TA,ALPH,BETA,P,PA,AA,CC,GAM,GAMA,DELT,   MAIN0011
     1CMC,CAD,COFC,COFD,F,TB,ALPO,ALPS,ALP,SUM2,EVAP,DV,DVP,CIO,CLK,CAP,MAIN0012
     2DVC,CHA,U0,U0,DD,SS,CON1,SR,OM,E,PSURR,ZETA,TSURR,TIME,CRIT,FA,     MAIN0013
     3TYP,ID,M,LA,J,MA,L,NX,NY,NTA,NTB,NTC,NAC,NXA,NXB,MXA,MXB,NXC,       MAIN0014
     4KPULSE,TCHAR,TOYM,ENDMND,ENDCAD,TOIS,NSTEP,TAUDIM,                  MAIN0015

     5SHAPET,CKO,NS,XC,DVRED,CKORED,CKIRED,RM,XS,CRITT,CKI,CON,UI,UO,     MAIN0016
     6CONA,ENERGO,ENERGA,ENDDMA,ENDCSA,TENDAB,TENDCH,TEND,TPEND,ANSTEP    MAIN0017
      COMMON PFACT,FMXA                                                   MAIN0018
C     FORMAT STATEMENTS                                                   MAIN0019
 500  FORMAT(7HOTIME    ,F8.4/34H TEMPERATURE IN CLOTH AND SKIN    ,12F7, MAIN0020
     14/34H                             ,12F7.4/8H SKIN    ,16F7.4/       MAIN0021
     210H PRESSURE ,21F5.2/ 11H SURF LOSS=,F10.4,8H   COND=,F10.4/ 4H C  MAIN0022
     3 18F6.3/ 4H D  18F6.3)                                              MAIN0023
 501  FORMAT (7F10.4)                                                     MAIN0024
 502  FORMAT (415)                                                        MAIN0025
 503  FORMAT(1H1, 98HTRANSIENT HEAT AND MOISTURE TRANSFER TO SKIN THROUGMAIN0026
     CH THERMALLY IRRADIATED CLOTH.N.Y.CMER-G.MIEDEL.)                    MAIN0027
C                                                                         MAIN0028
 504  FORMAT(1H0,8HUO      =,F9.4/9H UI      =,F9.4/9H DV*10  =,F9.4      MAIN0029
     1/9H KO*10  =,F9.4/9H KI*10  =,F9.4/9H PSURR  =,F9.4/9H TSURR  =,    MAIN0030
     2F9.4/9H CHA    =,F9.4/9H KC     =,F9.4/9H XS     =,F9.4/9H TAUDIM MAIN0031
     3=, F9.4/9H CRIT   =,F9.4/9H CLK    =,F9.4/9H CAP    =,F9.4/9H NXC  MAIN0031
     4   =,I4/9H NSTEP  =,I4)                                             MAIN0031
 506  FORMAT(10F5.1)                                                      MAIN0032
 507  FORMAT(12F6.4)                                                      MAIN0033
 512  FORMAT (I1,F9.4,2F10.4)                                             MAIN0034
C     ONCE FOR ALL PREPARATORY                                            MAIN0035
      READ 506,(TEMP(I),I=1,10)                                           MAIN0036
      READ 507,((PRES(I,J),J=1,12),I=1,10)                                MAIN0037
      READ 507,((DPT(I,J),J=1,12),I=1,10)                                 MAIN0038
      READ 507,((OMP(I,J),J=1,12),I=1,10)                                 MAIN0039
 902  DO 903 I=1,1000                                                     MAIN0040
      TA(I)=0                                                             MAIN0041
 903  T(I)=0                                                              MAIN0042
      DO 904 I=1,21                                                       MAIN0043
      P(I)=0                                                              MAIN0044
 904  PA(I)=0                                                             MAIN0045
      DD=0                                                                MAIN0046
      SS=0                                                                MAIN0047
      CON1=0                                                              MAIN0048
      TIME=0                                                              MAIN0049
      SUM2=0                                                              MAIN0050
      EVAP=0                                                              MAIN0051
      RI=0                                                                MAIN0052
      RS=0                                                                MAIN0053
      NXC=0                                                               MAIN0054
C     NXC CAN BE TAKEN [illegible] OR 18                                  MAIN0055
 1    READ 501,UO,UI,DVRE[illegible] RED,CKORED,PSURR,TSURR               MAIN0056
C     TERMINATE ON BLANK CARD                                             MAIN0057
      IF (UO)9999,9999,9998                                               MAIN0058
 9999 CALL EXIT                                                           MAIN0059
 9998 READ 501,CRIT,CLK,CAP,CHA,XC,XS,TAUDIM                              MAIN0060
      READ 502,NSTEP,ID,NY,NXC                                            MAIN0061
C     IRRADIATION PULSE DATA                                              MAIN0062
      READ 512,KPULSE,CIO,TCHAR,SHAPET                                    MAIN0063
C                                                                         MAIN0064
C     OBTAIN CONSTANTS DEPENDING ON MAX. RADIATION                        MAIN0065
      DV=DVRED/CIO                                                        MAIN0066
      CKI=CKIRED/CIO                                                      MAIN0067
      CKO=CKORED/CIO                                                      MAIN0068
      TOYM=1.                                                             MAIN0069
C                                                                         MAIN0070
      NTA =NXC/2                                                          MAIN0071
      NTC = ((30*XC)/2+7)/2                                               MAIN0072
      NTB = 15*NTA*NTC                                                    MAIN0073
      NXB =NXC-1                                                          MAIN0074
      NXA = NXC+3                                                         MAIN0075
      MXA =1                                                              MAIN0076
      MXB=NXA+1                                                           MAIN0077
      N=NXC+13                                                            MAIN0078
      CRITT=(453. - TSURR)/(C.K*CIO)                                      MAIN0079
      CONA = UO*XC                                                        MAIN0080
      FA = (2.-CONA)/(2.+CONA)                                            MAIN0081
      ALP=CHA+2.                                                          MAIN0082
      ALPO=1.+(2.*UI*XC)/(2.+(XS-XC)*UI)                                  MAIN0083
      ALPS=(1./UI+(XC+XS)+.5)/XS                                          MAIN0084
      ALPH(1) = ALP    -FA                                                MAIN0085
      DO 9 I=2,NXC                                                        MAIN0086
 9    ALPH(I)=ALP-1./ALPH(I-1)                                            MAIN0087
      ALPH(NXC+1)=((ALPH(NXC)*ALPO-1.)*(1.-ALPS)+(1.-ALPO))/(ALPS*ALPH(NMAIN0088
     1XC)*(1.-ALPO))                                                      MAIN0089
      ALPH(NXC+2)=(ALPH(NXC+1)*(ALPS*ALPH(NXC)-1.)/(ALPH(NXC+1)*ALPH(NXA  MAIN0090
     1C)*(ALPS-1.))                                                       MAIN0091
      CON=2./UI+XS-XC                                                     MAIN0092
      OM=(XC/CON)*XS*CKI                                                  MAIN0093
      SR=(XC*UI+2.)*CKI/2./UI                                             MAIN0094
      ZETA=XC*XC/CHA                                                      MAIN0095
 301  PRINT 503                                                           MAIN0096
      PRINT 504,UO,UI,DVRED,CKORED,CKIRED,PSURR,TSURR,CHA,XC,XS,TAUDIM,   MAIN0097
     1CRIT,CLK,CAP,NXC,NSTEP                                              MAIN0098
C                                                                         MAIN0099
C     DIMENSIONAL CONVERSION AND DATA PRINTOUT                            MAIN0100
```

```
      CALL PARA                                                         MAIN0101
      W=(2.*DV-CKI*XC)/(2.*DV+CKI*XC)                                   MAIN0102
 1803 DVC=CLK/CAP*C10/1000.                                             MAIN0103
C     IMPLICIT T EXPLICIT P SOLUTON, KNOWN TA PA                        MAIN0104
C     HERE FOR NEW TIME STEP                                            MAIN0105
 4005 GO TO (4001,4000,4000,4000),KPULSE                                MAIN0106
C     PROVIDES NEW VALUE FOR YOTM=INTENS./MAX.INTENSITY                 MAIN0107
 4000 CALL PULSE                                                        MAIN0108
C     SET IRRADIATION BOUNDARY CONDITION                                MAIN0109
 4001 E=2.*YOTM*XC/(2.*CONA)                                            MAIN0110
C     OPTIONAL DIFFUSIVITY CALC                                         MAIN0111
      GO TO (802,805),ID                                                MAIN0112
 802  DO 803 I=1,MXC                                                    MAIN0113
 803  DVP(I)=DV                                                         MAIN0114
      GO TO 21                                                          MAIN0115
 805  DO 806 I=1,MXC                                                    MAIN0116
 806  DVP(I)=DV*265.38/(.76-PA(I+1)-PSURR/1000.)/(TA(I+1)*C10*CLK+TSURR)MAIN0117
 21   DO 22 I=1,MXC                                                     MAIN0118
 22   AA(I)=DVP(I)*(PA(I)+PA(I+2)-2.*PA(I+1)) +CHA*TA(I+1)              MAIN0119
C     DRY IF TEMP IS ABOVE 180 C                                        MAIN0120
      MXA=1                                                             MAIN0121
      MXB=MXA+1                                                         MAINA121
      MXC=MXA-1                                                         MAIN0121
      DO 2206 I=1,MXC                                                   MAIN0122
      IF(T(I+1)-CRITT) 2203,2205,2205                                   MAIN0123
 2203 RH=(P(I+1)*1000.+PSURR)/(EXPF(-4860.975/(C10*CLK*T(I+1)+TSURR)   MAIN0124
     1+19.64787))                                                       MAIN0125
      IF(RH-.05) 2205,2205,2206                                         MAIN0126
 2205 AA(I)=CHA*TA(I+1)                                                 MAIN0127
      MXC=MXA                                                           MAIN0128
      MXA=MXA+1                                                         MAIN0129
      MXB=MXA+1                                                         MAIN0130
      IF(MXC-MXC) 2206,110,110                                          MAIN0131
 2206 CONTINUE                                                          MAIN0132
C     CHECK P GRADIENT IN AIR SPACE                                     MAIN0133
      IF (QG) 24,24,31                                                  MAIN0134
 24   IF (SUM2)25,25,31                                                 MAIN0135
C     NO CONDENSATION ON SKIN                                           MAIN0136
 25   SUM2=0.                                                           MAIN0137
      QQ=0.                                                             MAIN0138
      SS=0.                                                             MAIN0139
      GO TO 40                                                          MAIN0140
C     CONDENSATION ON SKIN                                              MAIN0141
 31   QQ=QN*CON1                                                        MAIN0142
      SS=SR*CON1                                                        MAIN0143
      SUM2=SUM2+CON1                                                    MAIN0144
C     CALCULATE T (IMPLICIT SOLUTION)                                   MAIN0145
 40   BETA(1) =E+AA(1)                                                  MAIN0146
      DO 42 I=2,MXC                                                     MAIN0147
 42   BETA(I)=BETA(I-1)/ALPH(I-1)+AA(I)                                 MAIN0148
      BETA(MXC+1)=(BETA(MXC)*(ALPO-ALPS)+ALPH(MXC)*((1.-ALPS)*QQ-(1.-ALPMAIN0149
     1O)*SS))/(ALPS*ALPH(MXC)*(1.-ALPO))                                MAIN0150
      BETA(MXC+2)=(ALPH(MXC)*SS+BETA(MXC)+BETA(MXC+1)/ALPH(MXC+1))/(ALPHMAIN0151
     1(MXC)*(ALPS-1.))                                                  MAIN0152
      DO 50 I=MXA,N                                                     MAIN0153
      ALPH(I)=ALP-1./ALPH(I-1)                                          MAIN0154
 50   BETA(I)=BETA(I-1)/ALPH(I-1) + CHA*TA(I+1)                         MAIN0155
      NN=N+1                                                            MAIN0156
      LA =N-2                                                           MAIN0157
      DO 55 I=0,LA                                                      MAIN0158
      J=N-I                                                             MAIN0159
 55   T(J)=(T(J+1)+BETA(J-1))/ALPH(J-1)                                 MAIN0160
      T(1)=E+FA*T(2)                                                    MAIN0161
      TVP=(T(MXC+3)+(    C- 110.5                                       MAIN0162
C     IMPLICIT T CALC CO LETED                                          MAIN0163
C     PREPARATORY FOR P CALC                                            MAIN0164
C     CALL DOUBLE INTERPOLATION SUBPROGRAM                              MAIN0165
 57   DO 63 I=MXA,MXC                                                   MAIN0166
 51   CALL DOUBIN(TA(I+1),PA(I+1),GPT,COFD(I))                          MAIN0167
      CMD(I)=C10*CLK/1000.*COFD(I)                                      MAIN0168
 52   CALL DOUBIN(TA(I+1),PA (I+1),DMP,COFC(I))                         MAIN0169
      CMC(I)=(DVP(I)*DVC)*(1000./COFC(I)+CAP*COFD(I))                   MAIN0170
      GAM(I)=2.+CMA/CMC(I)                                              MAIN0171
 63   CC(I)=(T(I)+T(I+2)-2.*T(I+1))*CMD(I)/CMC(I)+CMA/CMC(I)*PA(I+1)    MAIN0172
      GO TO 68                                                          MAIN0173
C     NO CONDENSATION                                                   MAIN0174
 68   GAMA(MXA)=GAM( MXA)-G                                             MAIN0175
      IF(MXC-2) 70,70,66                                                MAIN0176
 66   DO 69 I=MXB,MX9                                                   MAIN0177
 69   GAMA(I)=GAM(I)-1./GAMA(I-1)                                       MAIN0178
 70   GAMA(MXC)=GAM(MXC)-1.-1./GAMA(MXC-1)                              MAIN0179
      DELT(MXA)=CC(MXA)                                                 MAIN0180
      DO 75 I=MXB,MXC                                                   MAIN0181
 75   DELT(I)=CC(I)+DELT(I-1)/GAMA(I 1)                                 MAIN0182
      P(MXC+1)=DELT(MXC)/GAMA(MXC)                                      MAIN0183
      P(MXC+2)=P(MXC+1)                                                 MAIN0184
      DO 78 I=MXA,MX8                                                   MAIN0185
      J=MXC-I+MXC                                                       MAIN0186
 78   P(J+1)=(DELT(J)+P(J+2))/GAMA(J)                                   MAIN0187
      P(1)=G*P(MXB)                                                     MAIN0188
C     INTERPOLATE PRESSURE PROFILE IN DRY SLICES                        MAIN0189
      IF(MXA-1) 60,60,61                                                MAIN0190
 61   PFACT=(P(MXB)-P(1))/FMXA                                          MAIN0191
      DO 62 I=2,MXA                                                     MAIN0192
      FI=I                                                              MAIN0193
 62   P(I)=P(1)+(FI-1.)*PFACT                                           MAIN0194
 60   GO TO 100                                                         MAIN0195
 80   P(MXC+3)=(EXPF(-4860.975/(C10*CLK*TVP+TSURR)+19.64787)-PSURR)     MAIN0196
     1/1000.                                                            MAIN0197
C     CONDENSATION ON SKIN                                              MAIN0198
 83   WP=(1.-V)*P(MXC+3)/W                                              MAIN0199
      FMXA=MXA                                                          MAIN0200
      S=(2.*DV-CKO*XC)/(2.*DV+(2.*FMXA-1.)*CKO*XC)                      MAIN0201
```

```
      GAMA(MXA)=GAM(MXA)-G                                              MAIN0202
      DO 86 I=MXB,NXC                                                   MAIN0203
 86   GAMA(I)=GAM(I)-1./GAMA(I-1)                                       MAIN0204
      GAMA(NXC+1)=1./W-1./GAMA(NXC)                                     MAIN0205
      DELT(MXA)=CC(MXA)                                                 MAIN0206
      DO 90 I=MXB,NXC                                                   MAIN0207
 90   DELT(I)=DELT(I-1)/GAMA(I-1)+CC(I)                                 MAIN0208
      DELT(NXC+1)=DELT(NXC)/GAMA(NXC)+WW                                MAIN0209
      P(NXC+2)=DELT(NXC+1)/GAMA(NXC+1)                                  MAIN0210
      DO 95 I=MXA,NXC                                                   MAIN0211
      J=NXC-I+MXA                                                       MAIN0212
 95   P(J+2)=(DELT(J+1)+P(J+3))/GAMA(J+1)                               MAIN0213
      P(1)=G*P(MXB)                                                     MAIN0214
      IF(MXA-1) 92,92,93                                                MAIN0215
C     INTERPOLATE PRESSURE PROFILE IN DRY SLICES                        MAIN0216
 93   PFACT=(P(MXB)-P(1))/FMXA                                          MAIN0217
      DO 94 I=2,MXA                                                     MAIN0218
      FI=I                                                              MAIN0219
 94   P(I)=P(1)+(FI-1.)*PFACT                                           MAIN0220
 92   COM1=(P(NXC+2)+P(NXC+1))*.5-P(NXC+3)                              MAIN0221
      IF (COM1) 96,96,100                                               MAIN0222
 96   IF (SUM2) 65,65,100                                               MAIN0223
C     P CALC COMPLETED, MOVE T TO TA, P TO PA                           MAIN0224
 100  MA=M+1                                                            MAIN0225
      DO 102 I=1,MA                                                     MAIN0226
 102  TA(I)=T(I)                                                        MAIN0227
      DO 105 I=1,NXA                                                    MAIN0228
 105  PA(I)=P(I)                                                        MAIN0229
      EVAP =(P(1)+P(2))*.5 +EVAP                                        MAIN0230
C     PRINT OUT FOR MAIN PROGRAM                                        MAIN0231
      TIME=TIME+ZETA                                                    MAIN0232
C     RECORD DRY CLOTH SLICES, INTEGRATE MAX. CRIT. HEAT CONTENT OF SKINMAIN0233
C     CHANGE MODULUS AND TIME STEP IF PRESCRIBED                        MAIN0234
      CALL CHANGE(1)                                                    MAIN0235
      NX=NX+1                                                           MAIN0236
      IF (NY-NX) 116,116,115                                            MAIN0237
 116  PRINT 500,TIME,(T(N),N=1,26),(T(N),N=NTC,NTE,NTA),                MAIN0238
     1(P(N),N=1,21),EVAP,SUM2,(CMC(N),N=1,18),(CMD(N),N=1,18)           MAIN0239
      NX=0                                                              MAIN0240
 115  CALL SUBP                                                         MAIN0241
      NS=NS+1                                                           MAIN0242
      IF(NS-NSTEP) 4005,4005,119                                        MAIN0243
C     INDICATE END IF DRY-OUT                                           MAIN0244
 118  AS=STEP                                                           MAIN0245
      CALL CHANGE(1)                                                    MAIN0246
C     COMPUTE TOTAL ENERGY IN CASE OF STEP FUNCTION OR TRUE WAVE        MAIN0247
 119  CALL ERG                                                          MAIN0248
C     RUN OUT UNUSED CHANGE-CARDS,IF ANY                                MAIN0249
      CALL CHANGE(2)                                                    MAIN0250
      GO TO 902                                                         MAIN0251
      END                                                               MAIN0252
```

```
      SUBROUTINE SUBP                                                   SUBP0000
C     IMPLICIT P EXPLICIT T SOLUTION                                    SUBP0001
 900  DIMENSION ALPH(1000),AA(18),T(1000),TA(1000),P(21),PA(21),        SUBP0002
     1BETA(1000),CMC(18),CMD(18),COPC(18),COPD(18),GAM(18),GAMA(19),    SUBP0003
     2DELT(19),CC(18),DVP(18),P(3),TB(3),                               SUBP0004
     3L(15),TEMP(10), PT(10,12),OPT(10,12),DMP(10,12)                   SUBP0005
 901  COMMON TEMP,PRES,...,DMP,T,TA,ALPH,BETA,P,...,AA,CC,GAM,GAMA,DELT, SUBP0006
     1CMC,CMD,COPC,COPD,P,TB,ALF3,ALPS,ALP,SUM2,EVAP,DV,DVP,C10,CLK,CAP,SUBP0007
     2DVC,CMA,G,W,WW,QQ,SS,COM1,SR,QM,E,PSURR,ZETA,TSURR,TIME,CRIT,FA,  SUBP0008
     3TVP,ID,K,LA,J,MA,L,NX,NY,NTA,NTB,NTC,NXC,NXA,NXB,MXA,MXB,MXC,     SUBP0009
     4KPULSE,TCHAR,YOYM,ENORMD,ENOCSD,TDIS,NSTEP,TAUDIM,                SUBP0010
     5SHAPET,CKO,NS,KC,DVRED,CKONED,CAIAGO,RH,FS,CAITT,CKI,CON,UI,UO,   SUBP0011
     6CONA,ENERGO,ENERGA,ENORMA,ENOCSA,TENDAB,TENDCH,TEND,TPSND,NNSTEP  SUBP0012
      COMMON PFACT,FMXA                                                 SUBP0013
C     FORMAT STATEMENTS                                                 SUBP0014
 500  FORMAT(7HOTIME  ,F8.4/34H TEMPERATURE IN CLOTH AND SKIN   ,12F7, SUBP0015
     16/34H                           ,12F7.4/8H SKIN   ,16F7.4/        SUBP0016
     210H PRESSURE ,21F9.2/ 11H SURF LOSS=,F10.4,8H   COND=,F10.4/ 4H C SUBP0017
     3 10F6.3/ 4H D  10F6.3)                                            SUBP0018
 505  FORMAT(7H CYCLE F6.0)                                             SUBP0019
C     NEXT TIME INCREMENT                                               SUBP0020
C     OPTIONAL DIFFUSIVITY CALC                                         SUBP0021
 801  GO TO (802,805),10                                                SUBP0022
 802  DO 803 I=1,NXC                                                    SUBP0023
 803  DVP(I)=DV                                                         SUBP0024
      GO TO 57                                                          SUBP0025
 805  DO 806 I=1,NXC                                                    SUBP0026
 806  DVP(I)=DV*269.38/(.76-PA(I+2)-PSURR/1000.)/(TA(I+1)*C10*CLK+TSURR)SUBP0027
C     CALL DOUBLE INTERPOLATION SUBPROGRAM                              SUBP0028
 57   DO 63 I=MXA,NXC                                                   SUBP0029
 51   CALL DOUBIN (TA(I+1),PA(I+1),OPT,COPD(I))                         SUBP0030
      CMD(I)=C10*CLK/1000.*COPD(I)                                      SUBP0031
 52   CALL DOUBIN(TA(I+1),PA(I+1),DMP,COPC(I))                          SUBP0032
      CMC(I)=(DVP(I)*DVC)*(1000./COPC(I)+CAP*COPD(I))                   SUBP0033
      GAM(I)=2.+CMA/CMC(I)                                              SUBP0034
 63   CC(I)=(T(I)+T(I+2)-2.*T(I+1))*CMD(I)/CMC(I)+CMA/CMC(I)*PA(I+1)    SUBP0035
      MB=1                                                              SUBP0036
C     CHECK P GRADIENT AGAIN                                            SUBP0037
 20   IF (COM1) 202,202,62                                              SUBP0038
 202  IF (SUM2) 65,65,62                                                SUBP0039
C     NO COND ON SKIN, CALC IMPLICIT P FIRST TRIAL                      SUBP0040
 65   GAMA(MXA)=GAM(MXA)-G                                              SUBP0041
      IF(NXC-2) 70,70,68                                                SUBP0042
 68   DO 69 I=MXB,NXC                                                   SUBP0043
 69   GAMA(I)=GAM(I)-1./GAMA(I-1)                                       SUBP0044
 70   GAMA(NXC)=GAM(NXC)-1.-1./GAMA(NXC-1)                              SUBP0045
      DELT(MXA)=CC(MXA)                                                 SUBP0046
```

```
      DO 75 I=NXB,NXC
75    DELT(I)=CC(I)+DELT(I-1)/GAMA(I-1)
      P(NXC+1)=DELT(NXC)/GAMA(NXC)
      P(NXC+2)=P(NXC+1)
      DO 78 I=NXA,NXB
      J=NXC-I+NXC
78    P(J+1)=(DELT(J)+P(J+2))/GAMA(J)
      P(1)=G*P(NXB)
C     INTERPOLATE PRESSURE PROFILE IN DRY SLICES
      IF(NXA-1) 81,81,61
61    PFACT=(P(NXB)-P(1))/FNXA
      DO 62 I=2,NXA
      FI=I
62    P(I)=P(1)+(FI-1.)*PFACT
81    GO TO 250
C     CONDENSATION ON SKIN
82    WW=(1.-W)*P(NXC+3)/W
      GAMA(NXP)=GAM(NXA)-G
      DO 86 I=NXB,NXC
86    GAMA(I)=GAM(I)-1./GAMA(I-1)
      GAMA(NXC+1)=1./W-1./GAMA(NXC)
      DELT(NXA)=CC(NXA)
      DO 90 I=NXB,NXC
90    DELT(I)=DELT(I-1)/GAMA(I-1)+CC(I)
      DELT(NXC+1)=DELT(NXC)/GAMA(NXC)+WW
      P(NXC+2)=DELT(NXC+1)/GAMA(NXC+1)
      DO 95 I=NXA,NXC
      J=NXC-I+NXC
95    P(J+2)=(DELT(J+1)+P(J+3))/GAMA(J+1)
      P(1)=G*P(NXB)
      IF(NXA-1) 92,92,93
C     INTERPOLATE PRESSURE PROFILE IN DRY SLICES
93    PFACT=(P(NXB)-P(1))/FNXA
      DO 94 I=2,NXA
      FI=I
94    P(I)=P(1)+(FI-1.)*PFACT
C     FIRST TRIAL IMPLICIT P COMPLETED, PREPARATION FOR T CALC
92    NXD=NXA-1
      IF (NXD) 250,250,2501
2501  DO 2502 I=1,NXD
2502  AA(I)=CHA*TA(I+1)
250   DO 251 I=NXA,NXC
251   AA(I)=DVP(I)*(P(I)+P(I+2)-2.*P(I+1)) + CHA*TA(I+1)
C     CHECK P GRADIENT AGAIN
      IF (P(NXC+2)-P(NXC+1)) 257,253,257
C     NO COND ON SKIN
253   QQ=0.
      SS=0.
      SUM3=0.
      GO TO 40
C     COND ON SKIN
257   CON1 =(P(NXC+2)+P(NXC+1))*0.5-P(NXC+3).
      QQ=QH*CON1
      SS=SR*CON1
C     CALC IMPLICIT T
      GO TO (4001,4000,4000,4000),KPULSE
4000  CALL PULSE
C     SET IRRADIATION BOUNDARY CONDITION
4001  E=2.*TOTNXC/(2.*CON.)
40    BETA(1) =E*AA(1)
      DO 42 I=2,NXC
42    BETA(I)=BETA(I-1)/ALPH(I-1)+AA(I)
      BETA(NXC+1)=(BET [illegible] *(ALPB-ALPS)+ALPH(NXC)*(1.-ALPS)*QQ-(1.-ALP
     1B)*SS))/(ALPB*ALP [illegible] (1.-ALPO))
      BETA(NXC+2)=(ALPH(NX [illegible] )*SS+BETA(NXC)+BETA(NXC+1)/ALPH(NXC+1))/(ALPH
     1(NXC)*(ALPB-1.))
      DO 50 I=NXA,N
      ALPH(I)=ALP-1./ALPH(I-1)
50    BETA(I)=BETA(I-1)/ALPH(I-1) + CHA*TA(I+1)
      M=N+1
      LA =N-2
      DO 55 I=2,LA
      J=N-I
55    T(J)=(T(J+1)+BETA(J-1))/ALPH(J-1)
      T(1)=E*FACT(2)
C     IMPLICIT T CALC COMPLETED, FIRST TRIAL
      GO TO (300,400,420),MD
300   TD(1)=TVP
      TVP=(T(NXC+3)+T(NXC+4))*0.5
      TD(2)=TVP
      F(1)=TD(2)-TD(1)
      IF (ABSF(F(1))-CRIT) 100,100,300
300   P(NXC+3)=(EXPF(-4000.575/(C1O*CLA*TD(2)+TBURN)+10.64707)-PBURN)
     1/1000.
      MD=2
      N=N-1
      GO TO 200
400   F(2)=(T(NXC+3)+T(NXC+4))*0.5-TD(2)
      IF (ABSF(F(2))-CRIT) 100,100,410
410   TD(3)=-(TD(2)-TD(1))/(F(2)-F(1))*F(2)+TD(2)
      P(NXC+3)=(EXPF(-4000.575/(C1O*CLA*TD(3)+TBURN)+10.64707)-PBURN)
     1/1000.
      MD=3
      N=N-1
      GO TO 200
420   F(3)=(T(NXC+3)+T(NXC+4))*0.5 -TD(3)
      IF (ABSF(F(3))-CRIT.  100,100,421
421   IF (F(2)*F(3)) 422,100,423
422   F(1)=F(3)
      TD(1)=TD(3)
      CYCLE=CYCLE+1.
      GO TO 410
423   F(2)=F(3)
```

```
          TRA     D125                                                  DTAB0121
D112      CLA     -11,4                                                 DTAB0122
          STO     DELY                                                  DTAB0123
          CLA     DONE                                                  DTAB0124
          STO     DELXT                                                 DTAB0125
          STO     DELYT                                                 DTAB0126
          STO     SWITCH                                                DTAB0127
          CLA     -10,4                                                 DTAB0128
          STO     DELX                                                  DTAB0129
          SUB     DONE                                                  DTAB0130
          STO     ALPHA                                                 DTAB0131
          TNZ     D122                                                  DTAB0132
          STO     DELXT                                                 DTAB0133
D122      CLA     -8,4                                                  DTAB0134
          STO     X11                                                   DTAB0135
          CLA     -9,4                                                  DTAB0136
          STO     Y11                                                   DTAB0137
          CLA     -12,4                                                 DTAB0138
          STO     N                                                     DTAB0139
D126      CLA     -5,4                                                  DTAB0140
          STO     KK                                                    DTAB0141
          CLA     -4,4                                                  DTAB0142
          STO     LIST6                                                 DTAB0143
          ADD     DONE                                                  DTAB0144
          STO     KZ1                                                   DTAB0145
          CLA     -6,4                                                  DTAB0146
          ARS     18                                                    DTAB0147
          STA     D3                                                    DTAB0148
          STA     D13                                                   DTAB0149
          STA     D39                                                   DTAB0150
          ADD     K26                                                   DTAB0151
          STA     D54                                                   DTAB0152
          STA     D141                                                  DTAB0153
          STA     D144                                                  DTAB0154
          STA     D50,2                                                 DTAB0155
D1+1      CLA     0                                                     DTAB0156
          STO     SAVE                                                  DTAB0157
          CLA     REPL                                                  DTAB0158
D144      STO     0                                                     DTAB0159
          CLA     0,4                                                   DTAB0160
          SUB     N7                                                    DTAB0161
          ARS     18                                                    DTAB0162
          STA     D45                                                   DTAB0163
          CLA     -3,4                                                  DTAB0164
          STO     LIST7                                                 DTAB0165
          CLA     DONE                                                  DTAB0166
          STO     LIST5                                                 DTAB0167
          TRA     D1                                                    DTAB0168
REG1      PZE                                                           DTAB0169
REG2      PZE                                                           DTAB0170
REG4      PZE                                                           DTAB0171
          CLA     XDTABP          LOCATION ENTRY FOR DTABP              DTAB0172
          TRA     1,4                                                   DTAB0173
LIST6     PZE                     LIST FOR                              DTAB0174
LIST7     PZE                     USE                                   DTAB0175
LIST4     PZE                     OF                                    DTAB0176
LIST5     PZE                     TABP                                  DTAB0177
LIST4     PZE                     SUBROUTINE                            DTAB0178
LIST3     PZE                     X                                     DTAB0179
LIST2     PZE                     X                                     DTAB0180
LIST1     PZE     0,0,LIST1       X                                     DTAB0181
DONE      PZE     0,0,1                                                 DTAB0182
DTWO      PZE     0,0,2                                                 DTAB0183
A1        PZE     0,0,COMMON-1    ORIGIN OF AUX Z TABLE                 DTAB0184
A2        PZE     0,0,COMMON-2    ORIGIN OF AUX Y TABLE                 DTAB0185
SAVE      PZE     0,0,0           SAVE INSTR J28 FROM TABP SUBR         DTAB0186
ALPHA     PZE     0,0,0           ALPHA=0 IF X IS 1 DIM, 1 OTHERWISE    DTAB0187
X         PZE                     1ST INDEPENDENT ARG                   DTAB0188
Z         PZE                     2ND INDEPENDENT ARG                   DTAB0189
KK        PZE                     ORDER OF INTERPOL ON X                DTAB0190
KZ1       PZE                     KZ+1 IN INCREMENT                     DTAB0191
N         PZE                     NO OF X,Y PAIRS PER Z CURVE           DTAB0192
X11       PZE                     LOCATION OF X(1,1)                    DTAB0193
Y11       PZE                     LOCATION OF Y(1,1)                    DTAB0194
DELXT     PZE                     INCREMENT TO LOC NEXT X TABLE         DTAB0195
DELYT     PZE                     INCREMENT TO LOC NEXT Y TABLE         DTAB0196
DELX      PZE                     INCR TO NEXT X IN SAME TABLE          DTAB0197
DELY      PZE                     INCR TO NEXT Y IN SAME TABLE          DTAB0198
SWITCH    PZE                     ZERO TABLE IS ONE DIMENSIONAL         DTAB0199
K26       NZE     07                                                    DTAB0200
REPL      TRA     D3,0                                                  DTAB0201
N7        PZE     0,0,7                                                 DTAB0202
XDTABP    PZE     0,0,DB6                                               DTAB0203
 DTAB     SYN DB6                                                       DTAB0204
 XDTAB    SYN REG4+1                                                    DTAB0205
          END     0                                                     DTAB0206
```

```
*     FAP                                                               TAB 0000
      COUNT 220                                                         TAB 0001
      ENTRY TAB                                                         TAB 0002
      ENTRY XTAB                                                        TAB 0003
COMMON SYN -1                                                           TAB 0004
      REM X1 CONTAINS X WITH ADJUSTED SIGN                              TAB 0005
      REM COMMON-2 IS LBAS                                              TAB 0006
      REM K PUT GREATER THAN 9                                          TAB 0007
      REM COMMON CONTAINS X                                             TAB 0008
      REM COMMON-1 CONTAIN LOC OF LIST                                  TAB 0009
      REM COMMON FOR AUXILIARY                                          TAB 0010
      REM XTABLE FLOATS FROM COMMON-0                                   TAB 0011
```

```
         REM TO COMMON-8 WHEN K=5                                  TAB 0010
         REM Y TABLE FLOATS FROM COMMON-9                          TAB 0011
         REM TO COMMON-16                                          TAB 0012
         REM ON OV OR UNDER FLOW OR DCT                            TAB 0013
         REM ORIGINAL ARG IN ACC                                   TAB 0014
         REM 1 LIST (8) IF SOLN IS GOOD                            TAB 0015
         REM 2 LIST (8) IF ERROR                                   TAB 0016
         REM LIST (1)=LOCATION OF LIST (1)                         TAB 0017
         REM LIST (2)=LOCATION OF X TABLE                          TAB 0018
         REM LIST (3)=LOCATION OF Y TABLE                          TAB 0019
         REM LIST (4)=DEL X                                        TAB 0020
         REM LIST (5)=DEL Y                                        TAB 0021
         REM LIST (6)=K                                            TAB 0022
         REM LIST (7)=P                                            TAB 0023
         REM LIST (8)=1-SUCCESSFUL, 2-LARC?                        TAB 0024
TAB      LFTM                                                      TAB 0025
         TRA J71                                                   TAB 0026
J1       CLA 0,1              A=LOC OF X TABLE                     TAB 0027
J2       NOP                  CHS IF X(I+1) LESS THAN X(I)         TAB 0028
         CAS X1               X1 HAS SIGN ADJUSTED                 TAB 0029
         TRA J9               X LESS THAN X(I)                     TAB 0030
         TRA J9               X=X(I)                               TAB 0031
J6       TXI J7,1,0           X GREATER THAN X(I), D=DELTA X       TAB 0032
J7       TXI J8,2,0           D=DELTA Y                            TAB 0033
J8       TXL J1,1,0           K ODD(P-(K+1)/2-1),K EVEN(P-(K/2+1)-1) TAB 0034
J9       CLA K2               LOC OF K IN ADDRESS                  TAB 0035
         LBT                                                       TAB 0036
         TRA J13              K EVEN                               TAB 0037
         TRA J26              K ODD                                TAB 0038
J13      CLA 0,1              A=LOC OF XTABLE                      TAB 0039
         FSB COMMON           LOCATION OF X                        TAB 0040
         SSP                                                       TAB 0041
         STO COMMON-2         ERASABLE                             TAB 0042
J17      TIX J18,1,0          D=DELTA X                            TAB 0043
J18      CLA 0,1              A=LOC OF XTAB                        TAB 0044
         FSB COMMON                                                TAB 0045
         SSP                                                       TAB 0046
         FSB COMMON-2                                              TAB 0047
         TMI J23              X CLOSER TO X(I)                     TAB 0048
J23      TXL J24,1,0          DECREMENT SAME AS J6      TAB 34,1   TAB 0049
J23A     TIX J23B,1,0         DECR DELTAX               TAB 34,2   TAB 0050
J23B     TIX J23,2,0          DECR DELTAY               TAB 34,3   TAB 0051
J24      TXI J26,1,0          X CLOSER TO X(I+1)D=DELTA X          TAB 0052
J25      TIX J26,2,0          D=DELTA Y                            TAB 0053
J26      TXI J27,1,0          -(K/2)DELTA X,-(K+1)/2 DELTA X       TAB 0054
J27      TXI J28,2,0          -(K/2)DELTA Y,-(K+1)/2 DELTA Y       TAB 0055
J28      LXD K1,4             K1=0,0, K+1                          TAB 0056
J29      CLA COMMON                                                TAB 0057
J30      FSB 0,1              A=LOC OF X TABLE                     TAB 0058
         STO COMMON-2,4                                            TAB 0059
J31      TXI J32,1,0          D=DELTA X                            TAB 0060
J32      TIX J29,4,1                                               TAB 0061
         LXD K1,4                                                  TAB 0062
J34      CLA 0,2              A=Y TABLE                            TAB 0063
         STO COMMON-8,4                                            TAB 0064
J36      TXI J37,2,0          D=DELTA Y                            TAB 0065
J37      TIX J34,4,1                                               TAB 0066
         LXD K,1              K=0,0,5                              TAB 0067
J39      DCT                  BEGIN AITKEN INTERPOLATION           TAB 0068
J40      TOV J41                                                   TAB 0069
J41      PXD 0,1                                                   TAB 0070
J42      PDX 0,2                                                   TAB 0071
J43      TOV J44                                                   TAB 0072
J44      CLA COMMON-2,2                                            TAB 0073
         FSB COMMON-3,1                                            TAB 0074
         STO COMMON-2         ERASE, X(I)-X(I+1)                   TAB 0075
         LDQ COMMON-9,1                                            TAB 0076
         FMP COMMON-2,2                                            TAB 0077
         STO K1               ERASE, Y(I) (X-X(I+1))               TAB 0078
         LDQ COMMON-3,1                                            TAB 0079
         FMP COMMON-8,2                                            TAB 0080
         CHS                                                       TAB 0081
         FAD K1                                                    TAB 0082
         TOV J67                                                   TAB 0083
         TQO J56                                        TAB 33,1   TAB 0084
J56      FDP COMMON-1                                   TAB 33,2   TAB 0085
         TQO J67                                        TAB 34     TAB 0086
         STO COMMON-8,2                                 TAB 34,1   TAB 0087
         TIX J43,2,1                                               TAB 0088
         TIX J41,1,1                                               TAB 0089
         DCT                                                       TAB 0090
         TRA J67              DIVIDE CHECK ON                      TAB 0091
         CLA DONE             PREPARE NORMAL EXIT                  TAB 0092
J61      STO 8                A=LIST (8)                           TAB 0093
         CLA COMMON-9                                              TAB 0094
         LXD REG1,1                                                TAB 0095
         LXD REG2,2                                                TAB 0096
         LXD REG4,4                                                TAB 0097
         EFTM                                                      TAB 0098
         TRA 1,4                                                   TAB 0099
J67      CLA COMMON           SET ERROR RETURN                     TAB 0100
         STO COMMON-9                                              TAB 0101
         CLA DTWO                                                  TAB 0102
         TRA J61                                                   TAB 0103
J71      SXD REG1,1           ENTRY POINT FOR TABLE                TAB 0104
         SXD REG2,2                                                TAB 0105
         SXD REG4,4                                                TAB 0106
         STO COMMON           X                                    TAB 0107
         STO COMMON-1         LOCATION OF LIST                     TAB 0108
         CLA COMMON-1                                              TAB 0109
         COM                                                       TAB 0110
         ADD DONE                                                  TAB 0111
         PDX 0,4              2-COMPLEMENT OF LIST LOCATION        TAB 0112
```

```
         CLA -1,4           ADDRESS OF X TABLE                      TAB 0113
         ARS 18                                                     TAB 0114
         STA J1                                                     TAB 0115
         STA J13                                                    TAB 0116
         STA J18                                                    TAB 0117
         STA J30                                                    TAB 0118
         STA J137                                                   TAB 0119
         STA J139                                                   TAB 0120
         CLA -2,4                                                   TAB 0121
         ARS 18                                                     TAB 0122
         STA J34                                                    TAB 0123
         CLA -5,4                                                   TAB 0124
         STO K                                                      TAB 0125
         ADD DONE                                                   TAB 0126
         STO K1                                                     TAB 0127
         SUB DONE                                                   TAB 0128
         ARS 18                                                     TAB 0129
         STA K2                                                     TAB 0130
         CLA -3,4           ACC HAS DELTA X                         TAB 0131
         STD J6                                                     TAB 0132
         STD J17                                                    TAB 0133
         STD J24                                                    TAB 0134
         STD J31                                                    TAB 0135
         STD J23A                                                   TAB 0136
         CLA -4,4           DELTA Y IN ACC          TAB137,1        TAB 0137
         STD J7                                                     TAB 0138
         STD J25                                                    TAB 0139
         STD J36                                                    TAB 0140
         STD J23B                                                   TAB 0141
         LXD K,1                                    TAB141,1        TAB 0142
         LDQ DONE+1,1                                               TAB 0143
         MPY -3,4                                                   TAB 0144
         ALS 17                                                     TAB 0145
         STO COMMON-2       (AK/2) DELTAX                           TAB 0146
         COM                                                        TAB 0147
         ADD DONE                                                   TAB 0148
         STD J26                                                    TAB 0149
         LDQ DONE+1,1                                               TAB 0150
         MPY -4,4                                                   TAB 0151
         ALS 17                                                     TAB 0152
         STO COMMON-8       (AK/2)DELTAY, TEMP ERAS                 TAB 0153
         COM                                                        TAB 0154
         ADD DONE                                                   TAB 0155
         STD J27                                                    TAB 0156
         CLA K2                                                     TAB 0157
         LBT                                                        TAB 0158
         TRA J126           K EVEN                                  TAB 0159
         TRA J130           K ODD                                   TAB 0160
J126     CLA COMMON-2                                               TAB 0161
         ADD -3,4                                                   TAB 0162
         STO COMMON-2                                               TAB 0163
         CLA COMMON-8                                               TAB 0164
         ADD -4,4                                                   TAB 0165
         STO COMMON-8                                               TAB 0166
J130     CLA -6,4                                                   TAB 0167
         SUB DONE                                                   TAB 0168
         LRS 35                                                     TAB 0169
         MPY -3,4                                                   TAB 0170
         ALS 17                                                     TAB 0171
         SUB COMMON-2                                               TAB 0172
         STO J8                                                     TAB 0173
         STO J25                                                    TAB 0174
J137     CLA 0                                      TAB173,1        TAB 0175
         LXD J17,1          *STAB,DETERMINE DIRECTION               TAB 0176
J139     FSB 0,1            OF MONOTONICITY                         TAB 0177
         TPL J144           X(1)-X(2)                               TAB 0178
         CLA NOP                                                    TAB 0179
         STO J2                                                     TAB 0180
         CLA COMMON                                                 TAB 0181
         TRA J148                                                   TAB 0182
J144     CLA CHS                                                    TAB 0183
         STO J2                                                     TAB 0184
         CLA COMMON                                                 TAB 0185
         CHS                                                        TAB 0186
J148     STO X1                                                     TAB 0187
         CLA 0,4                                                    TAB 0188
         SUB SEVEN                                                  TAB 0189
         ARS 18                                                     TAB 0190
         STA J61                                                    TAB 0191
         LXD COMMON-2,1                                             TAB 0192
         LXD COMMON-8,2                                             TAB 0193
         CLA -6,4                                                   TAB 0194
         SUB X1                                     TAB194,1        TAB 0195
         TNZ J1                                     TAB194,2        TAB 0196
         PDX 0,1                                    TAB194,3        TAB 0197
         PDX 0,2                                    TAB194,4        TAB 0198
         TRA J28                                    TAB194,5        TAB 0199
J156     CLA LOCATE                                 TAB 195         TAB 0200
         TRA 1,4                                                    TAB 0201
K        PZE 0,0,0          LOCATING SUB ROUTINE                    TAB 0202
K1       PZE 0,0,0          B,0,K                                   TAB 0203
F2       PZE 0,0,0          C,0,K+1                                 TAB 0204
X1       PZE                K,0,0                                   TAB 0205
         PZE 0,0,5          X WITH ADJUSTED SIGN                    TAB 0206
         PZE 0,0,3                                                  TAB 0207
DTWO     PZE 0,0,2                                                  TAB 0208
         PZE 0,0,1                                                  TAB 0209
DONE     PZE 0,0,1                                                  TAB 0210
NOP      NOP                                                        TAB 0211
CHS      CHS                                                        TAB 0212
SEVEN    PZE 0,0,7                                                  TAB 0213
REG1     PZE                                                        TAB 0214
REG2     PZE                                                        TAB 0215
```

```
 REGA  PZE                                                              TAB 0216
LOCATE PZE 0,0,J71                                                      TAB 0217
 XTAB  SYN J156                                                         TAB 0218
       END                                                              TAB 0219


      SUBROUTINE PULSE                                                  PUL50000
C     ROUTINE TO COMPUTE REL. IRRADIATION INTENSITY IO/IOMAX            PUL50001
C     AS FUNCTION OF TIME                                               PUL50002
 900  DIMENSION ALPH(1000),AA(18),T(1000),TA(1000),P(21),PA(21),        PUL50003
     1BETA(1000),CMC(18),CMD(18),COFC(18),COFD(18),GAM(18),GAMA(19),    PUL50004
     2DELT(19),CC(18),DVP(18),F(3),TB(3),                               PUL50005
     3L(13),TEMP(10),PRES(10,12),DPT(10,12),DMP(10,12)                  PUL50006
 901  COMMON TEMP,PRES,DPT,DMP,T,TA,ALPH,BETA,P,PA,AA,CC,GAM,GAMA,DELT, PUL50007
     1CMC,CMD,COFC,COFD,F,TB,ALPG,ALPS,ALP,SUM2,EVAP,DV,DVP,CIO,CLK,CAP,PUL50008
     2DVC,CRA,G,U,UW,GO,SS,CON1,SR,OM,E,PSURR,ZETA,TSURR,TIME,CRIT,FA,  PUL50009
     3TVP,IO,M,LA,J,MA,L,MX,NY,NTA,NTB,NTC,NXC,NXA,NXB,MXA,MXB,MXC  ,   PUL50010
     4KPULSE,TCHAR,YOYM,ENDRMD,ENDCSD,TDIS,NSTEP,TAUOIN,                PUL50011
     5SHAPE1,CKO,NS,XC,DVRED,CKORED,CKIRED,RH,XS,CRITT,CK1,CON,UI,UD,   PUL50012
     6COMA,ENERGD,ENERGA,ENORMA,ENDCSA,TENDAB,TENDCH,TEND,TPEAB,XNSTEP  PUL50013
      COMMON PFACT,FMXA                                                 PUL50014
C     COMPUTES YOYM = RAD. INTENSITY/MX. RAD.INTENSITY                  PUL50015
C     COMPUTE DIM.LESS TIME/ DIM.LESS PEAK TIME                         PUL50016
      TPLS=TIME/TCHAR                                                   PUL50017
C     BRANCH FOR STEP,SQUARE WAVE,TRAPEZOIDAL WAVE,TRUE WAVE            PUL50018
      GO TO (1,2,3,4),KPULSE                                            PUL50019
C     STEP FUNCTION                                                     PUL50020
 1    YOYM = 1.                                                         PUL50021
      GO TO 30                                                          PUL50022
C     SQUARE WAVE                                                       PUL50023
 2    IF (TIME - TCHAR) 10,11,11                                        PUL50024
 10   YOYM = 1.                                                         PUL50025
      GO TO 20                                                          PUL50026
 11   YOYM = 0.0                                                        PUL50027
      GO TO 20                                                          PUL50028
C     TRAPEZOIDAL WAVE                                                  PUL50029
 3    IF (TIME - ENDRMD) 13,14,14                                       PUL50030
 13   YOYM=TIME/ENDRMD                                                  PUL50031
      GO TO 20                                                          PUL50032
 14   IF (TIME-ENDCSD) 1,15,15                                          PUL50033
 15   IF (TIME-TCHAR) 16,11,11                                          PUL50034
 16   YOYM=(TCHAR-TIME)/ENDRMD                                          PUL50035
      GO TO 20                                                          PUL50036
C     TRUE WAVE                                                         PUL50037
 4    TDIS=TIME/TCHAR                                                   PUL50038
      IF (TDIS - .3) 21,22,22                                           PUL50039
 21   YOYM= .969*TDIS                                                   PUL50040
      GO TO 20                                                          PUL50041
 22   IF (TDIS - .65) 23,24,24                                          PUL50042
 23   YOTRY=1.72*TDIS-.347                                              PUL50043
      IF (YOTRY-YOYM) 21,21,33                                          PUL50044
 33   YOYM=YOTRY                                                        PUL50045
      GO TO 20                                                          PUL50046
 24   IF (TDIS - 1.4) 25,27,27                                          PUL50047
 25   YOYM = 1.-1.02*(TDIS-1.05)**2                                     PUL50048
      GO TO 20                                                          PUL50049
 27   YOYM = 1.634*EXPF(-1.64*LOGF(TDIS))                               PUL50050
 20   PRINT 31,YOYM                                                     PUL50051
 31   FORMAT(10H IO/IOMAX=,F5.3)                                        PUL50052
 30   RETURN                                                            PUL50053
      END                                                               PUL50054


      SUBROUTINE PARA                                                   PARA0000
C     DIMENSIONAL CONVERSION AND DATA PRINTOUT                          PARA0001
 900  DIMENSION ALPH(1000),AA(18),T(1000),TA(1000),P(21),PA(21),        PARA0002
     1BETA(1000),CMC(18),CMD(18),COFC(18),COFD(18),GAM(18),GAMA(19),    PARA0003
     2DELT(19),CC(18),DVP(18),F(3),TB(3),                               PARA0004
     3L(13),TEMP(10),PRES(10,12),DPT(10,12),DMP(10,12)                  PARA0005
 901  COMMON TEMP,PRES,DPT,DMP,T,TA,ALPH,BETA,P,PA,AA,CC,GAM,GAMA,DELT, PARA0006
     1CMC,CMD,COFC,COFD,F,TB,ALPG,ALPS,ALP,SUM2,EVAP,DV,DVP,CIO,CLK,CAP,PARA0007
     2DVC,CRA,G,U,UW,GO,SS,CON1,SR,OM,E,PSURR,ZETA,TSURR,TIME,CRIT,FA,  PARA0008
     3TVP,IO,M,LA,J,MA,L,MX,NY,NTA,NTB,NTC,NXC,NXA,NXB,MXA,MXB,MXC  ,   PARA0009
     4KPULSE,TCHAR,YOYM,ENDRMD,ENDCSD,TDIS,NSTEP,TAUOIN,                PARA0010
     5SHAPE1,CKO,NS,XC,DVRED,CKORED,CKIRED,RH,XS,CRITT,CK1,CON,UI,UD,   PARA0011
     6COMA,ENERGD,ENERGA,ENORMA,ENDCSA,TENDAB,TENDCH,TEND,TPEAB,XNSTEP  PARA0012
      COMMON PFACT,FMXA                                                 PARA0013
 499  FORMAT (31HMAXIMUM IRRADIATION INTENSITY=,F9.2,12H CAL/CM2SEC.)   PARA0014
 550  FORMAT(72H TRUE PULSE DISTRIBUTION. HERE BY PULSE WIDTH IS MEANT LPARA0015
     1OCATION OF PEAK.)                                                 PARA0016
 519  FORMAT (14H0STEP FUNCTION)                                        PARA0017
 514  FORMAT (12H0SQUARE WAVE)                                          PARA0018
 515  FORMAT(50H0TRAPEZOIDAL PULSE. TANGENT OF RAMP=,F7.3,35H CAL/CM2*SEPARA0019
     1C/UNIT DIM.LESS TIME,OR ,F7.3,20H IN NORMALIZED DISTRIBUTION.)    PARA0020
 516  FORMAT(67H                          DIMENSIONLESS        ABSOLUTE PARA0021
     1TIME SCALE )                                                      PARA0022
 517  FORMAT(21H END OF [illegible]. RAMP    =,F8.4,13H SEC/SEC      ,F8.4,4H SECPARA0023
 518  FORMAT(21H E D OF CONST. LEVEL=,F8.4,13H SEC/SEC      ,F8.4,4H SECPARA0024
 519  FORMAT(21H P[illegible]E WIDTH          =,F8.4,13H SEC/SEC      ,F8.4,4H SECPARA0025
 521  FORMAT(21H TOTAL ENERGY       =,F8.4,13H CAL/CM2SEC   ,F8.4,8H CAL/CPARA0026
     1M2)                                                               PARA0027
 520  FORMAT(21H TIME LIMIT SET      =,F8.4,13H SEC/SEC      ,F8.4,4H SECPARA0028
 503  FORMAT (1H0=                                                      PARA0029
     1     =,F7.2,12H*PULSE WIDTH)                                      PARA0030
 522  FORMAT (1H1)                                                      PARA0031
      XNSTEP=NSTEP                                                      PARA0032
      TEND=XNSTEP*ZETA*2.                                               PARA0033
```

```
C       ABSOLUTE END OF PROCESS                                                PARA0034
        TENDAB=TEND*TAUDIM                                                     PARA0035
C       END OF PROCESS IN DISTRIBUTION CURVE FOR TRUE WAVE                     PARA0036
        TENDCH=TEND/TCHAR                                                      PARA0037
        GO TO (498,320,321,320),KPULSE                                         PARA0038
C       INTERVALS AT TRAPEZOIDAL CURVE, DIM.LESS AND ABSOLUTE                  PARA0039
C       END OF RAMP                                                            PARA0040
  321   ENDRMO=SHAPET                                                          PARA0A40
        PHI=TCHAR/ENDRMO                                                       PARA0041
        PHIAB=CIO/ENDRMO                                                       PARA0A41
        ENDRMA=ENDRMO*TAUDIM                                                   PARA0042
C       END OF CONST. LEVEL                                                    PARA0043
        ENDCSD=TCHAR-ENDRMO                                                    PARA0044
        ENDCSA=ENDCSD*TAUDIM                                                   PARA0045
C       ABSOLUTE PULSE WIDTH                                                   PARA0046
  320   TPEND=TCHAR*TAUDIM                                                     PARA0047
C       PULSE AREA = ENERGY, DIM.LESS AND ABSOLUTE                             PARA0048
  300   GO TO (498,302,303,498),KPULSE                                         PARA0049
  302   ENERGO=CIO*TCHAR                                                       PARA0050
        GO TO 304                                                              PARA0051
C       TRAPEZE                                                                PARA0052
  303   ENERGO=CIO*(TCHAR-ENDRMO)                                              PARA0053
  304   ENERGA=ENERGO*TAUDIM                                                   PARA0054
C       DIMENSIONAL CONVERSION FINISHED                                        PARA0055
C       COMPUTED AT END OF PROCESS                                             PARA0056
  498   PRINT 499,CIO                                                          PARA0057
C       PULSE FORM                                                             PARA0058
        GO TO (306,307,308,330),KPULSE                                         PARA0059
  330   PRINT 530                                                              PARA0060
        GO TO 309                                                              PARA0061
  306   PRINT 513                                                              PARA0062
        GO TO 309                                                              PARA0063
  307   PRINT 514                                                              PARA0064
        GO TO 309                                                              PARA0065
  308   PRINT 515,PHIAB,PHI                                                    PARA0066
  309   PRINT 516                                                              PARA0067
        GO TO (310,340,341,340),KPULSE                                         PARA0068
  341   PRINT 517,ENDRMO,ENDRMA                                                PARA0069
        PRINT 518,ENDCSD,ENDCSA                                                PARA0070
  340   PRINT 519,TCHAR,TPEND                                                  PARA0071
        GO TO (310,311,311,310),KPULSE                                         PARA0072
  311   PRINT 521,ENERGO,ENERGA                                                PARA0073
  310   PRINT 520,TEND,TENDAB                                                  PARA0074
        GO TO (350,344,344,344),KPULSE                                         PARA0075
  344   PRINT 343,TENDCH                                                       PARA0076
  350   PRINT 522                                                              PARA0077
        RETURN                                                                 PARA0078
        END                                                                    PARA0079


        SUBROUTINE CHANGE(ICH)                                                 CHAN0000
C                                                                              CHAN0001
C       1. THIS ROUTINE RECORDS THE NUMBER OF DRY CLOTH SLICES.                CHAN0002
C       2. IF A DATA CARD WITH CRIT. TEMPERATURE AND K*C*RHO OF SKIN IS        CHAN0003
C       ENCOUNTERED, FOLLOWING THE NORMAL DATA CARDS, THE MAX. HEAT            CHAN0004
C       CONTENT OF THE SKIN ABOVE T-CRIT, ATTAINED AT ANY TIME, WILL BE        CHAN0005
C       COMPUTED.                                                              CHAN0006
C       3. THIS ROUTINE ALSO CHANGES THE MODULUS CMA TO A NEW VALUE AND AT CHAN0007
C       A TIME PRESCRIB [illegible] DATA CARD CARD FOLLOWING NORMAL DATA OR    CHAN0008
C       T-CRIT-CARD. AN [illegible] R OF CHANGE-CARDS POSSIBLE.                CHAN0009
C       1 BLANK CARD IS RE[illegible]ED AFTER EACH DATA SET,AND 2 BLANK CARDS  CHAN0010
C       AFTER THE LAST DATA SET OF A RUN.                                      CHAN0011
C                                                                              CHAN0012
  900   DIMENSION ALPH(1000),AA(10),T(1000),TA(1000),P(21),PA(21),             CHAN0013
       1BETA(1000),CMC(10),CMD(10),COFC(10),COFD(10),GAM(10),GAMA(19),         CHAN0014
       2DELT(19),CL(10),DVP(10),F(3),TB(3),                                    CHAN0015
       3L(13),TEMP(10),PRES(10,12),DPT(10,12),DMP(10,12)                       CHAN0016
C       BESIDES, THE NUMBER OF DRY SLICES IS REDUCED.                          CHAN0017
  901   COMMON TEMP,PRES,DPT,DMP,T,TA,ALPH,BETA,P,PA,AA,CC,GAM,GAMA,DELT, CHAN0018
       1CMC,CMD,COFC,COFD,F,TB,ALPO,ALPS,ALP,SUM2,EVAP,DV,DVP,CIO,CLX,CAP,CHAN0019
       4DVC,CMA,U,W,DW,DD,SS,COMI,SR,DM,E,PSURR,ZETA,TSURR,TIME,CRIT,FA,       CHAN0020
       3TVP,IU,M,LA,J,MA,L,NR,NY,NTA,NTB,NTC,NXC,NXA,NAB,NBA,NEB,MEC,          CHAN0021
       4KPULSE,TCHAR,YOYM,ENDRMO,ENDCSD,TDIS,NSTEP,TAUDIM,                     CHAN0022
       5SHAPET,LEO,NS,KC,DVRED,CKORED,CKIRED,RM,ZB,CRITT,CKI,CON,UI,UD,        CHAN0023
       6CDMA,ENERGO,ENERGA,ENDRMA,ENDCSA,TENDAB,TENDCH,TEND,TPEND,NNSTEP       CHAN0024
        COMMON PFACT,FMXA                                                      CHAN0025
C       SKIP UNUSED CHANGE-CARDS,IF ANY,AT END OF RUN FOR EACH DATA SET.       CHAN0026
        GO TO (81,83),ICH                                                      CHAN0027
   83   IF(CHTIM) 82,100,82                                                    CHAN0028
   82   PRINT 84,CHTIM,CHACMA                                                  CHAN0029
   84   FORMAT(23H0UNUSED CHANGE-CARD ,2F10.4)                                 CHAN0030
   85   READ 2,CHTIM,CHACMA                                                    CHAN0031
        GO TO 83                                                               CHAN0032
   81   NR=NR+1                                                                CHAN0033
        INWID=INWID                                                            CHAN0A33
        IF(TIME-ZETA) 30,41,3                                                  CHAN0034
C       INITIALIZE DRY SLICES COUNT                                            CHAN0035
   41   NCH=0                                                                  CHAN0036
        KWAIT=0                                                                CHAN0037
C       INITIALIZE INTEGRATOR                                                  CHAN0038
        TWPO=0.                                                                CHAN0039
        SAO=0.                                                                 CHAN0040
        STIME=0.                                                               CHAN0041
        INWID=1                                                                CHAN0042
C       READ TCRIT-CARD                                                        CHAN0043
        READ 43,TCRIT,CROK                                                     CHAN0044
   43   FORMAT(2F10.7)                                                         CHAN0045
        IF (TCRIT-273.) 71,70,70                                               CHAN0046
C       HERE IF 1ST CARD A T-CRIT-CARD                                         CHAN0047
   70   TCRITD=(TCRIT-TSURR)/CIO/CLX                                           CHAN0048
```

```
      GO TO 40
C     HERE IF 1ST CARD A CHANGE-CARD OR BLANK
   71 CHTIM=TCRIT
      CHACHA=CROK
      TCRIT=0.
      GO TO 30
    3 IF(CHTIM) 30,30,66
C     CHECK WAITING STATUS
   66 IF(KWAIT) 21,6,21
    6 IF(TIME-CHTIM) 30,5,5
    5 IF(TIME-ZETA-CHTIM) 4,30,30
    4 LLCHA=CHACHA
    8 LCHA=CHA
   21 IF(XMODF(NX*LLCHA,LCHA)) 50,20,50
C     PUT IN WAITING STATUS
   50 KWAIT=1
      GO TO 30
   20 NY=(NY*LLCHA)/LCHA
      NX=(NX*LLCHA)/LCHA
C     LEAVE WAITING STATUS
      KWAIT=0
      CHA=CHACHA
      ALP=CHA+2.
      ALPH(1)=ALP-FA
      DO 9 I=2,NXC
    9 ALPH(I)=ALP-1./ALPH(I-1)
      ALPH(NXC+1)=((ALPH(NXC)*ALPQ-1.)*(1.-ALPS)+(1.-ALPQ))/(ALPS*ALPH(N
     1XC)*(1.-ALPQ))
      ALPH(NXC+2)=(ALPH(NXC+1)*ALPS*ALPH(NXC)-1.)/(ALPH(NXC+1)*ALPH(NX
     1C)*(ALPS-1.))
      ZETA=XC*XC/CHA
      PRINT 12,CHA,NY,TIME
   12 FORMAT(20H0NEW PARAMETERS CHA=,F10.4,4H NY=,I5,8H AT TIME,F8.4)
C     READ NEXT CHANGE-CARD, OR BLANK CARD IF NO MORE CHANGES.
   40 READ 2, CHTIM,CHACHA
    2 FORMAT(2F10.4)
   30 NX=NX-1
   33 IF(NXA-NCH) 31,122,31
C     RECORD NUMBER OF DRY SLICES.
   31 PRINT 32,NXC,TIME
   32 FORMAT(1H ,I5,20H SLICES DRY AT TIME=,F8.4)
      NCH=NXA
C     HEAT CONTENT OF SKIN ABOVE CRITICAL LEVEL
  122 IF(TCRIT) 100,100,1221
 1221 IF(NS-NSTEP) 124,123,123
  123 GO TO (125,126,133,100), INHIB
  124 GO TO (125,125,100,100), INHIB
C     TRIGGER WHEN SKIN SURFACE TEMPERATURE = MAXIMUM
  125 IF(TVP-TVPO) 126,126,101
  126 IF(T(NXC+4)-TCRITD) 132,132,127
C     INTEGRATE
C     FIND SIMPSON RANGE
  127 NACA=NXC+4
      DO 202 K=NACA,M,2
      IF(T(K)-TCRITD) 204,203,202
  202 CONTINUE
      K=M
  203 K=K+2
  204 S=0.
      NVAL=K-3-(NXC+4)
      IF(NVAL-2) 210,205,205
C     SIMPSON RULE INTEGRATION
  205 SE=0.
      SO=0.
      ENV1=2*NVAL
      NAC5=NXC+5
      KM5=K-5
      DO 206 I=NAC5,KM5,2
  206 SE=SE+T(I)
      IF(NVAL-2) 209,209,207
  207 KM6=K-6
      DO 208 I=NAC6,KM6,2
  208 SO=SO+T(I)
  209 S=XS/3.*(T(NXC+4)+4.*SE+2.*SO+T(K-3)-ENV1*TCRITD)
C     CONTRIBUTION FROM TRAPEZOID AND TRIANGLE
  210 S=S+XS/2.*((TVP+T(NXC+4))/2.-TCRITD+(T(K-3)-TCRITD)**2/(T(K-3)
     1-T(K-1)))
C     DIMENSIONALIZATION FOR CAL/CM**2
      SA=CROK*CLR*CIO*CLA*S
C
  128 IF(SA-SAO) 129,130,130
  129 INHIB=3
      GO TO 100
  130 INHIB=2
      SAO=SA
      STIME=TIME
  132 IF(NS-NSTEP) 101,133,133
  133 PRINT 134,SAO,TCRIT,STIME
  134 FORMAT(1H0,37HMAX. HEAT CONTENT OF SKIN =,E12.5,20H CAL/CM**2 ABOV
     1E T-CRIT =,F5.1,12H K. AT TIME ,F8.4)
      INHIB=4
  101 TVPO=TVP
  100 RETURN
      END


      SUBROUTINE ERG
C     ROUTINE TO COMPUTE TOTAL ENERGY ABSORBED
C     IN CASE OF STEP FUNCTION OR TRUE PULSE
  900 DIMENSION ALPH(1000),AA(10),T(1000),A(1000),P(2),PA(2),
```

```
      1BETA(1000),CMC(18),CMD(18),COFC(18),COFD(18),GAM(18),GAMA(19),        ERG 0004
      2DELT(19),CC(16),DVP(18),F(3),TB(3),                                   ERG 0005
      3L(13),TEMP(10),PRES(10,12),DPT(10,12),DMP(10,12)                      ERG 0006
901   COMMON TEMP,PRES,DPT,DMP,T,TA,ALPH,BETA,P,PA,AA,CC,GAM,GAMA,DELT,     ERG 0007
      1CMC,CMD,COFC,COFD,F,TB,ALPO,ALPS,ALP,SUM2,EVAP,DV,DVP,CIO,CLK,CAP,   ERG 0008
      2DVC,CHA,G,W,WW,QG,SS,COM1,GR,QM,E,PWURR,ZETA,TEURR,TIME,CRIT,FA,     ERG 0009
      3TVP,IC,M,LA,J,MA,L,NX,NY,NTA,NTB,NTC,NAC,NXA,NXB,MXA,MXB,MXC,        ERG 0010
      4KPULSE,TCHAR,YOYM,ENDRMD,ENDCSD,TDIS,NSTEP,TAUDIN,                   ERG 0011
      5SHAPET,CKD,MS,XC,DV*FD,CKORED,CKINFD,RM,XS,CRITT,CKI,COM,UE,UO,      ERG 0012
      6COMA,ENERGD,ENERGA,ENORMA,ENDCSA,TENDAB,TENDCM,TFND,TPEND,ANSTEP     ERG 0013
      COMMON PFACT,PMXA                                                     ERG 0014
      GO TO (1,100,100,2),KPULSE                                            ERG 0015
1     ENERGD=CIO*TIME                                                       ERG 0016
3     ENERGA=ENERGD*TAUDIN                                                  ERG 0017
      PRINT 516                                                             ERG 0018
516   FORMAT(67H                      DIMENSIONLESS          ABSOLUTE       ERG 0019
      XTIME SCALE )                                                         ERG 0020
      PRINT 521,ENERGD,ENERGA                                               ERG 0021
521   FORMAT(21H TOTAL ENERGY        =,F8.4,13H CAL/CM2SEC  ,F8.4,8H CAL/ERG 0022
      XCM2)                                                                 ERG 0023
100   RETURN                                                                ERG 0024
2     IF (TDIS-.3) 10,10,11                                                 ERG 0025
10    ENERGD=CIO*TCHAR*.2829*TDIS**2                                        ERG 0026
      GO TO 3                                                               ERG 0027
11    IF (TDIS-.65) 12,12,13                                                ERG 0028
12    ENERGD=CIO*TCHAR*(.052129+.66*TDIS**2-.347*TDIS)                      ERG 0029
      GO TO 3                                                               ERG 0030
13    IF (TDIS-1.4) 14,14,15                                                ERG 0031
14    ENERGD=CIO*TCHAR*(-.4903683+TDIS-.6733333*(TDIS-1.05)**3)             ERG 0032
      GO TO 3                                                               ERG 0033
15    ENERGD=CIO*TCHAR*(2.695877-2.240625*TDIS**(-.64))                     ERG 0034
      GO TO 3                                                               ERG 0035
      END                                                                   ERG 0036
```

```
*       FAP
        COUNT 4
        ENTRY (F2PM)                                                        F2PM    1
*       DUMMY (F2PM)                                                        F2PM    2
(F2PM)  CALL EXIT                                                           F2PM    3
        END                                                                 F2PM    4
```

APPENDIX F

SUMMARY OF COMPUTER SOLUTIONS ON MOIST CLOTH - SKIN SIMULANT SYSTEM

The theoretical results for the temperature response of the moist opaque cloth - skin simulant system are summarized in the following diagrams. The listings of the numerical solutions and the master diagrams are in the files of the Fuels Research Laboratory, Department of Chemical Engineering, MIT.

For reference see List of Figures.

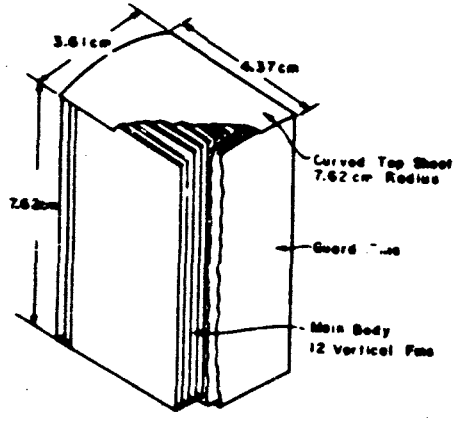

FIG. I.5 SKIN SIMULANT NO. 10

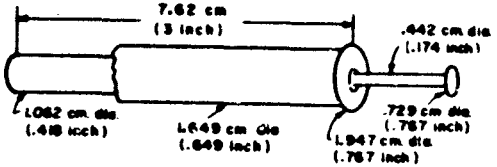

(a) Simulant proper (Inner Cylinder pulled out Outer Guard Cylinder Cut-away)

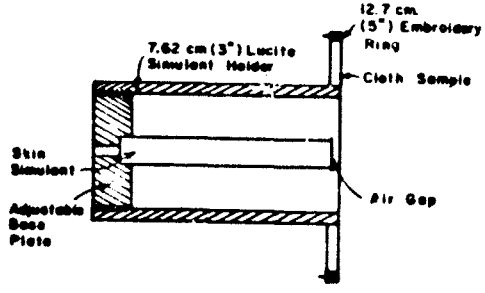

(b) Assembly

FIG. I.6 SKIN SIMULANT NO. II B

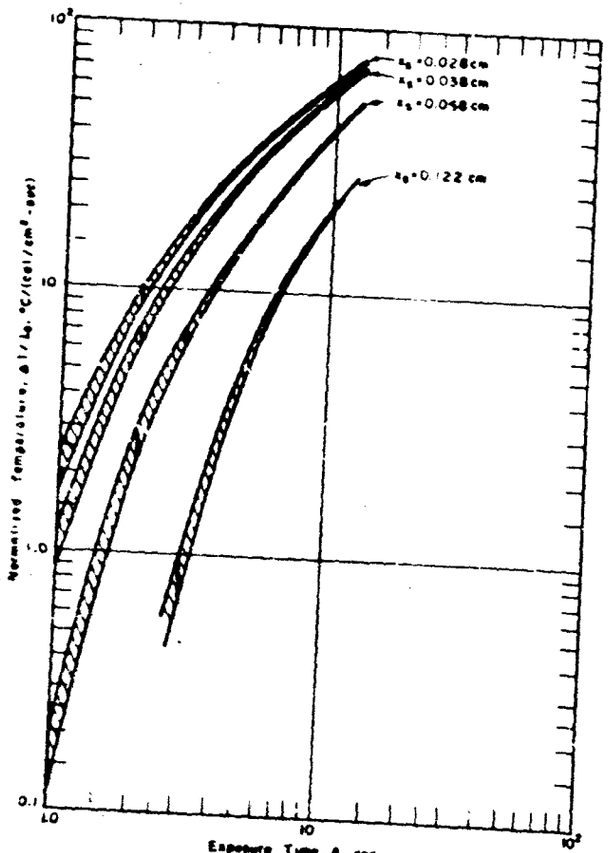

FIG 17 EXPERIMENTAL RESULTS ON DRY OPAQUE (DEEP BLACK, BLACK, DARK GRAY) CLOTH - SKIN SIMULANT SYSTEM

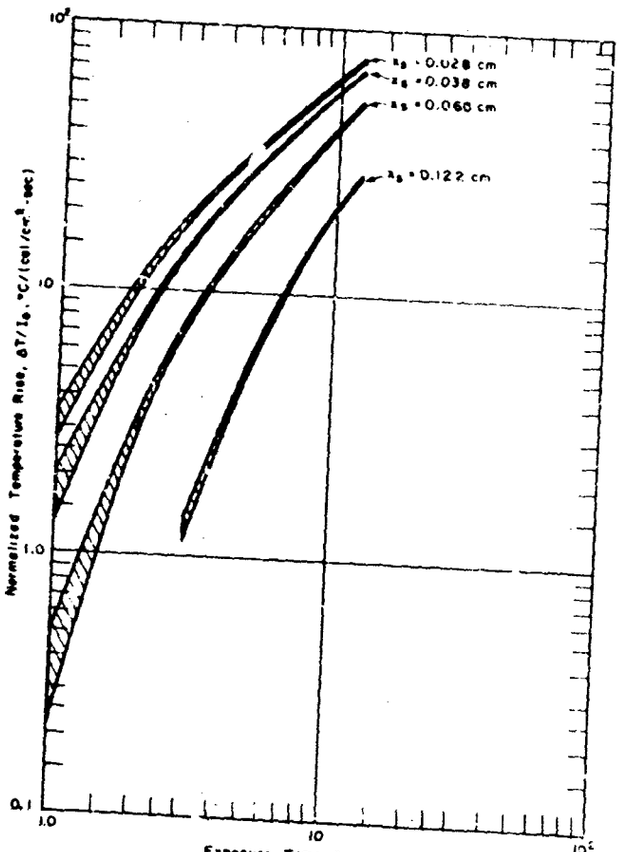

FIG. 18 EXPERIMENTAL RESULTS ON DRY MEDIUM GRAY CLOTH-SKIN SIMULANT SYSTEM

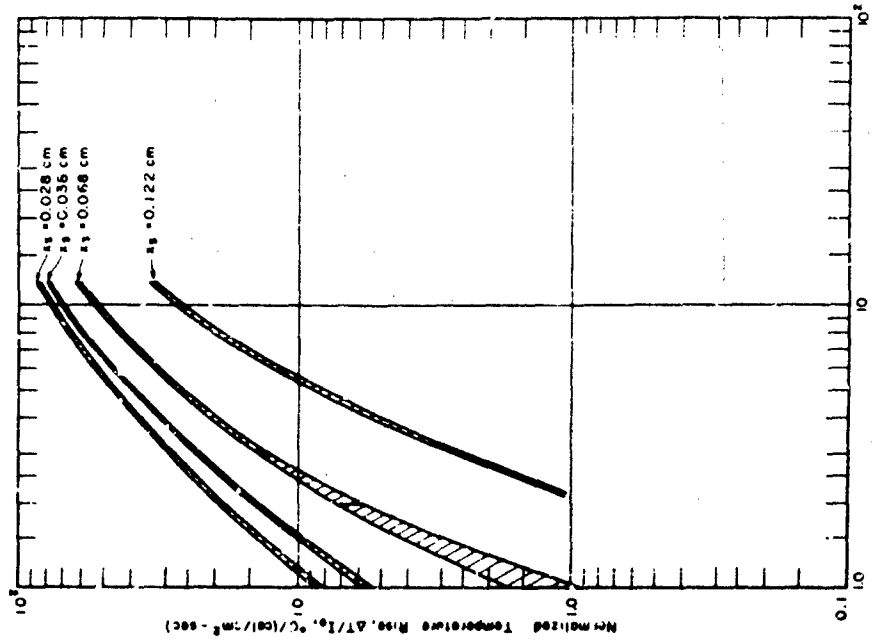

FIG. 8 EXPERIMENTAL RESULTS ON DRY WHITE (WITH CMC) CLOTH-SKIN SIMULANT SYSTEM

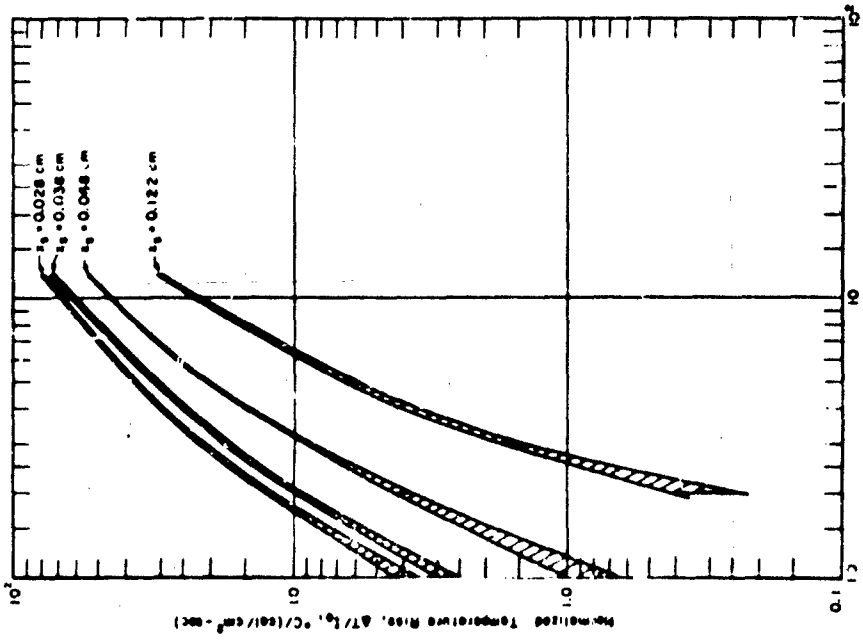

FIG. 9 EXPERIMENTAL RESULTS ON DRY LIGHT GREY CLOTH-SKIN SIMULANT SYSTEM

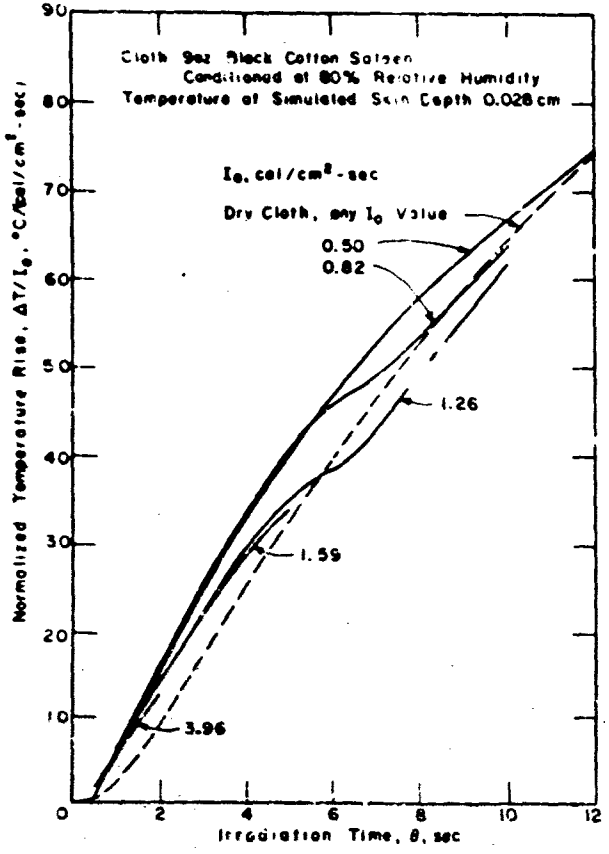

FIG. I.11 HEAT TRANSFER TO SKIN SIMULANT THROUGH MOIST OPAQUE CLOTH

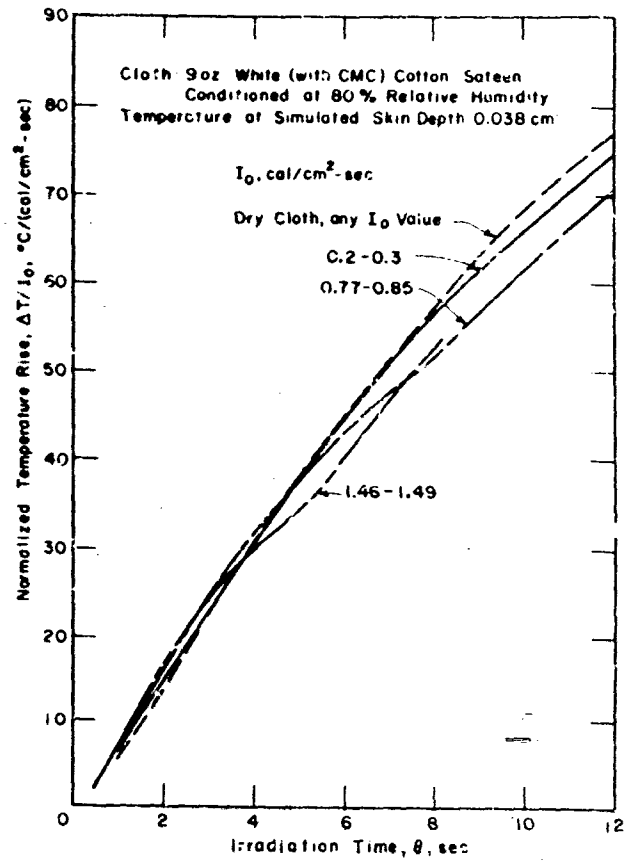

FIG. I.12 HEAT TRANSFER TO SKIN SIMULANT THROUGH MOIST DIATHERMANOUS CLOTH

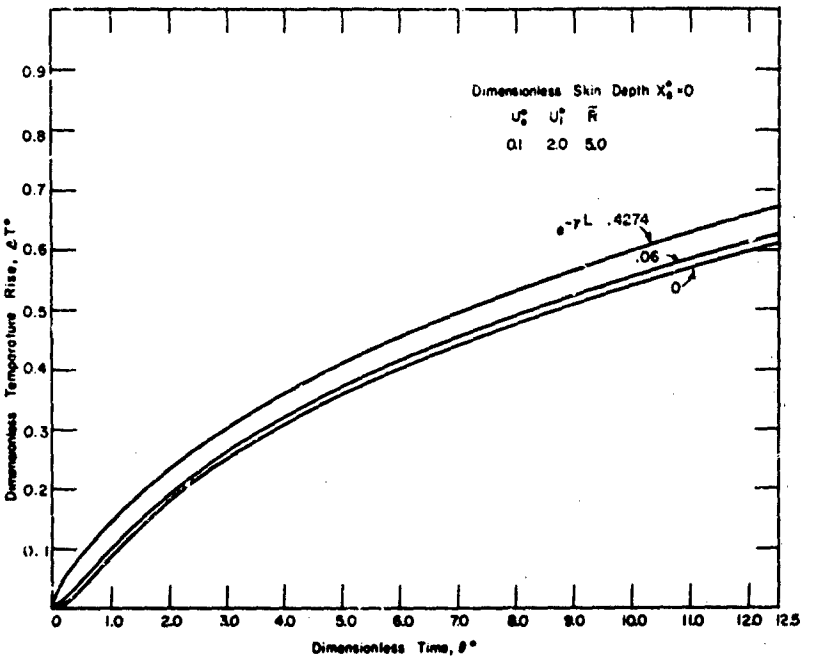

FIG. 1.13 EFFECT OF CLOTH DIATHERMANCY ON THE HEAT TRANSFER TO THE SKIN SIMULANT

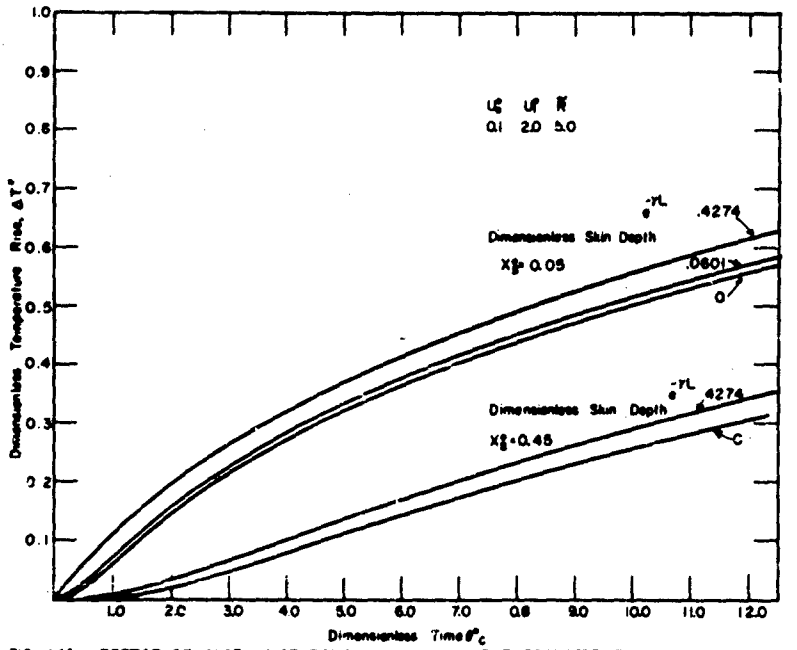

FIG 1.14 EFFECT OF CLOTH DIATHERMANCY ON THE HEAT TRANSFER TO THE SKIN SIMULANT

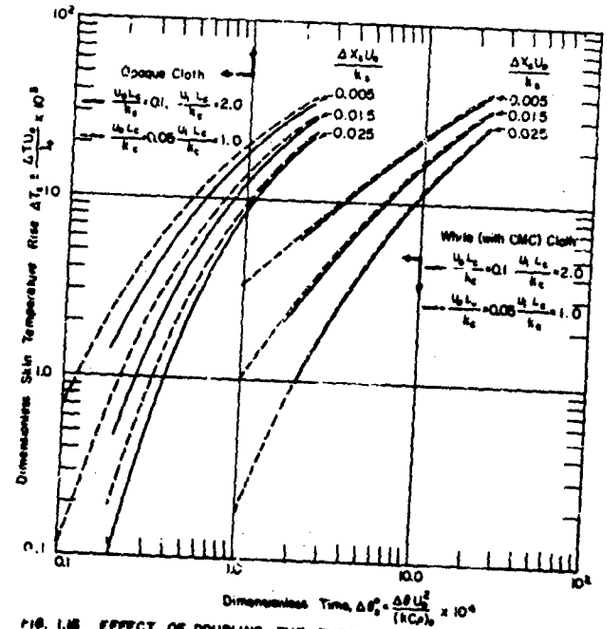

FIG. 1.15 EFFECT OF DOUBLING THE THERMAL CONDUCTANCE OF CLOTH ON THE HEAT TRANSFER TO THE SKIN SIMULANT.

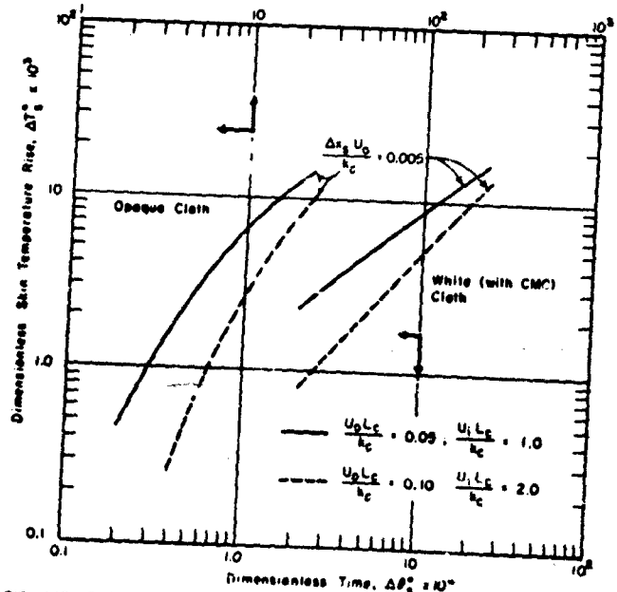

FIG. 1.16 EFFECT OF HALVING THE THICKNESS OF CLOTH ON THE HEAT TRANSFER TO THE SKIN SIMULANT

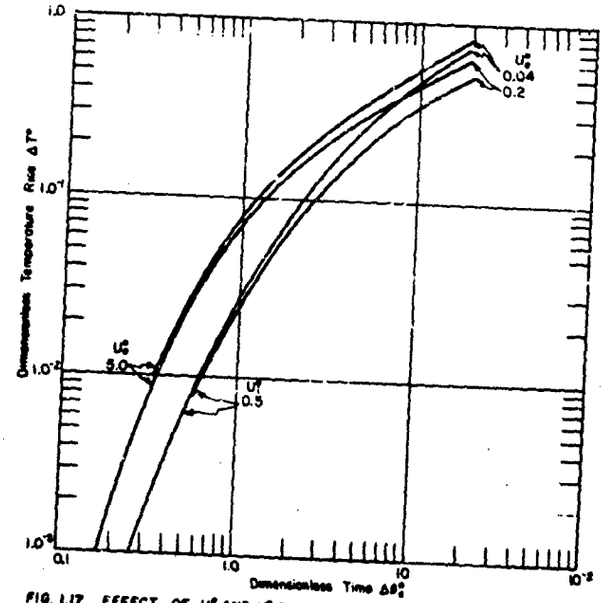

FIG. 1.17 EFFECT OF U_o^* AND U_i^* ON THE HEAT TRANSFER TO SIMULANT THROUGH DRY OPAQUE CLOTH

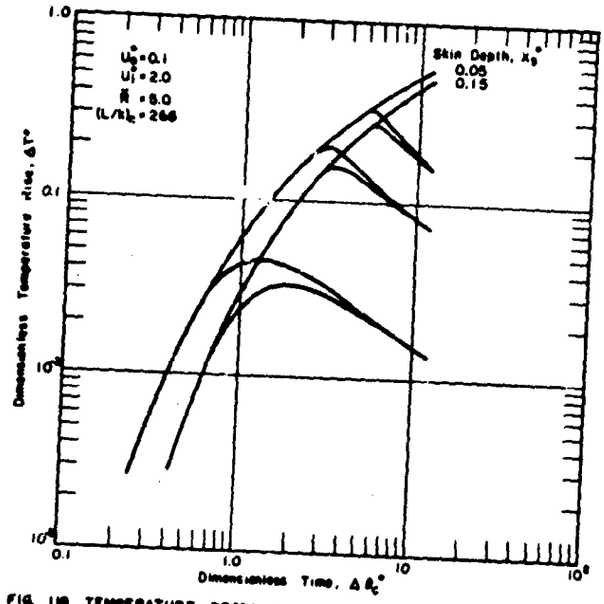

FIG. 1.18 TEMPERATURE RESPONSE IN SKIN SIMULANT DURING AND AFTER IRRADIATION. SYSTEM: DRY OPAQUE CLOTH IN "CONTACT" WITH SKIN SIMULANT

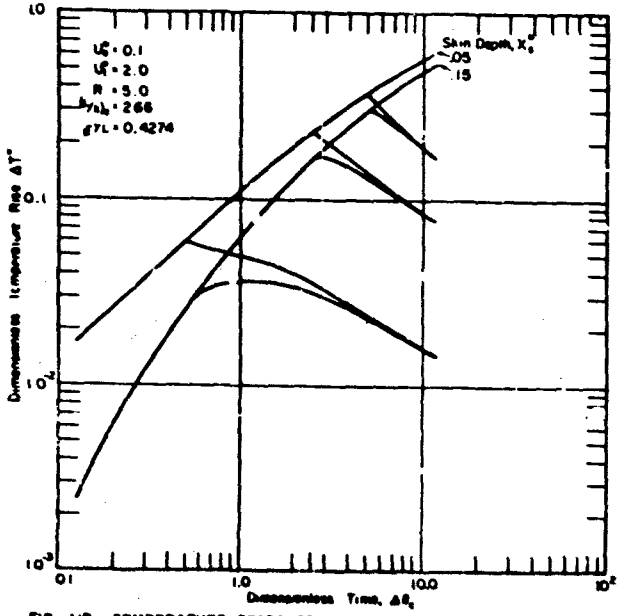

FIG. L19 TEMPERATURE RESPONSE IN SKIN SIMULANT DURING AND AFTER IRRADIATION. SYSTEM: DRY WHITE (WITH CMC) CLOTH IN "CONTACT" WITH SKIN SIMULANT

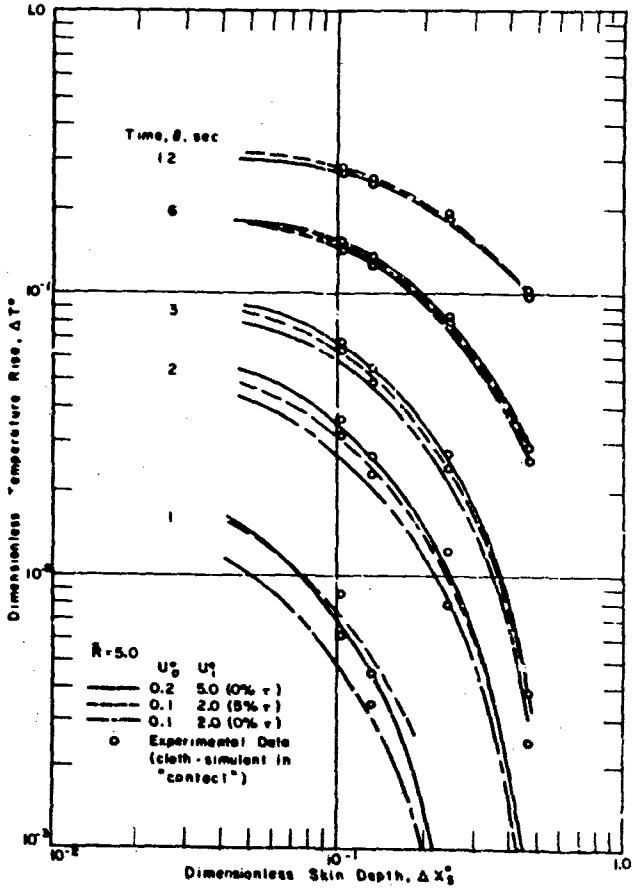

FIG. L20 COMPARISON OF EXPERIMENTAL RESULTS ON DRY OPAQUE CLOTH-SKIN SIMULANT SYSTEM WITH THEORETICAL ANALYSIS. EFFECT OF U_0^*, U_1^* AND τ

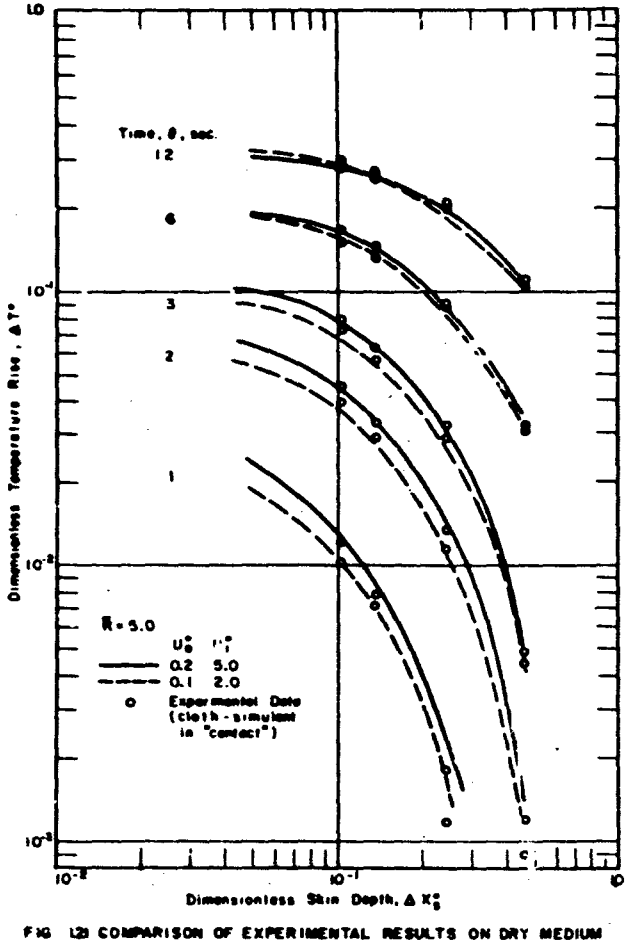

FIG. 121 COMPARISON OF EXPERIMENTAL RESULTS ON DRY MEDIUM GRAY CLOTH - SIMULANT SYSTEM WITH THEORETICAL ANALYSIS. EFFECT OF U°_{0} AND U°_{1}

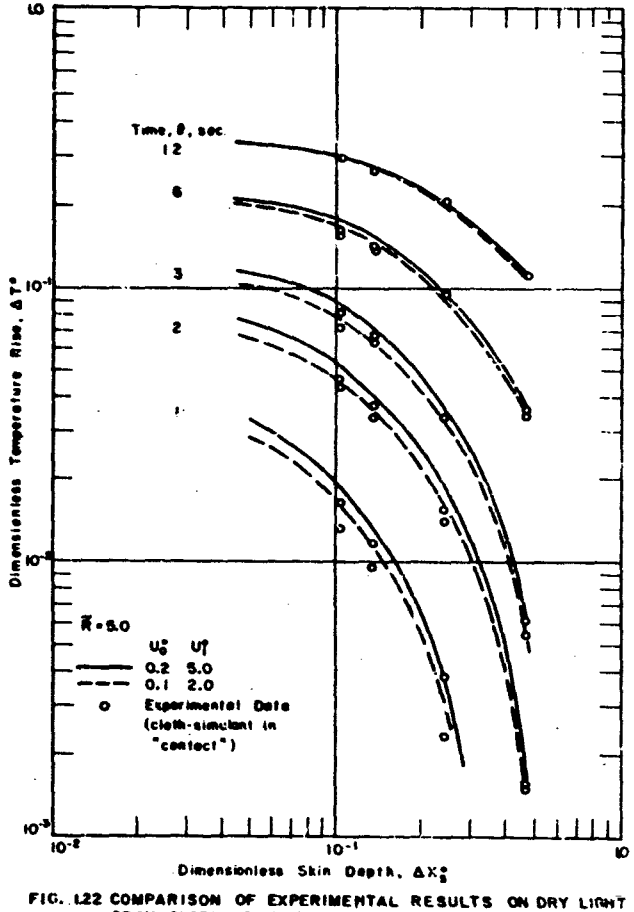

FIG. 122 COMPARISON OF EXPERIMENTAL RESULTS ON DRY LIGHT GRAY CLOTH - SKIN SIMULANT SYSTEM WITH THEORETICAL ANALYSIS. EFFECT OF U°_{0} AND U°_{1}

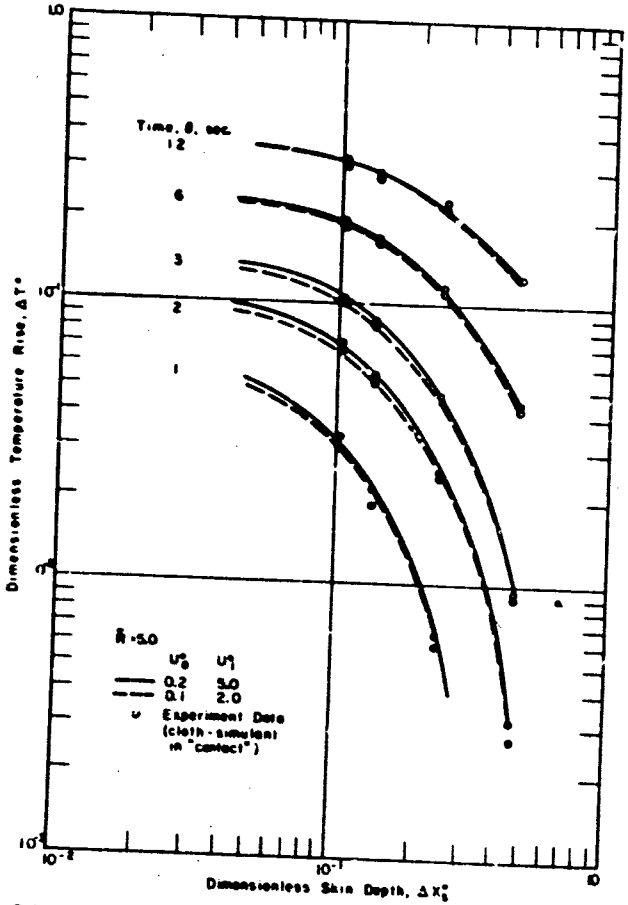

FIG. 1.23 COMPARISON OF EXPERIMENTAL RESULTS ON DRY WHITE (WITH CMC) CLOTH-SKIN SIMULANT SYSTEM WITH THEORETICAL ANALYSIS. EFFECT OF U_0° AND U_1°

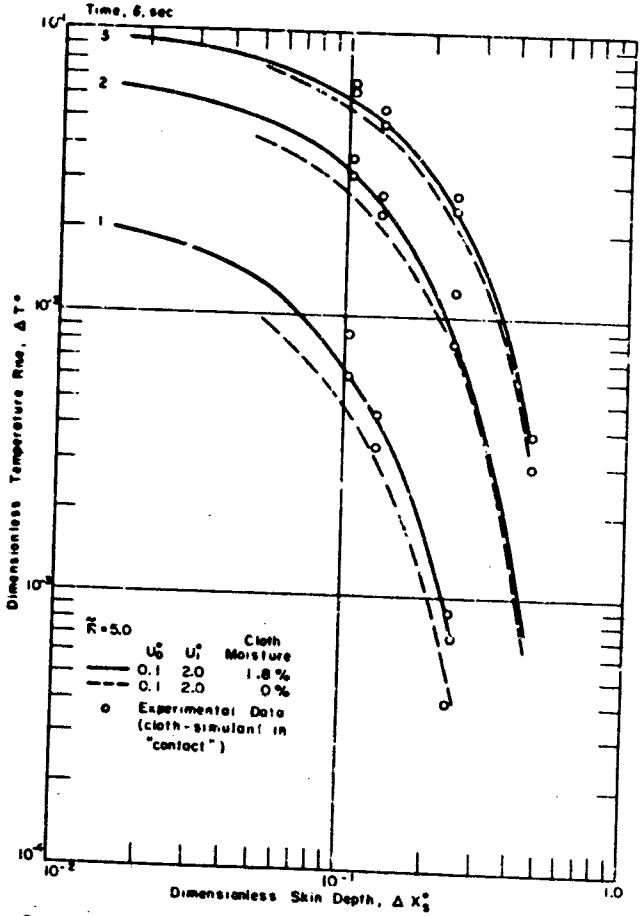

FIG. 1.24 COMPARISON OF EXPERIMENTAL RESULTS ON DRY OPAQUE CLOTH-SKIN SIMULANT SYSTEM WITH THEORETICAL ANALYSIS. EFFECT OF RESIDUAL MOISTURE IN CLOTH

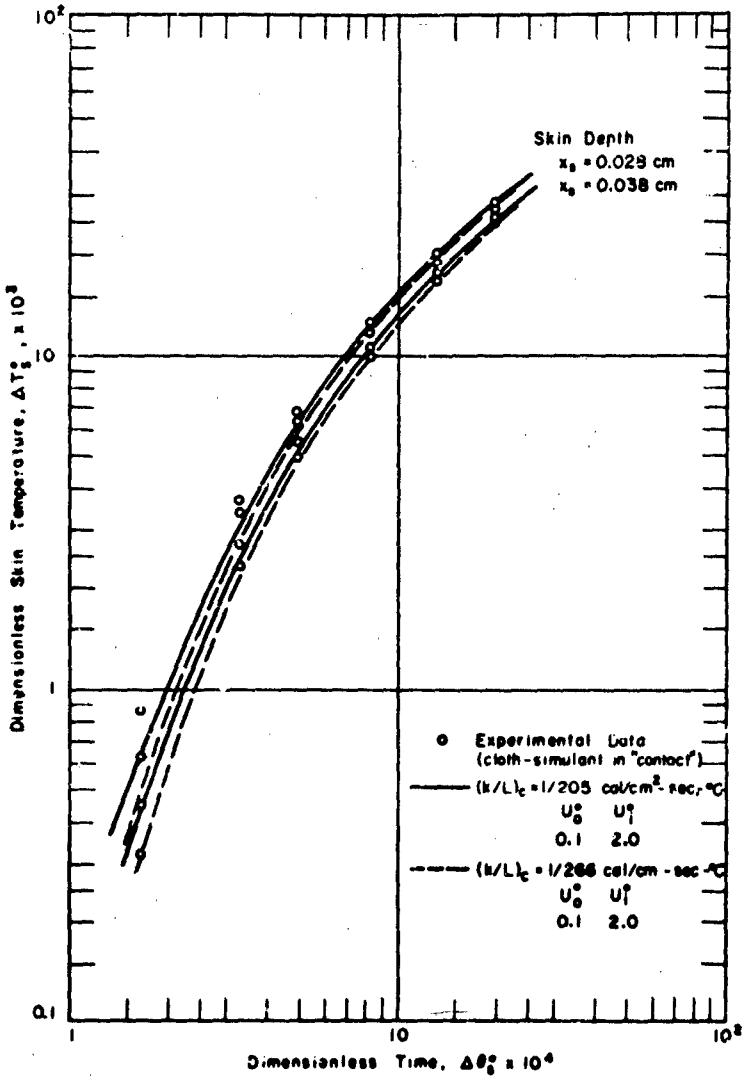

FIG 12B COMPARISON OF EXPERIMENTAL RESULTS ON DRY OPAQUE CLOTH - SKIN SIMULANT SYSTEM WITH THEORETICAL ANALYSIS. EFFECT OF THERMAL CONDUCTANCE OF CLOTH.

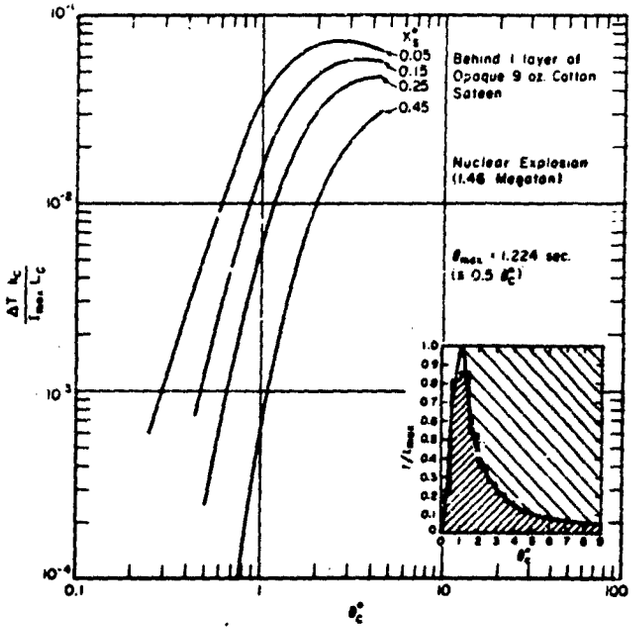

FIG. 1.26 TEMPERATURE RESPONSE IN CLOTHED SKIN SIMULANT EXPOSED TO NON-SQUARE WAVE RADIATION (NUCLEAR EXPLOSION PULSE)

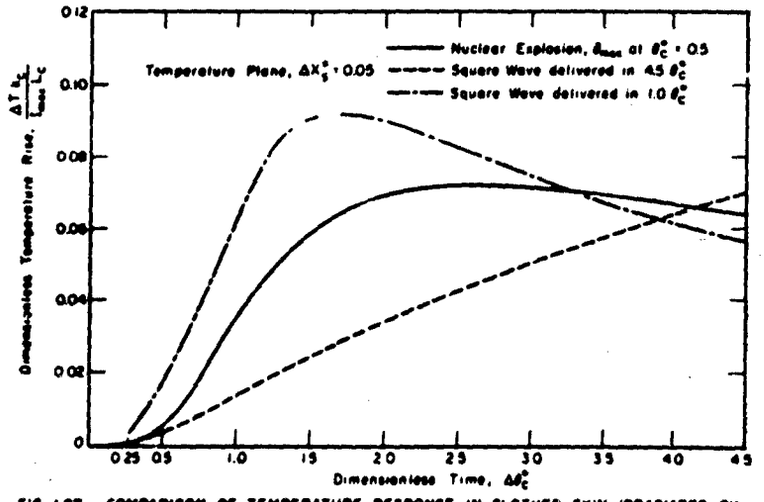

FIG. 1.27 COMPARISON OF TEMPERATURE RESPONSE IN CLOTHED SKIN IRRADIATED BY SQUARE WAVE RADIATION AND RADIATION FROM A NUCLEAR EXPLOSION

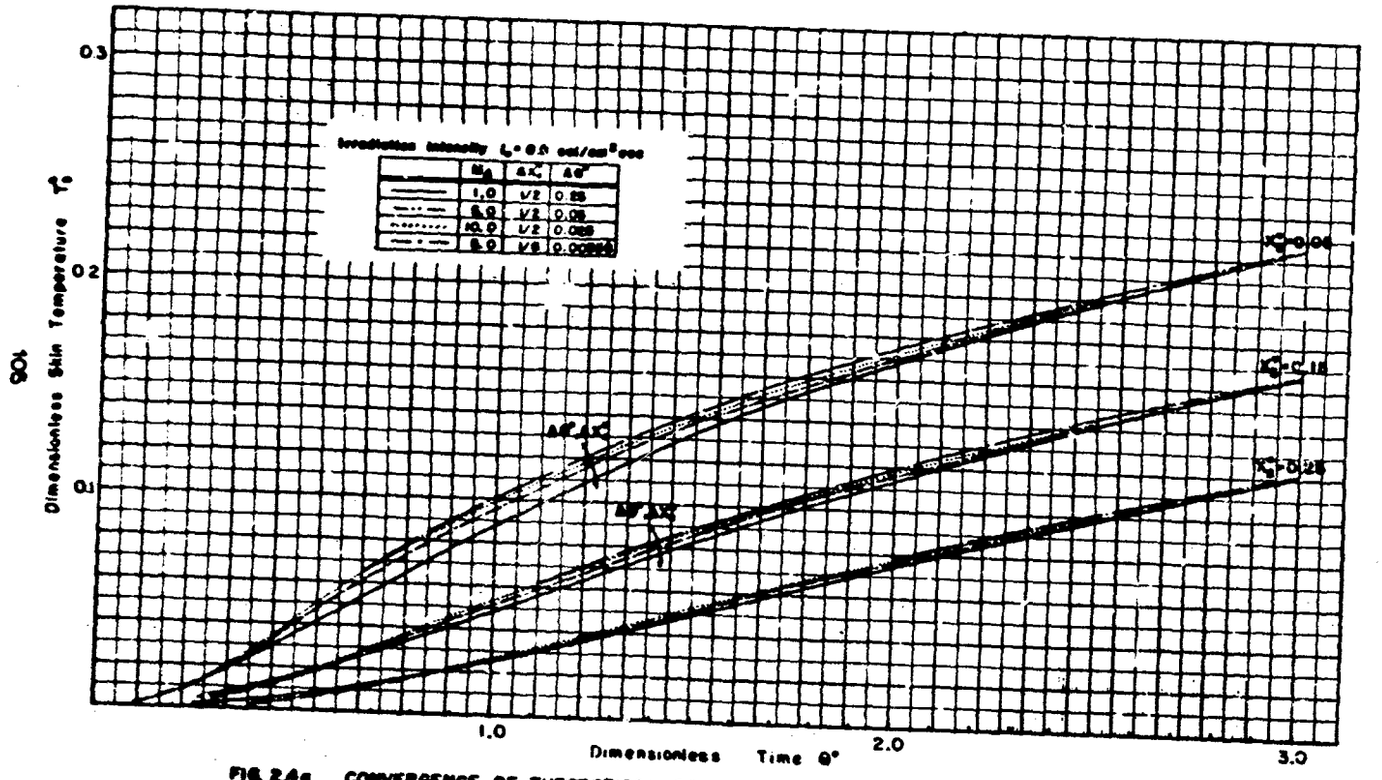

FIG. 2.4a CONVERGENCE OF THEORETICAL SOLUTION. EFFECT OF M_A, $\Delta X_c'$ AND $\Delta\theta^*$ ON TEMPERATURE RESPONSE OF SKIN SIMULANT.

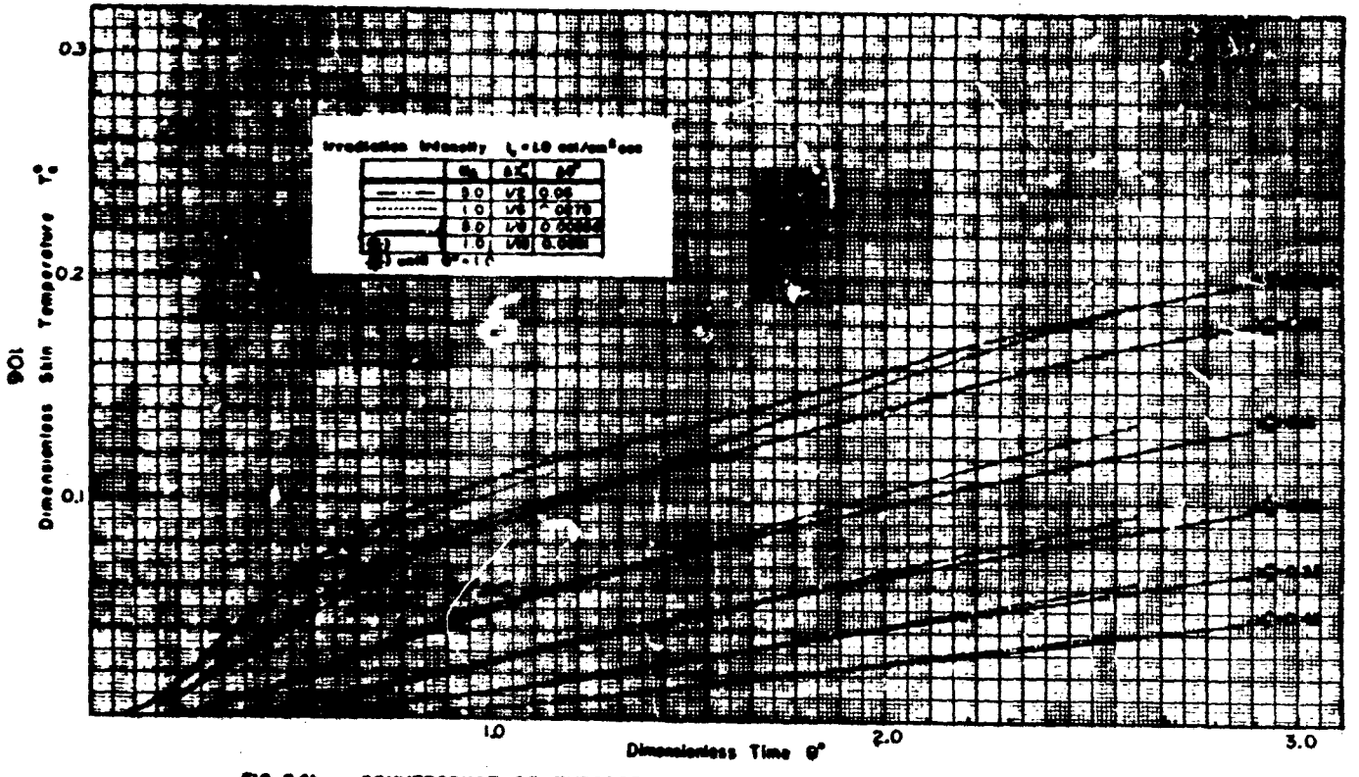

FIG. 2.4b CONVERGENCE OF THEORETICAL SOLUTION.
EFFECT OF M_A, ΔX_i^* AND $\Delta\theta^*$ ON TEMPERATURE RESPONSE OF SKIN SIMULANT.

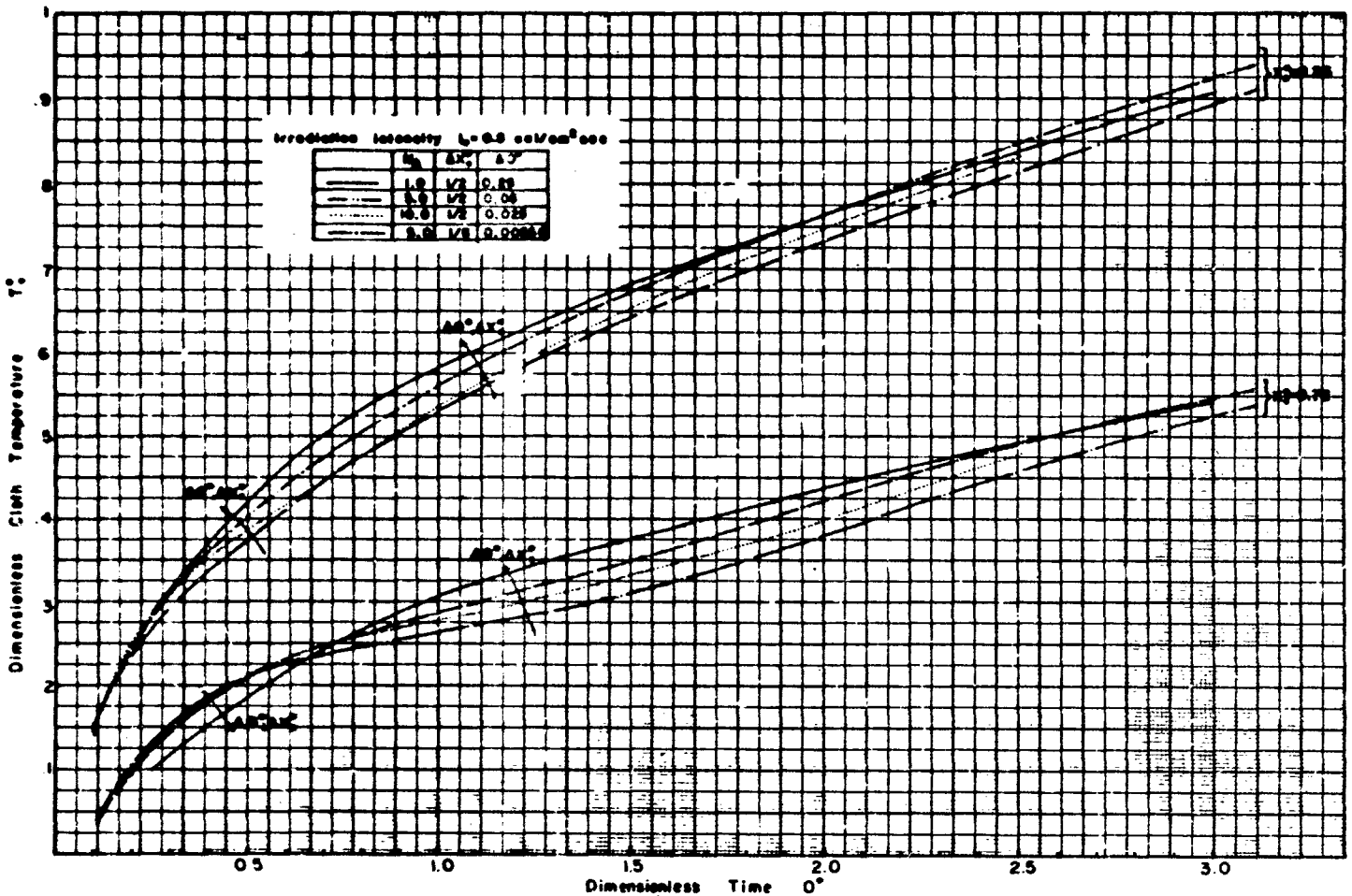

FIG. 2.4c CONVERGENCE OF THEORETICAL SOLUTION.
EFFECT OF Ma, ΔX_c° AND $\Delta\theta^\circ$ ON TEMPERATURE RESPONSE OF CLOTH.

FIG. 2.5 TRIDIAGONAL EQUATION SYSTEM
FOR SOLUTION OF EQUATION (2.14)

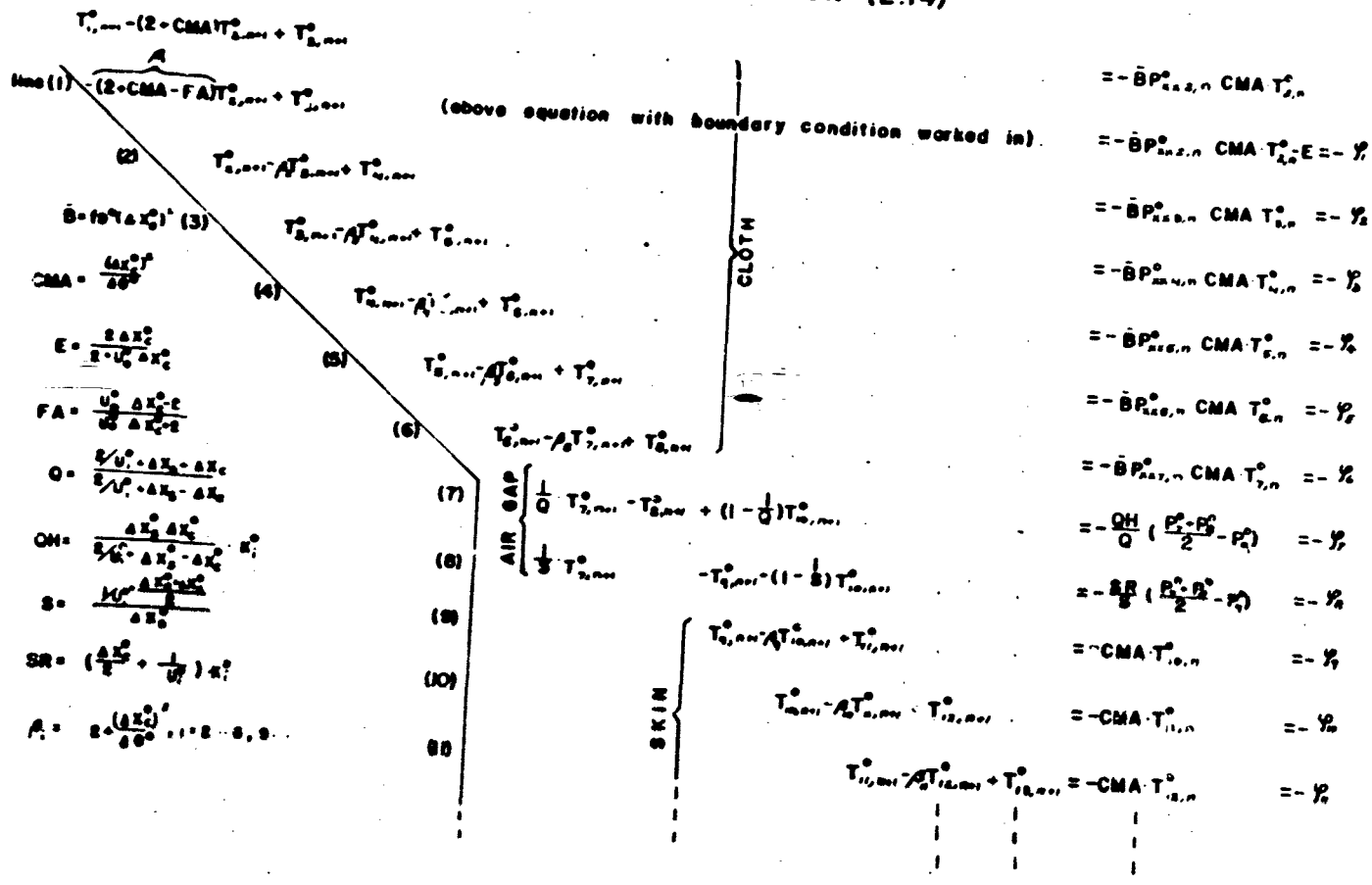

FIG. 2.6 BIDIAGONAL EQUATION SYSTEM
FOR SOLUTION OF EQUATION (2.14)

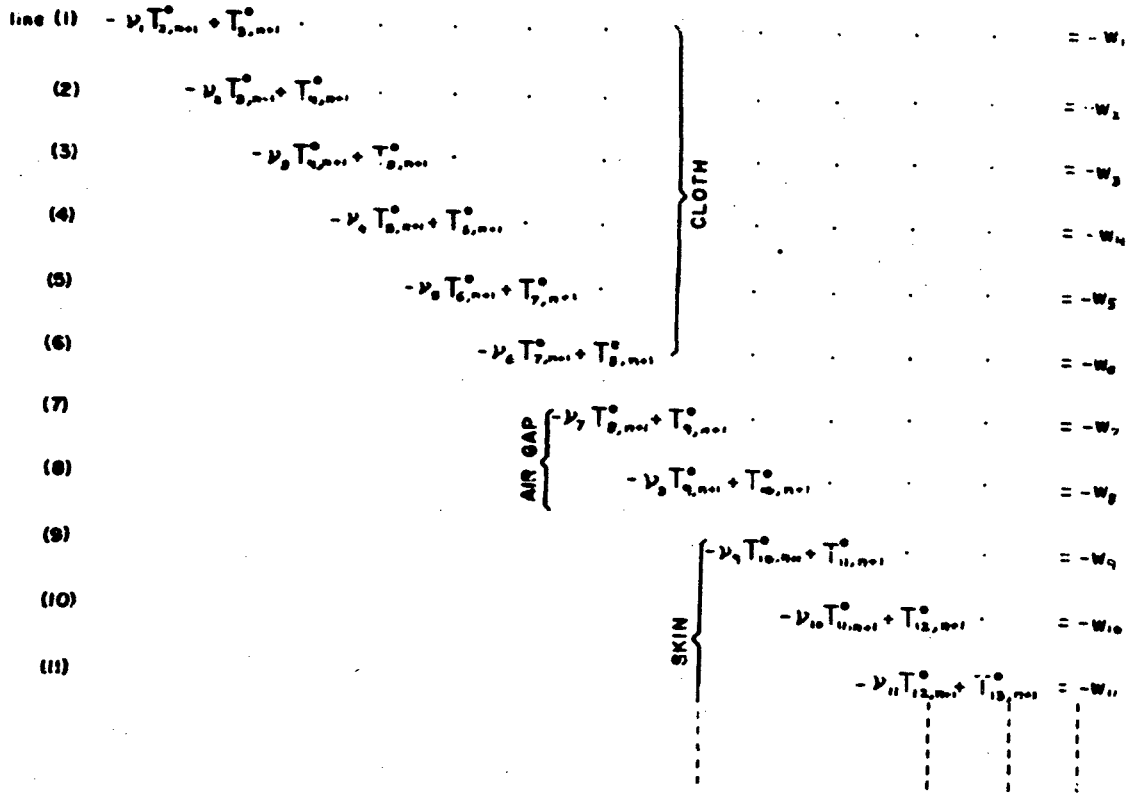

FIG. 2.7 FLOW-CHART OF MAIN PROGRAM
MOIST CLOTH-SKIN SIMULANT SYSTEM

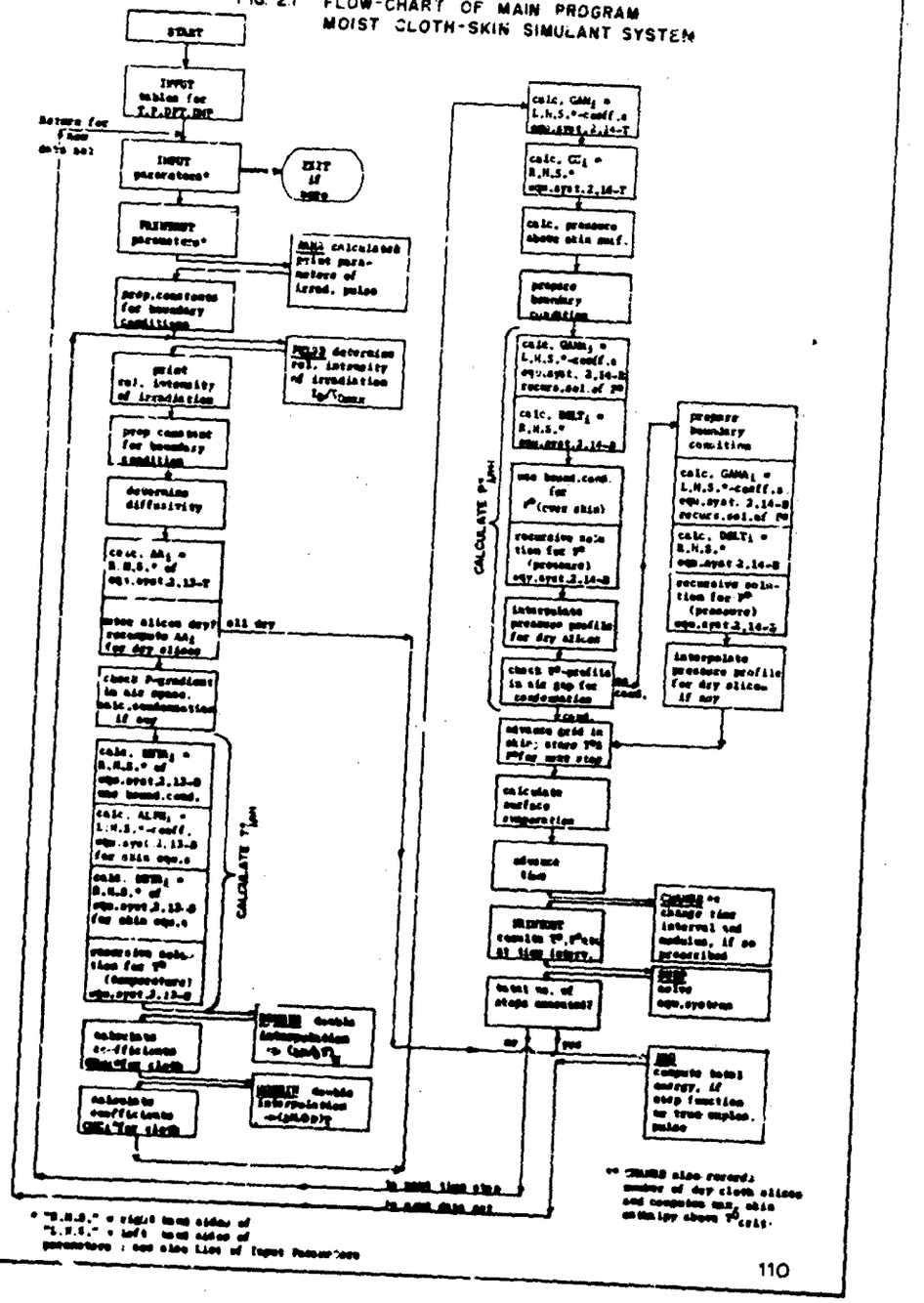

FIG. 2.8 FLOW-CHART OF SUBROUTINE SUBP
MOIST CLOTH-SKIN SIMULANT SYSTEM

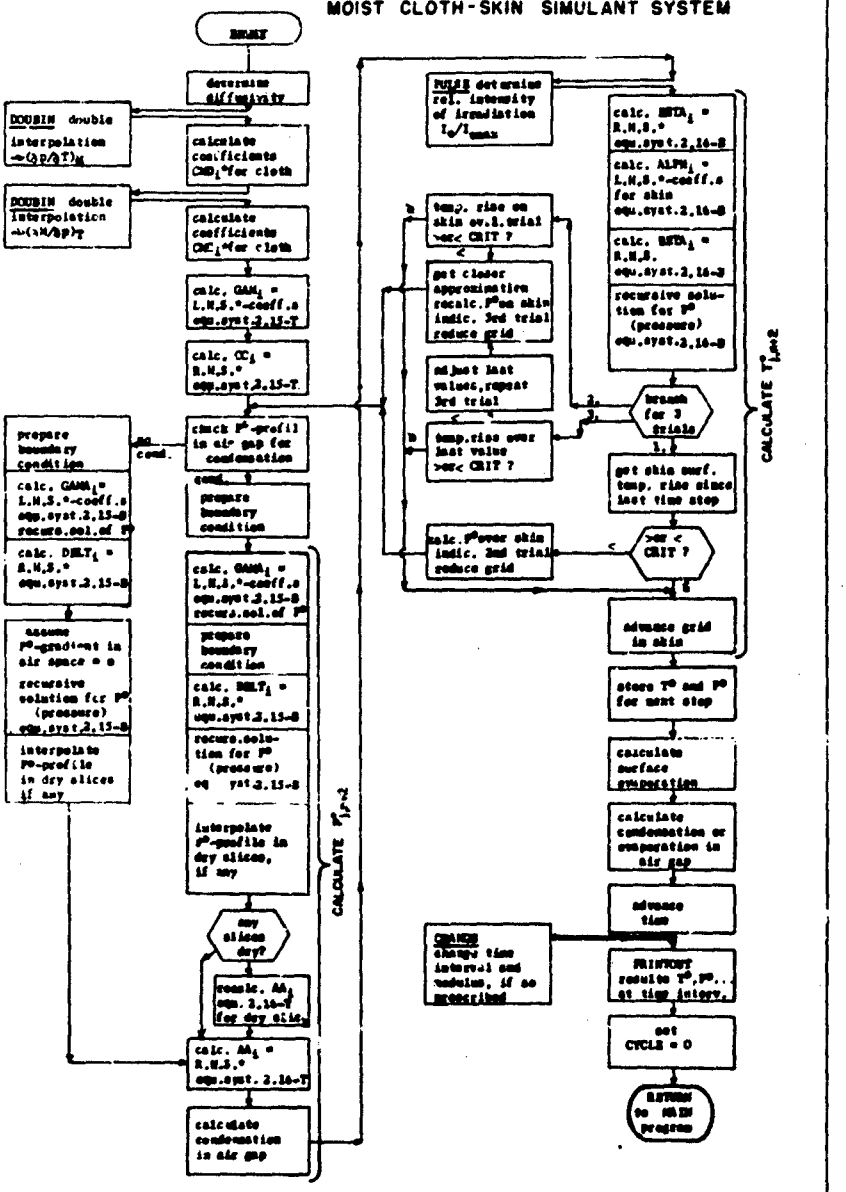

* "R.H.S." = right hand sides of
"L.H.S." = left hand sides of

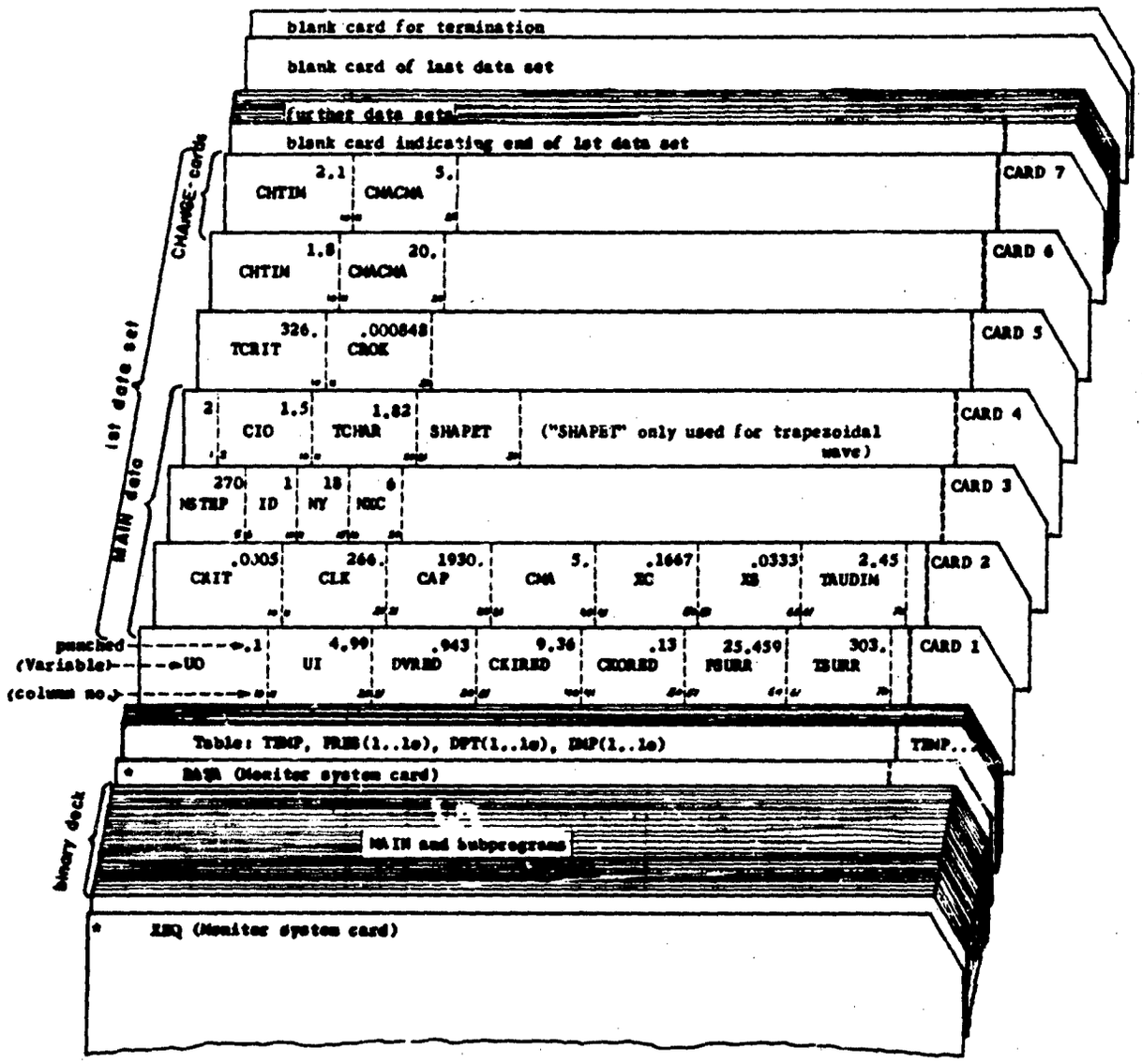

FIG. 2.9 MAKE-UP OF RUN CARD DECK

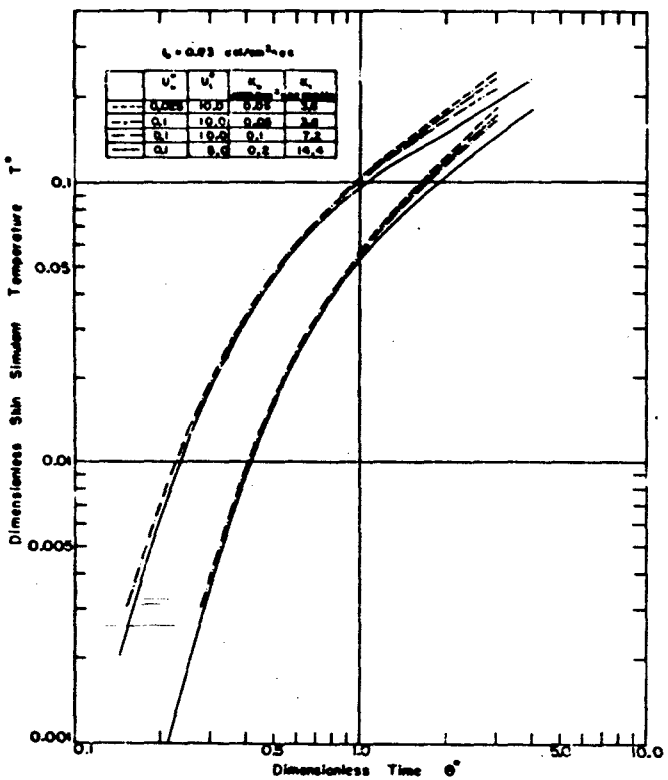

FIG. 2.10 THEORETICAL SOLUTION FOR MOIST CLOTH - SKIN SIMULANT SYSTEM (OPAQUE). INFLUENCE OF HEAT AND MASS TRANSFER COEFFICIENTS.

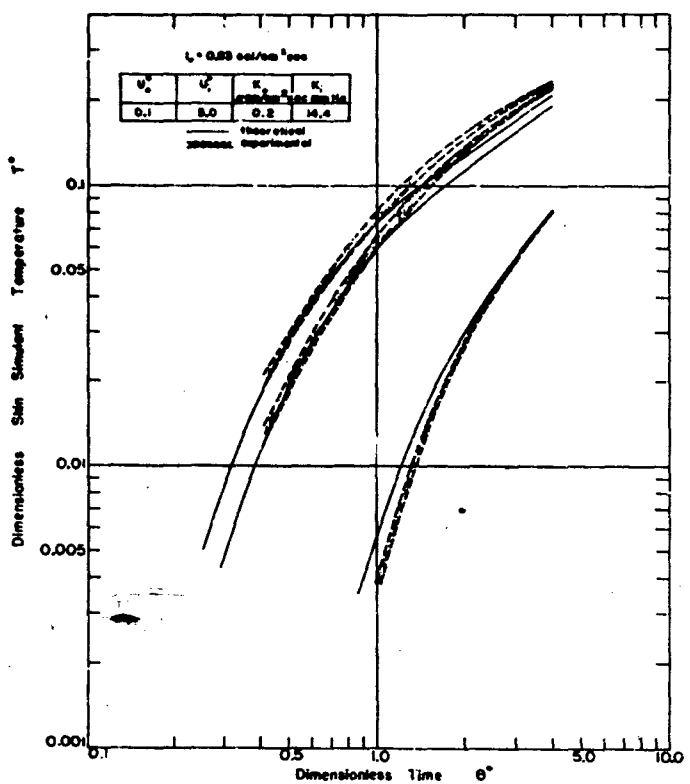

FIG. 2.11 TEMPERATURE RESPONSE OF MOIST CLOTH - SKIN SIMULANT SYSTEM (OPAQUE). COMPARISON OF THEORETICAL AND EXPERIMENTAL RESULTS.

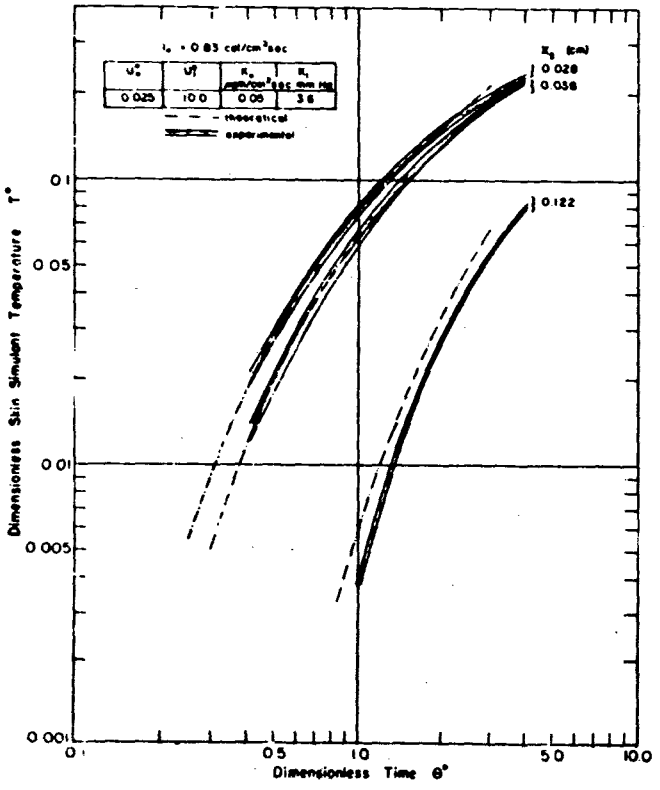

FIG. 2.12 TEMPERATURE RESPONSE OF MOIST CLOTH - SKIN SIMULANT SYSTEm (OPAQUE). COMPARISON OF THEORETICAL AND EXPERIMENTAL RESULTS.

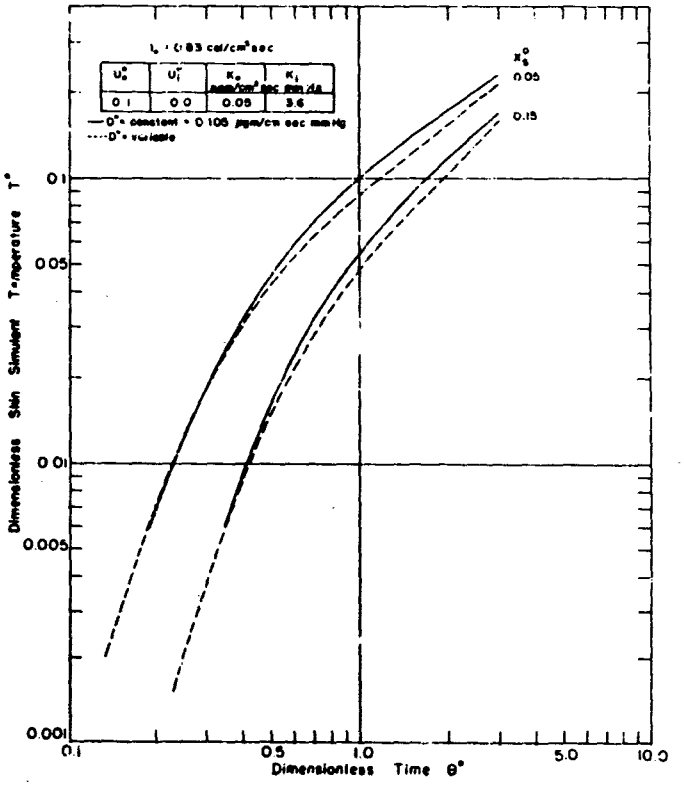

FIG. 2.13 THEORETICAL SOLUTION FOR MOIST CLOTH - SKIN SIMULANT SYSTEM (OPAQUE). INFLUENCE OF FIXED OR VARIABLE DIFFUSIVITY.

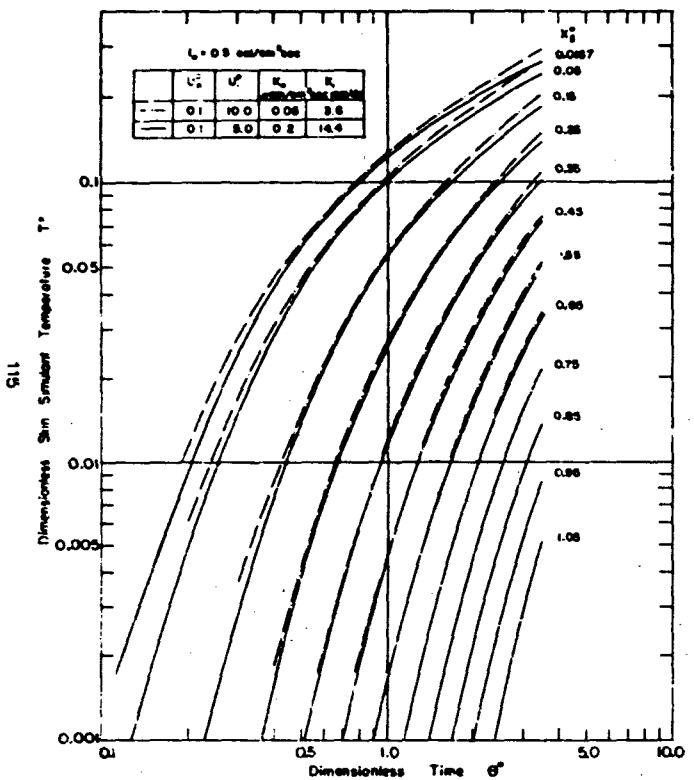

FIG. 2.14 THEORETICAL SOLUTION FOR MOIST CLOTH - SKIN SYSTEM (OPAQUE). INFLUENCE OF TRANSFER COEFFICIENTS.

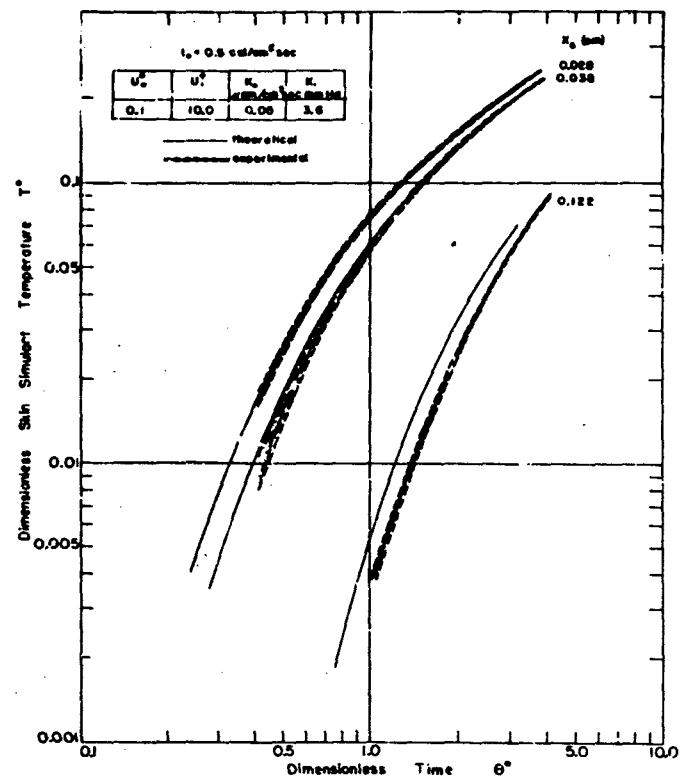

FIG. 2.15 TEMPERATURE RESPONSE OF MOIST CLOTH - SKIN SIMULANT SYSTEM (OPAQUE). COMPARISON OF THEORETICAL AND EXPERIMENTAL RESULTS.

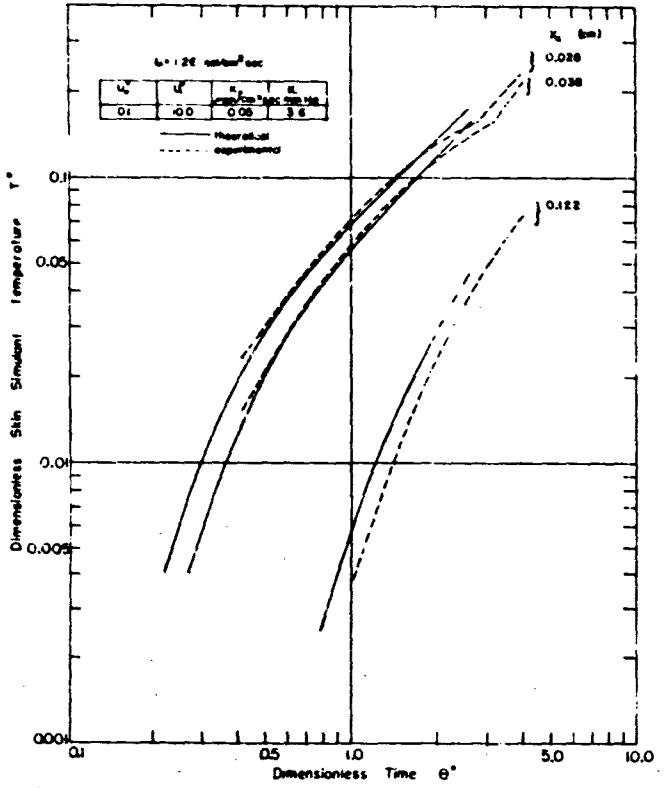

FIG. 2.16 TEMPERATURE RESPONSE OF MOIST CLOTH - SKIN SIMULANT SYSTEM (OPAQUE). COMPARISON OF THEORETICAL AND EXPERIMENTAL RESULTS.

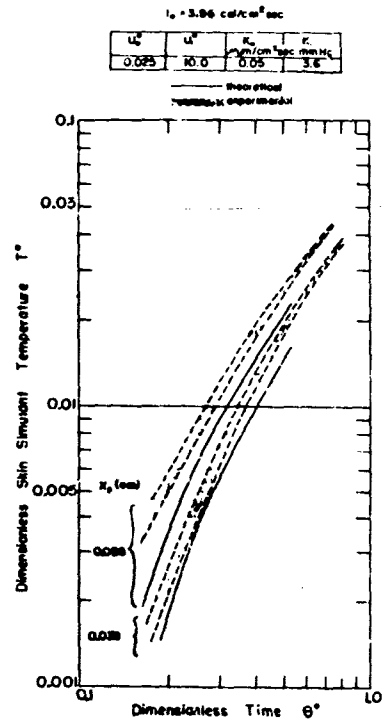

FIG. 2.17 TEMPERATURE RESPONSE OF MOIST CLOTH - SKIN SIMULANT SYSTEM (OPAQUE). COMPARISON OF THEORETICAL AND EXPERIMENTAL RESULTS.

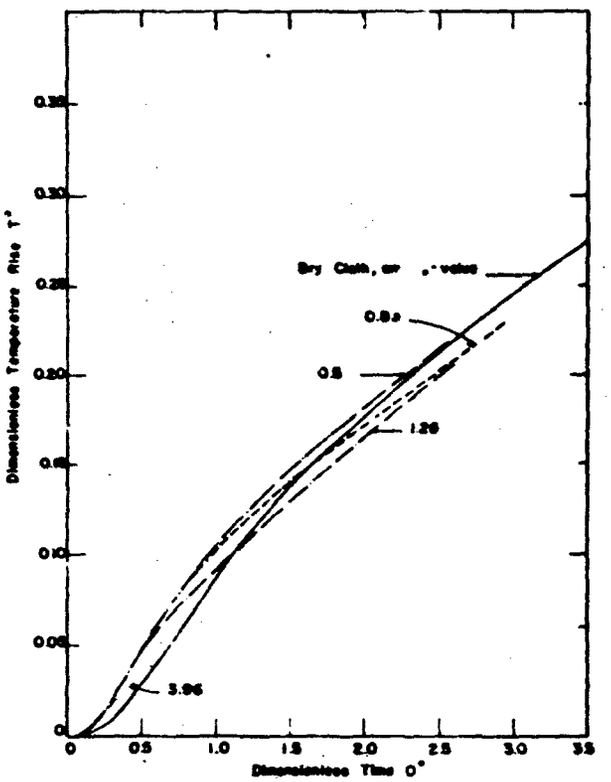

FIG 2.18 EFFECT OF INTENSITY ON THE TEMPERATURE RESPONSE OF A MOIST CLOTH-SKIN SIMULANT SYSTEM. (THEORETICAL SOLUTION)
CLOTH = OPAQUE. RELATIVE HUMIDITY = 9.1%
TEMPERATURE = 30°C

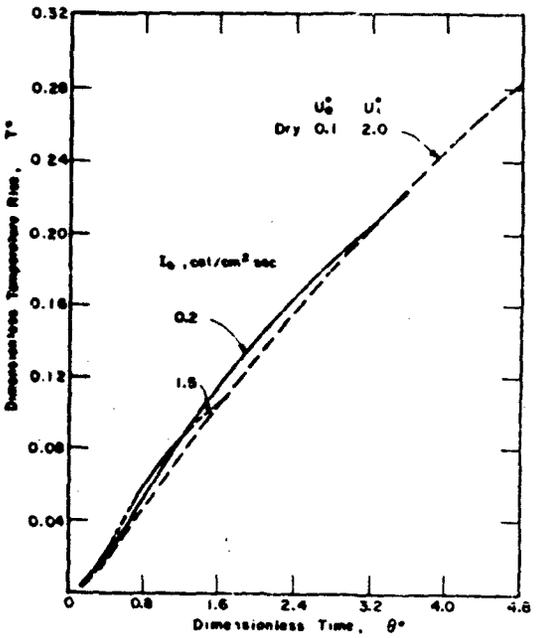

FIG 2.19 EFFECT OF INTENSITY ON THE TEMPERATURE RESPONSE OF A MOIST CLOTH-SKIN SIMULANT SYSTEM. (THEORETICAL SOLUTION)
CLOTH = WHITE, W-4, 9.1% MOISTURE, 80% RELATIVE HUMIDITY, T_0 = 30°C
TEMPERATURE RESPONSE AT X_0^* = 0.15

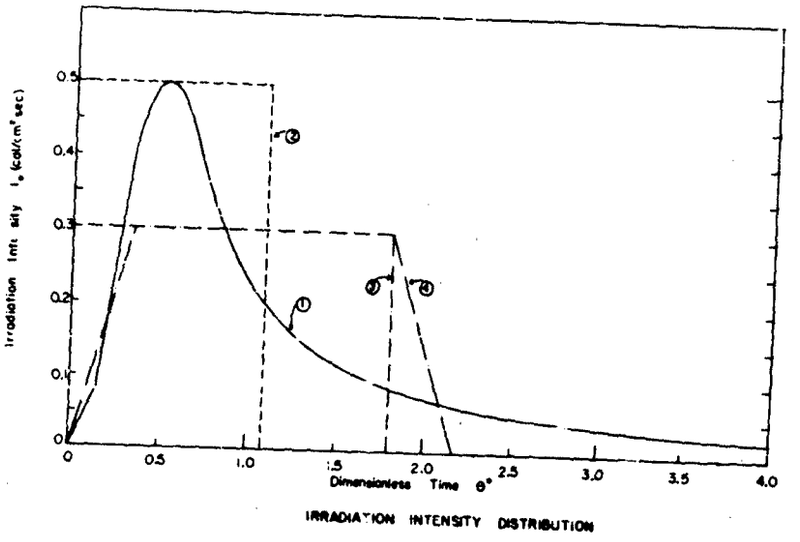

IRRADIATION INTENSITY DISTRIBUTION

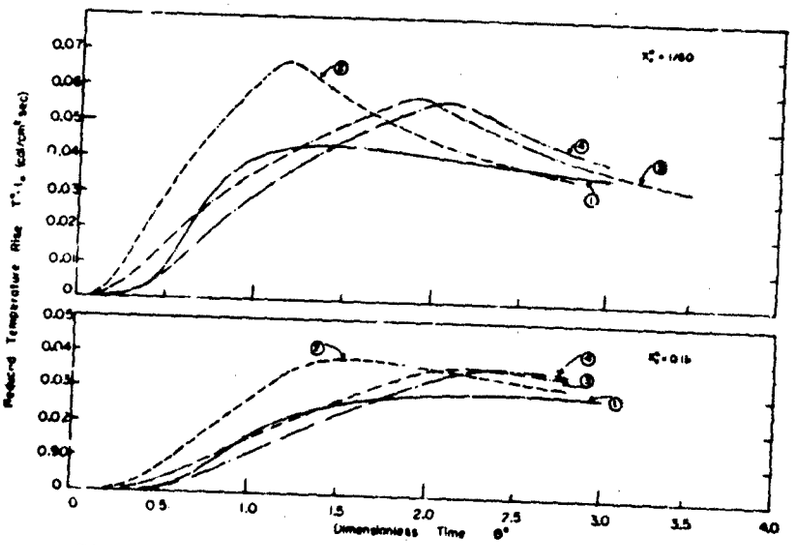

FIG 2.20 TEMPERATURE RESPONSE OF A MOIST OPAQUE CLOTH - SKIN SIMULANT SYSTEM. INFLUENCE OF IRRADIATION PULSE SHAPE; PULSE AREA = 0.545 cal/cm² sec

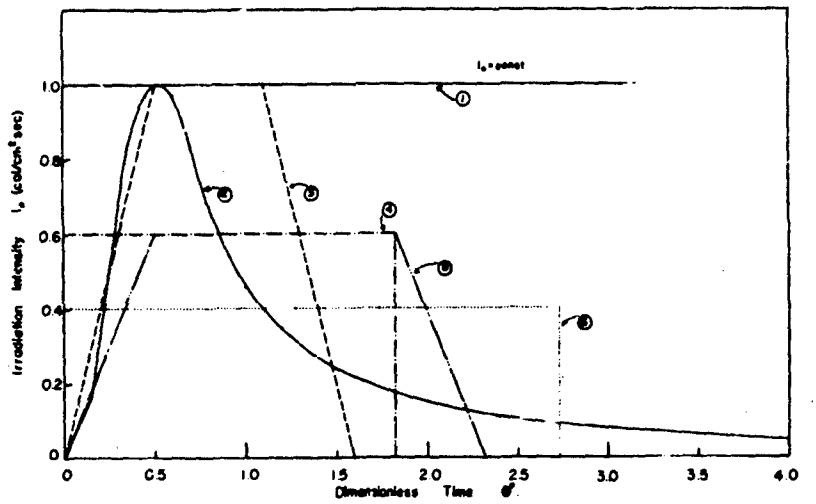

IRRADIATION INTENSITY DISTRIBUTION

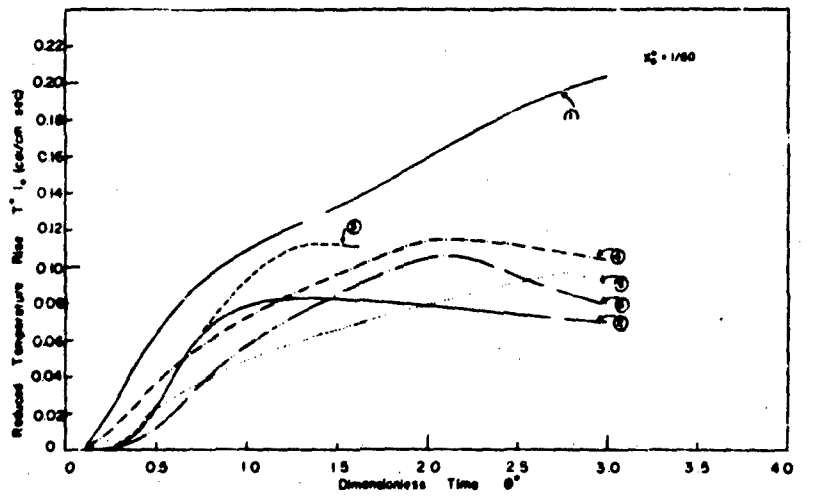

FIG. 2.21 TEMPERATURE RESPONSE OF A MOIST OPAQUE CLOTH - SKIN SIMULANT SYSTEM. INFLUENCE OF IRRADIATION PULSE SHAPE; PULSE AREA = 1.09 cal/cm² sec

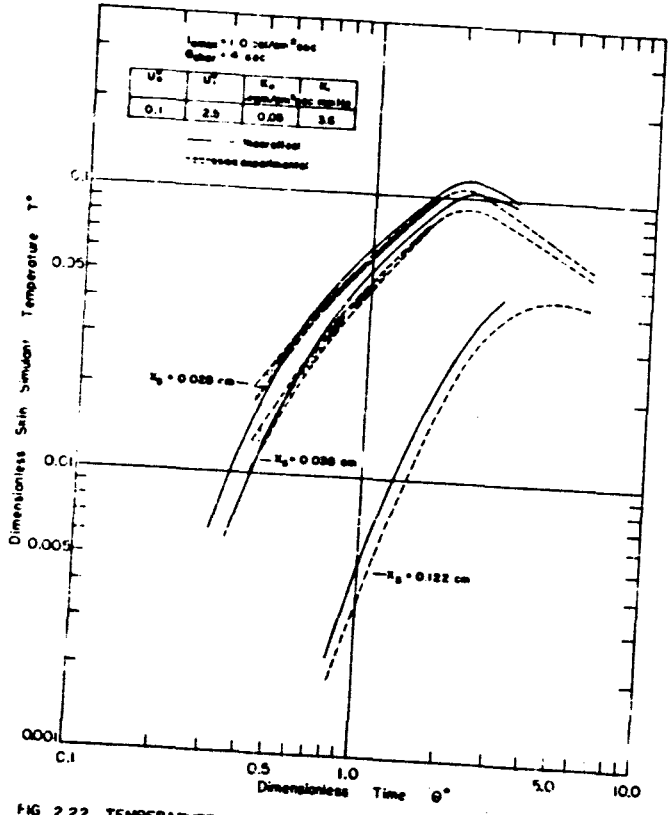

FIG 2.22 TEMPERATURE RESPONSE OF A MOIST CLOTH - SKIN SIMULANT SYSTEM (OPAQUE). COMPARISON OF THEORETICAL AND EXPERIMENTAL RESULTS FOR SQUARE WAVE IRRADIATION.

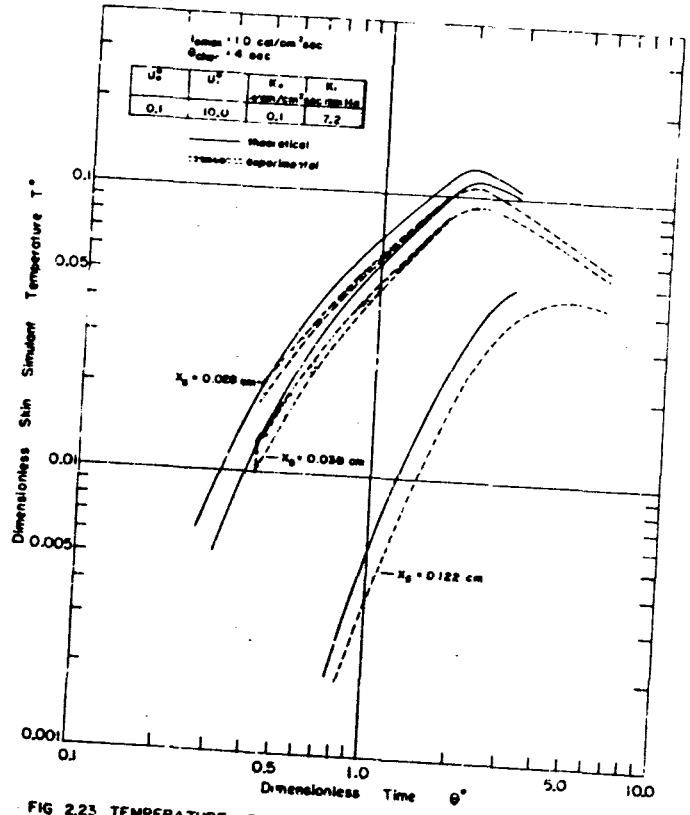

FIG 2.23 TEMPERATURE RESPONSE OF A MOIST CLOTH - SKIN SIMULANT SYSTEM (OPAQUE). COMPARISON OF THEORETICAL AND EXPERIMENTAL RESULTS FOR SQUARE WAVE IRRADIATION.

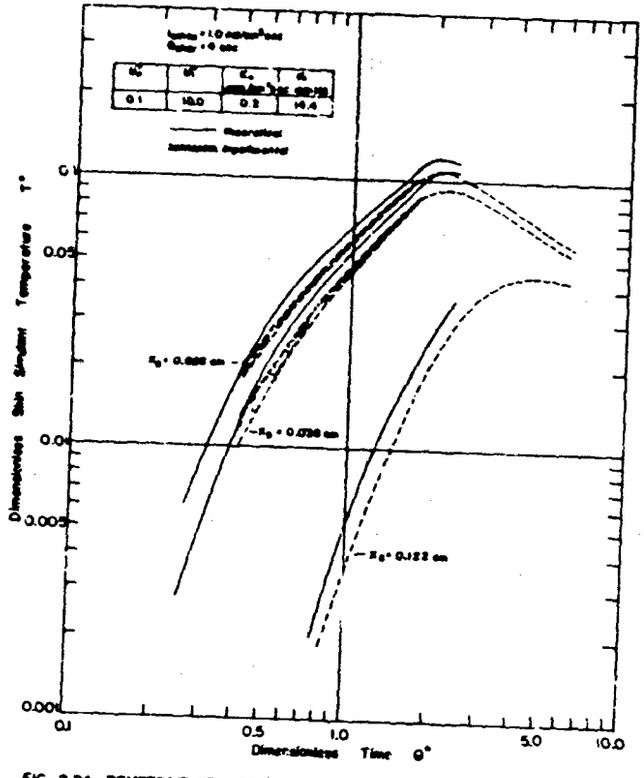

FIG. 2.24 TEMPERATURE RESPONSE OF A MOIST CLOTH-SKIN SIMULANT SYSTEM (OPAQUE). COMPARISON OF THEORETICAL AND EXPERIMENTAL RESULTS FOR SQUARE WAVE IRRADIATION.

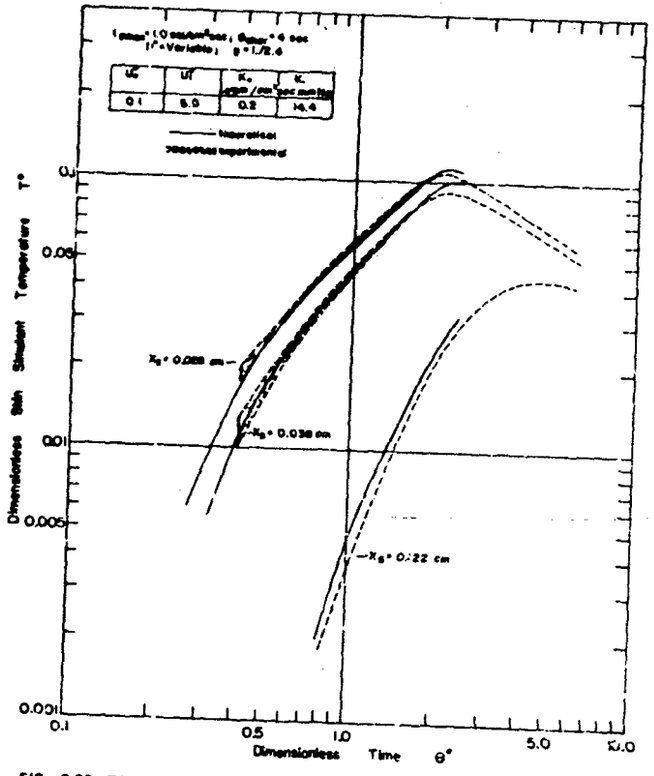

FIG. 2.25 TEMPERATURE RESPONSE OF A MOIST CLOTH-SKIN SIMULANT SYSTEM (OPAQUE). COMPARISON OF THEORETICAL AND EXPERIMENTAL RESULTS FOR SQUARE WAVE IRRADIATION.

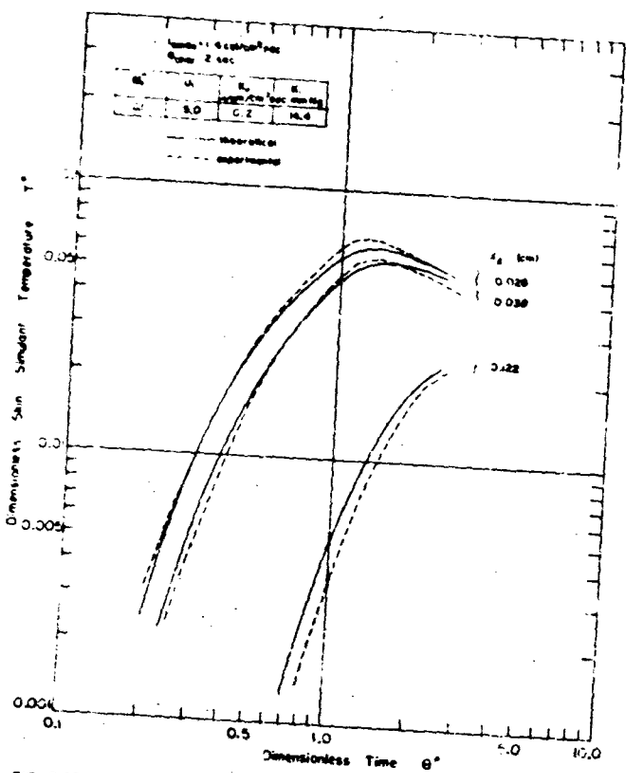

FIG 2 26 TEMPERATURE RESPONSE OF A MOIST CLOTH SKIN SIMULANT SYSTEM (OPAQUE). COMPARISON OF THEORETICAL AND EXPERIMENTAL RESULTS FOR SQUARE WAVE IRRADIATION.

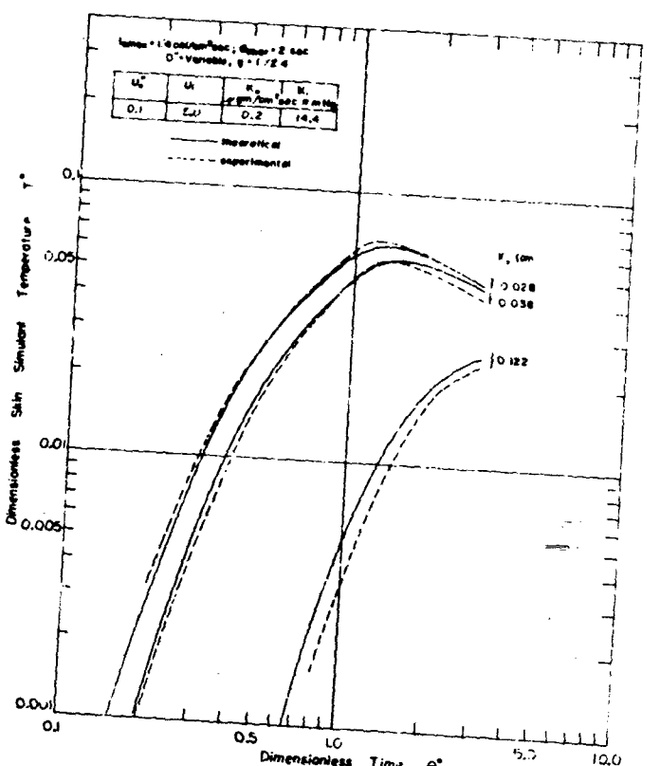

FIG 2 27 TEMPERATURE RESPONSE OF A MOIST CLOTH-SKIN SIMULANT SYSTEM (OPAQUE). COMPARISON OF THEORETICAL AND EXPERIMENTAL RESULTS FOR SQUARE WAVE IRRADIATION.

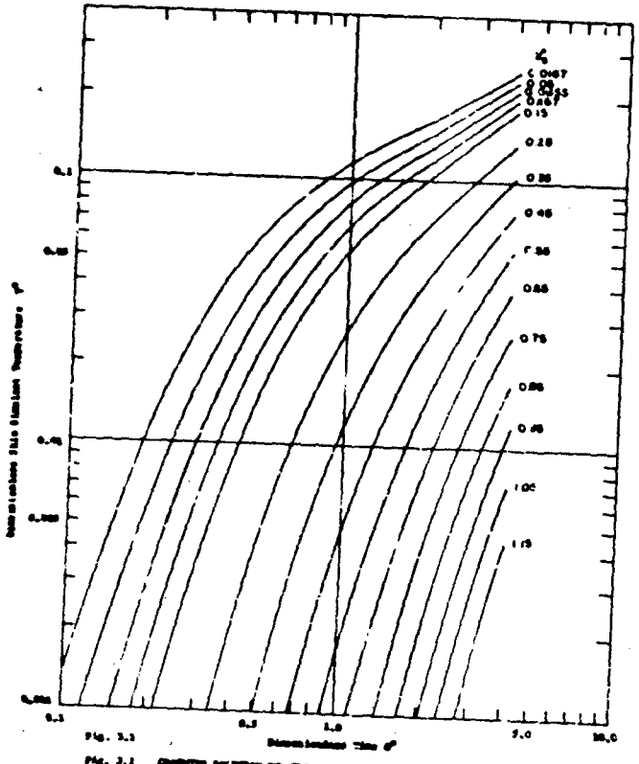

Fig. 5.1

Fig. 5.1 COMPUTER SOLUTION FOR THE MOIST CLOTH - SKIN SIMULANT SYSTEM

Constant Irradiation
I_o = 0.85 cal/cm² sec
Temperature = 30 °C.
α'_o = 0.1
α'_1 = 5.0
Relative Humidity = 80 %
E_o = 0.2 gm/cm² second
E_1 = 14.4 " "

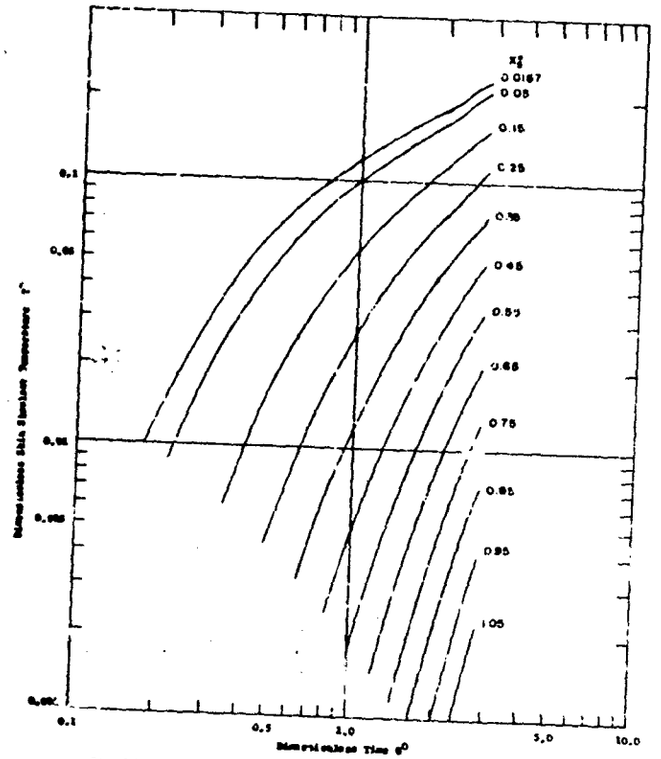

Fig. 5.2 COMPUTER SOLUTION FOR THE MOIST CLOTH - SKIN SIMULANT SYSTEM

Constant Irradiation
I_o = 0.83 cal/cm² sec
Temperature = 30 °C.
α'_o = 0.1
α'_1 = 50.0
Relative Humidity = 80 %
E_o = 0.1 gm-cm² second
E_1 = 7.2 " "

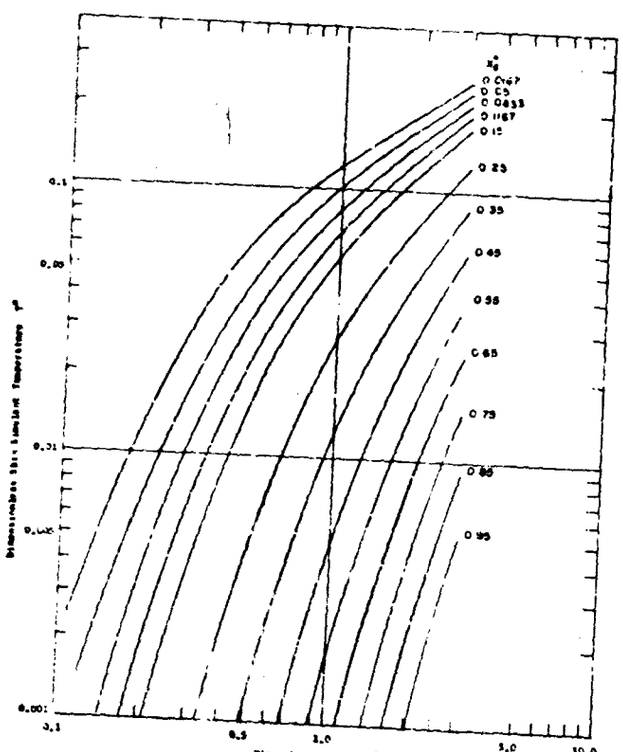

Fig. 3.3 COMPUTER SOLUTION FOR THE MOIST CLOTH – SKIN SIMULANT SYSTEM
Constant Irradiation
I_0 = 0.83 cal/cm² sec
Temperature = 30 °C.
Relative Humidity = 80 %
θ_0^* = 0.1
θ_1^* = 10.0
E_0 = 0.05 μgm/cm² sec mmHg
E_1 = 3.6 " "

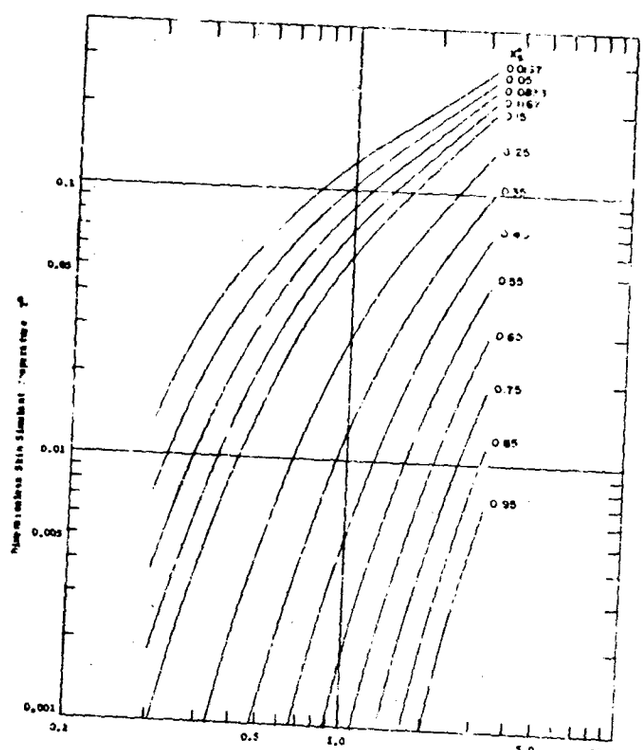

Fig. 3.4 COMPUTER SOLUTION FOR THE MOIST CLOTH – SKIN SIMULANT SYSTEM
Constant Irradiation
I_0 = 0.83 cal/cm² sec
Temperature = 30 °C.
Relative Humidity = 80 %
θ_0^* = 0.025
θ_1^* = 10.0
E_0 = 0.05 μgm/cm² sec mmHg
E_1 = 3.6 " "

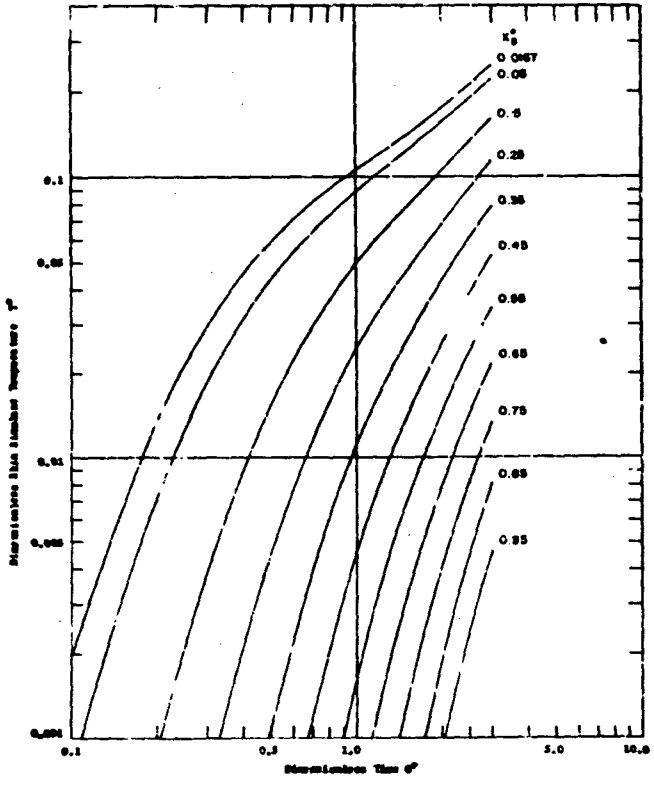

Fig. 3.5 COMPUTER SOLUTION FOR THE MOIST CLOTH - SKIN SIMULANT SYSTEM

Constant Irradiation
I_o = 0.83 cal/cm²sec
Temperature = 30 °C. Relative Humidity = 80 %
W_o^o = 0.1 E_o = 0.05 μgm/cm² secondg
W_1^o = 10.0 E_1 = 3.6 " "
Variable Diffusivity D'

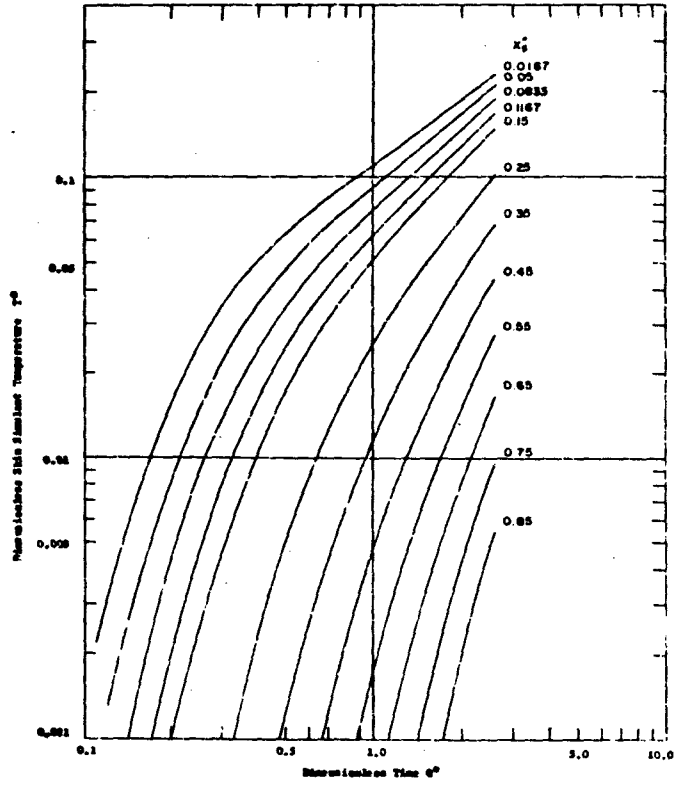

Fig. 3.6 COMPUTER SOLUTION FOR THE MOIST CLOTH - SKIN SIMULANT SYSTEM

Constant Irradiation
I_o = 1.24 cal/cm²sec
Temperature = 30 °C. Relative Humidity = 80 %
W_o^o = 0.1 E_o = 0.05 μgm/cm² secondg
W_1^o = 10.0 E_1 = 3.6 " "

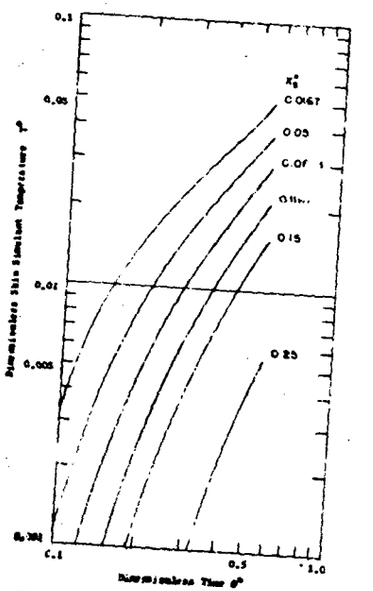

Fig. 3.7 COMPUTER SOLUTION FOR THE MOIST CLOTH - SKIN SIMULANT SYSTEM

Constant Irradiation
I_c = 3.00 cal/cm²sec
Temperature = 30 °C.
$G_0^* = 0.083$
$W_1^* = 30.0$
Relative Humidity = 80 %
E_0 = 0.05 μgm/cm² seconds
E_1 = 3.0 " "

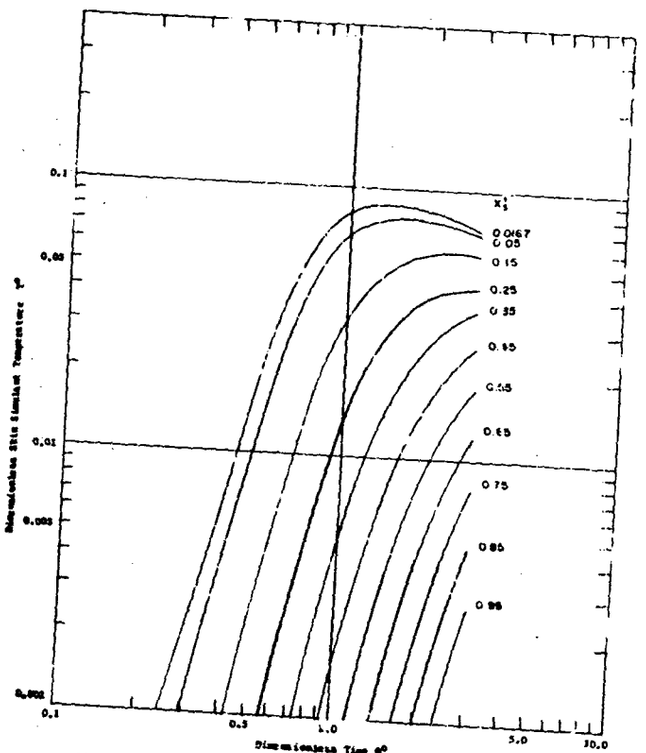

Fig. 3.8 COMPUTER SOLUTION FOR THE MOIST CLOTH - SKIN SIMULANT SYSTEM

Thermonuclear Irradiation Pulse
I_{max} = 0.3 cal/cm²sec;
G_{Char}^0 = 0.3
Temperature = 30 °C.
G_0^0 = 0.1
W_1^0 = 5.0
Relative Humidity = 80 %
E_0 = 0.2 μgm/cm² seconds
E_1 = 16.0 " "

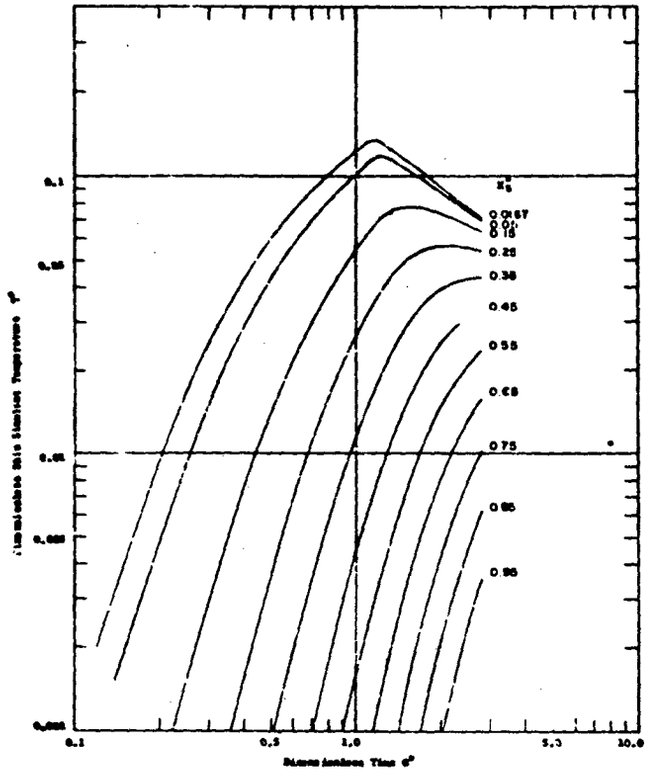

Fig. 3.9 COMPUTER SOLUTION FOR THE MOIST CLOTH - SKIN SIMULANT SYSTEM

Square Wave Irradiation
I_{max} = 0.3 cal/cm² sec; θ'_{Char} = 1.00
Temperature = 30 °C. Relative Humidity = 60 %
θ'_0 = 0.1 K_0 = 0.2 μgm/cm² seconds
θ'_1 = 5.0 K_1 = 14.4 " "

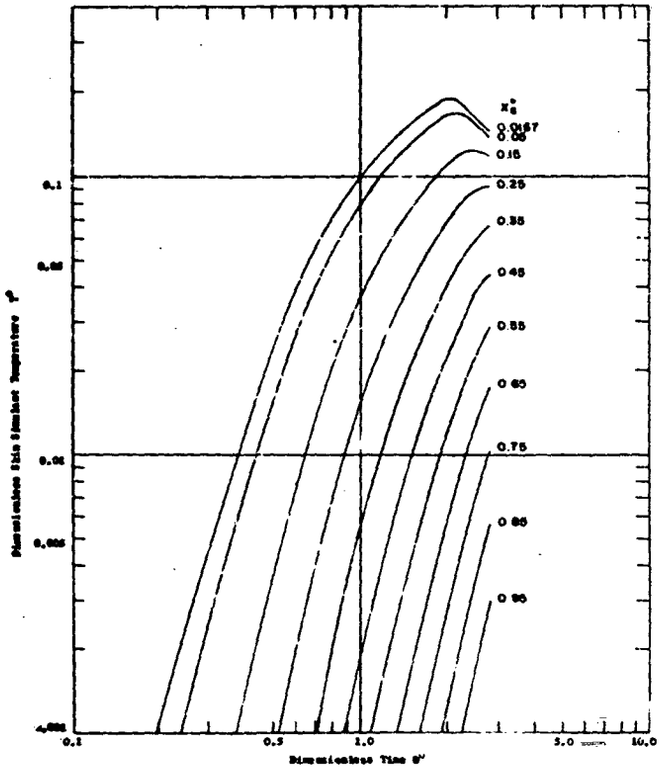

Fig. 3.10 COMPUTER SOLUTION FOR THE MOIST CLOTH - SKIN SIMULANT SYSTEM

Trapezoidal Wave Irradiation
I_{max} = 0.3 cal/cm² sec; θ'_{Char} = 2.17; θ'_{Pr} = 0.35
Temperature = 30 °C. Relative Humidity = 60 %
θ'_0 = 0.1 K_0 = 0.2 μgm/cm² seconds
θ'_1 = 5.0 K_1 = 14.4 " "

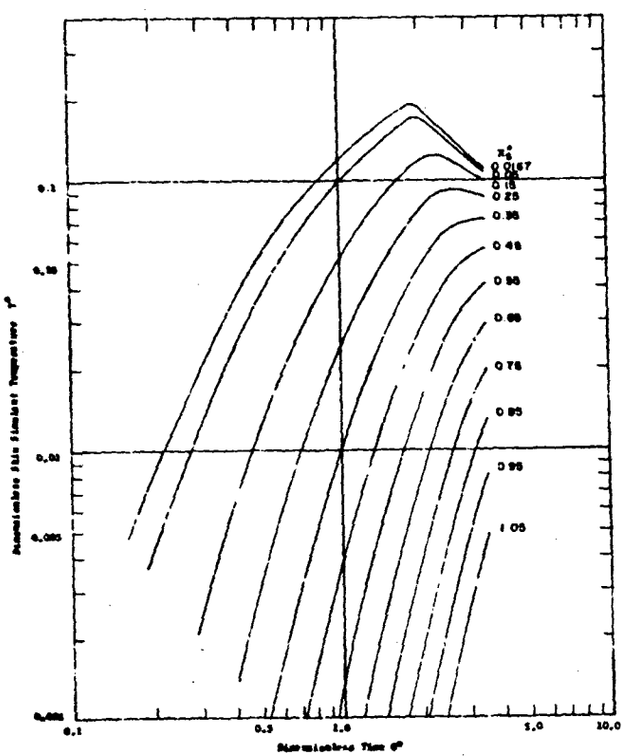

Fig. 3.11 COMPUTER SOLUTION FOR THE MOIST CLOTH - SKIN SIMULANT SYSTEM

Square Wave Irradiation
I_{max} = 0.3 cal/cm²sec; θ^*_{Char} = 1.85
Temperature = 30 °C. Relative Humidity = 80 %
θ^*_0 = 0.1 E_o = 0.2 μgm/cm²seconds
θ^*_1 = 3.0 E_1 = 14.4 " "

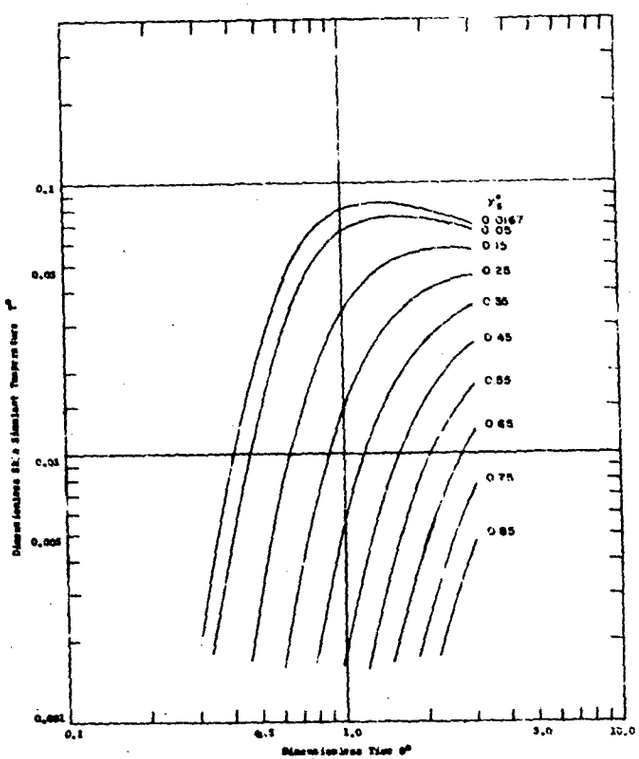

Fig. 3.12 COMPUTER SOLUTION FOR THE MOIST CLOTH - SKIN SIMULANT SYSTEM

Thermonuclear Irradiation Pulse
I_{max} = 1.0 cal/cm²sec; θ^*_{Char} = 0.3
Temperature = 30 °C. Relative Humidity = 80 %
θ^*_0 = 0.1 E_o = 0.2 μgm/cm²seconds
θ^*_1 3.0 E_1 = 14.4 " "

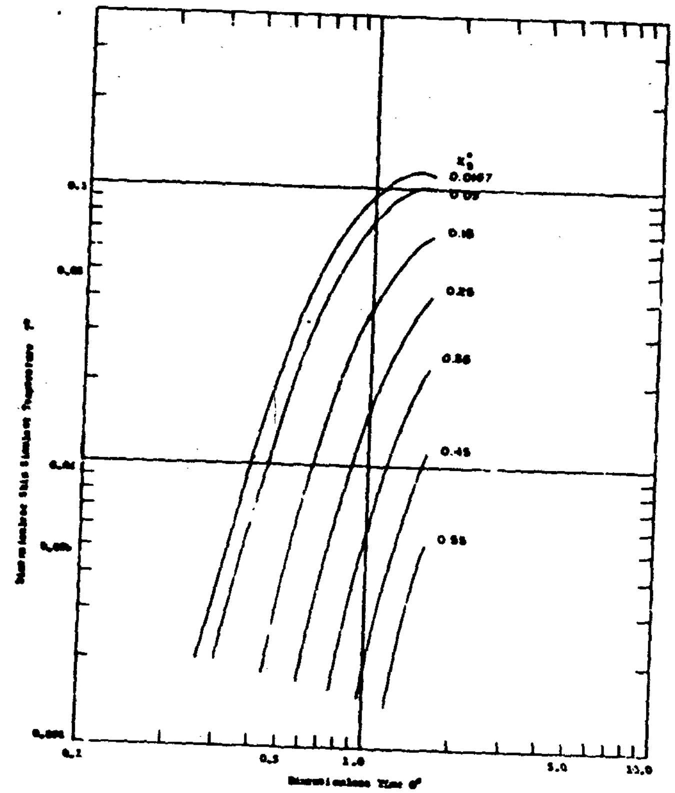

Fig. 3.13 COMPUTER SOLUTION FOR THE MOIST CLOTH - SKIN SIMULANT SYSTEM
Trapezoidal Wave Irradiation
I_{max} = 1.0 cal/cm² sec; θ^*_{char} = 1.90; θ^*_{tr} = 0.5
Temperature = 30 °C. Relative Humidity = 80 %
U_o^o = 0.1 K_o = 0.2 μgm/cm² second/g
U_i^o = 5.0 K_i = 14.4 " "

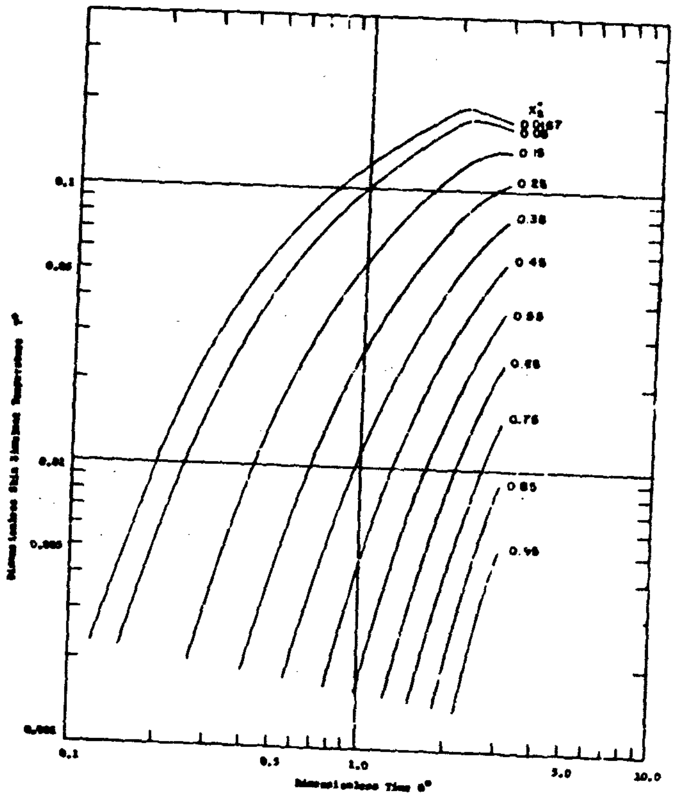

Fig. 3.14 COMPUTER SOLUTION FOR THE MOIST CLOTH - SKIN SIMULANT SYSTEM
Square Wave Irradiation
I_{max} = 0.6 cal/cm² sec; θ^*_{char} = 1.82
Temperature = 30 °C. Relative Humidity = 80 %
U_o^o = 0.1 K_o = 0.2 μgm/cm² second/g
U_i^o = 5.0 K_i = 14.4 " "

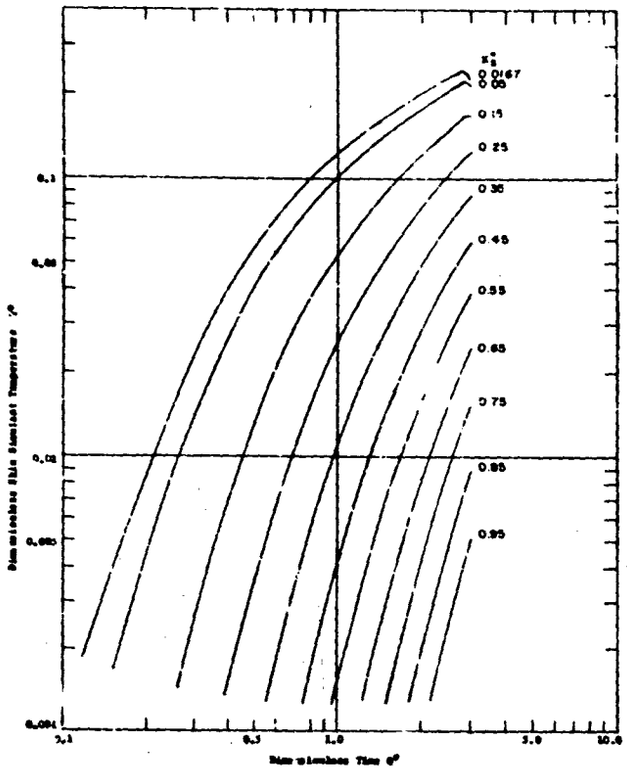

Fig. 3.15 COMPUTER SOLUTION FOR THE MOIST CLOTH - SKIN SIMULANT SYSTEM

Square Wave Irradiation
I_{max} = 0.4 cal/cm²sec; θ^o_{Char} = 2.73
Temperature = 30 °C. Relative Humidity = 80 %
θ^o_0 = 0.1 E_0 = 0.2 μgm/cm² seconds
θ^o_1 = 5.0 E_1 = 14.4 " "

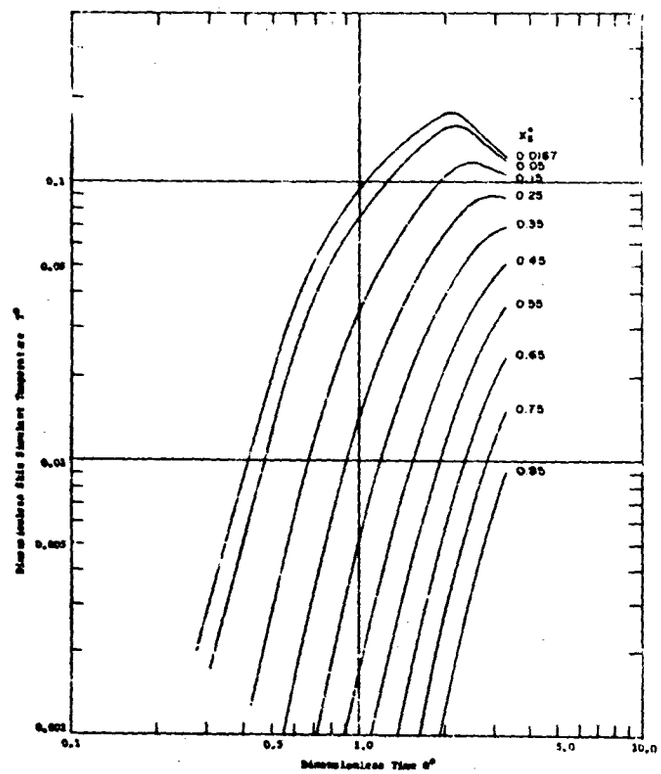

Fig. 3.16 COMPUTER SOLUTION FOR THE MOIST CLOTH - SKIN SIMULANT SYSTEM

Trapezoidal Wave Irradiation
I_{max} = 0.4 cal/cm²sec; θ^o_{Char} = 2.32; θ^o_{cr} = 0.5
Temperature = 30 °C. Relative Humidity = 80 %
θ^o_0 = 0.1 E_0 = 0.2 μgm/cm² seconds
θ^o_1 = 5.0 E_1 = 14.4 " "

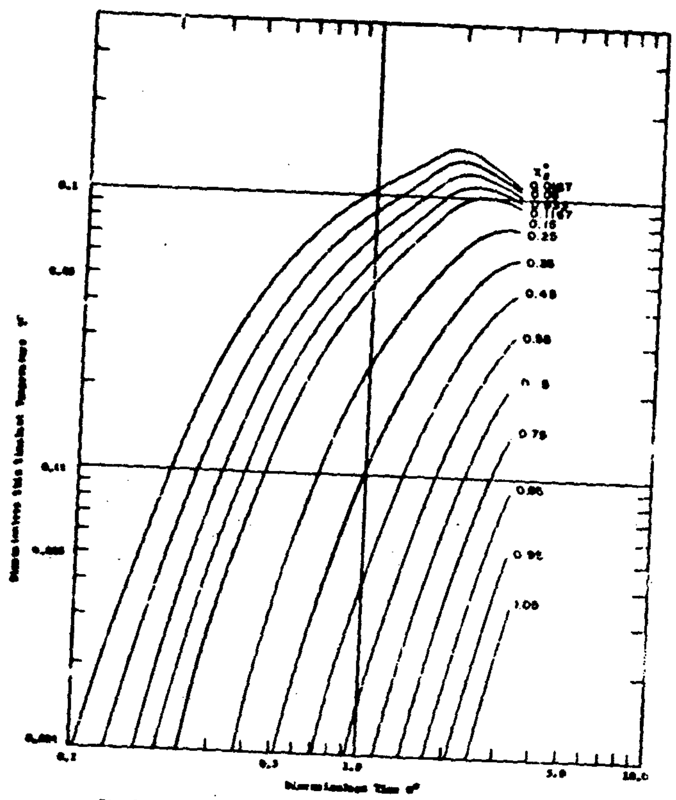

Fig. 3.17 COMPUTER SOLUTION FOR THE MOIST CLOTH - SKIN SIMULANT SYSTEM

Square Wave Irradiation

I_{omax} = 1.00 cal/cm² sec; θ_{dmax} = 4 sec

Temperature = 30 °C. Relative Humidity = 65 %

U_o^0 = 0.1 E_o = 0.08 μgm/cm² seconds

U_1^0 = 2.5 E_1 = 2.6 " "

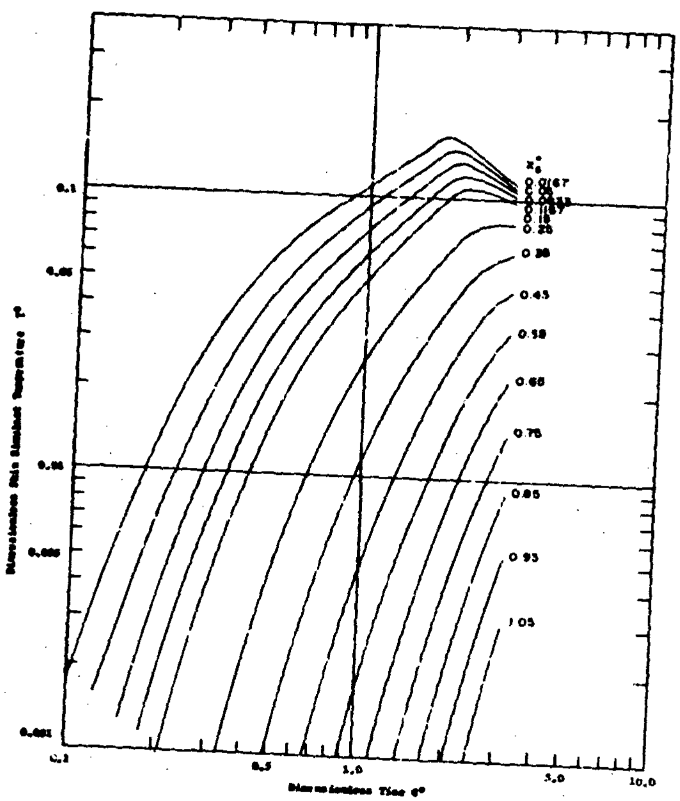

Fig. 3.18 COMPUTER SOLUTION FOR THE MOIST CLOTH - SKIN SIMULANT SYSTEM

Square Wave Irradiation

I_{omax} = 1.00 cal/cm² sec; θ_{dmax} = 4 sec

Temperature = 30 °C. Relative Humidity = 65 %

U_o^0 = 0.1 E_o = 0.1 μgm/cm² seconds

U_1^0 = 10.0 E_1 = 7.2 " "

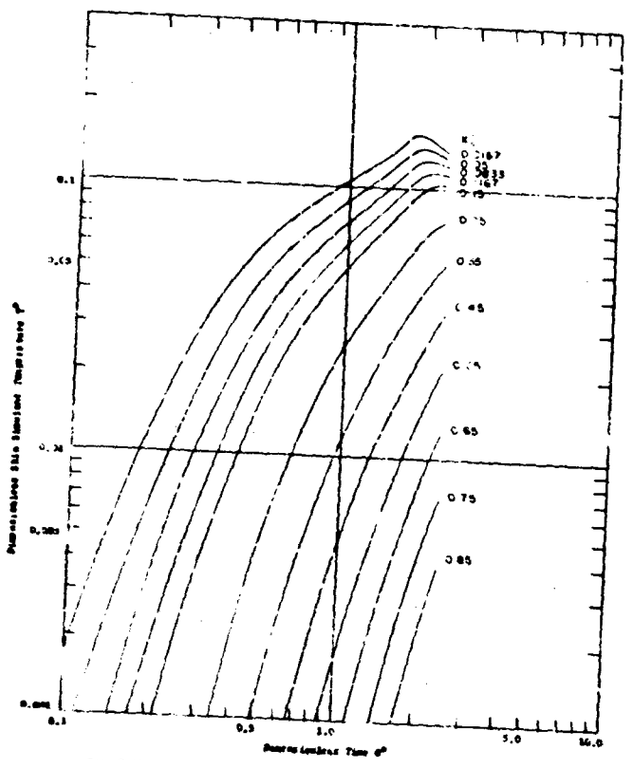

Fig. 3.19 COMPUTER SOLUTION FOR THE MOIST CLOTH - SKIN SIMULANT SYSTEM

Square Wave Irradiation
I_{max} = 3.03 cal/cm² sec; θ_{time} = 4 sec
Temperature = 32 °C. Relative Humidity = 65 %
$D_0^* = 0.1$ E_0 = 0.2 mgm/cm² seconds
$D_1^* = 10.0$ E_1 = 34.4 " "

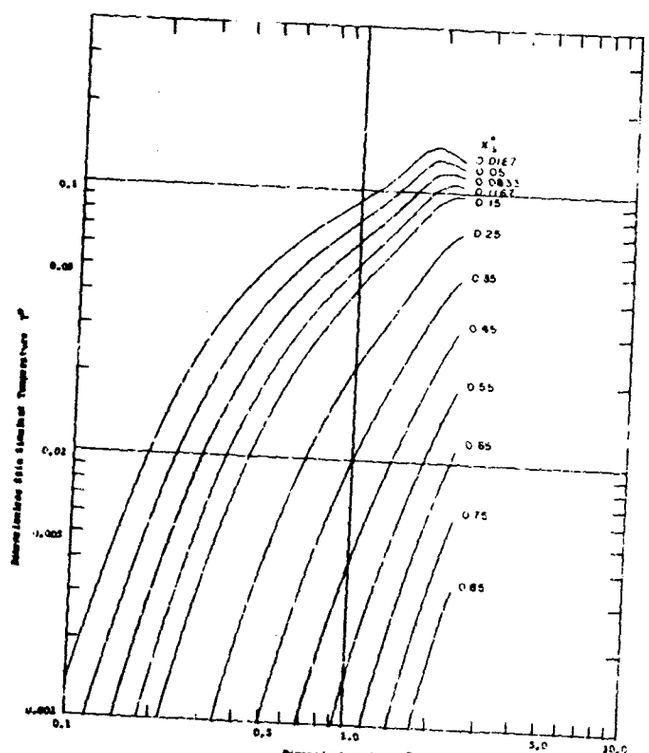

Fig. 3.20 COMPUTER SOLUTION FOR THE MOIST CLOTH - SKIN SIMULANT SYSTEM

Square Wave Irradiation
I_{max} = 3.03 cal/cm² sec θ_{time} = 4 sec
Temperature = 32 °C. Relative Humidity = 65 %
$D_0^* = 0.1$ E_0 = 0.2 mgm/cm² seconds
$D_1^* = 5.0$ E_1 = 34.4 " "
Variable Diffusivity D^*

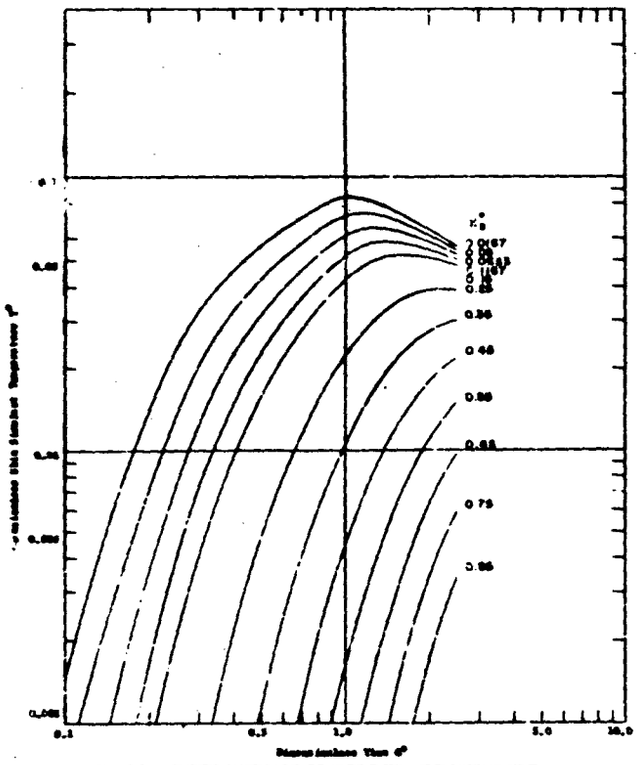

Fig. 3.21 COMPUTER SOLUTION FOR THE MOIST CLOTH - SKIN SIMULANT SYSTEM

Square Wave Irradiation
I_{max} = 1.4 cal/cm²sec; θ_{time} = 2 sec
Temperature = 38 °C. Relative Humidity = 65 %
$\alpha_0^* = 0.1$ K_2 = 0.2 gm/cm²seconds
$\alpha_1^* = 3.0$ K_1 = 14.4 " "

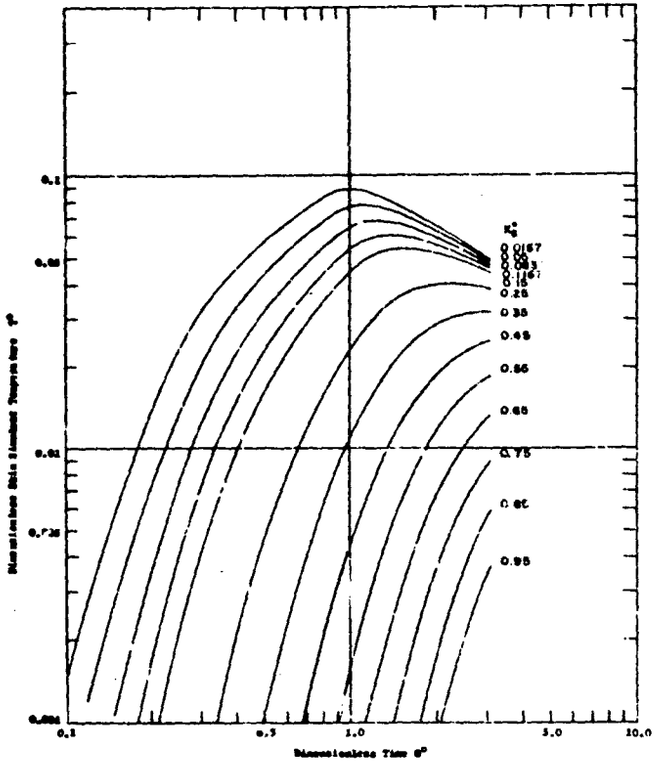

Fig. 3.22 COMPUTER SOLUTION FOR THE MOIST CLOTH - SKIN SIMULANT SYSTEM

Square Wave Irradiation
I_{max} = 1.4 cal/cm²sec; θ_{time} = 2 sec
Temperature = 38 °C. Relative Humidity = 65 %
$\alpha_0^* = 0.1$ K_2 = 0.2 gm/cm²seconds
$\alpha_1^* = 3.0$ K_1 = 14.4 " "
Variable Diffusivity D*

APPENDIX G

EQUILIBRIUM DATA ON MOIST CLOTH

This data is used in the numerical solution of transient heat and moisture transfer through cloth.

TABLE G.1

EQUILIBRIUM MOISTURE CONTENT OF CLOTH AS A FUNCTION OF TEMPERATURE AND RELATIVE HUMIDITY

T, °C \ RH, % M	.05	.1	.2	.3	.4	.5	.6	.65	.7	.75	.8	.85	.9	.95
20	.015	.021	.030	.038	.047	.055	.065	.070	.077	.085	.095	.109	.128	.156
30	.013	.018	.027	.035	.044	.052	.061	0.67	.073	.081	.091	.103	.121	.147
40	.011	.016	.025	.033	.041	.049	.058	.064	.070	.077	.086	.099	.115	.142
50	.010	.015	.023	.031	.039	.047	.056	.061	.067	.075	.084	.096	.113	.139
60	.009	.013	.021	.029	.037	.045	.054	.059	.065	.072	.081	.094	.110	.143
70	.008	.012	.020	.027	.035	.043	.052	.057	.062	.069	.079	.092	.111	.151
80	.007	.011	.018	.026	.033	.041	.050	.054	.060	.067	.077	.092	.114	.157
90	.006	.010	.018	.025	.032	.039	.047	.051	.057	.065	.077	.095	.118	.164
100	.006	.009	.017	.024	.030	.037	.045	.049	.054	.062	.073	.092	.122	.169
110	.005	.009	.016	.022	.029	.035	.042	.046	.051	.058	.068	.097	.119	.166
120	.004	.009	.015	.021	.028	.034	.040	.044	.043	.055	.064	.083	.112	.160

Date of Urquhardt and Williams (22)

TABLE G.2

GRADIENTS OF EQUILIBRIUM MOISTURE CONTENT OF CLOTH

AS FUNCTIONS OF TEMPERATURE AND PARTIAL WATER VAPOR PRESSURE

i	T (°K)	j →												
↓	↓													
	303.	1.454	2.959	7.320	10.32	12.36	15.96	19.28	22.17	24.86	26.29	27.17	27.96	PRES 1
	313.	3.175	6.040	13.91	19.43	23.24	29.78	35.33	40.20	44.65	46.96	48.30	49.48	PRES 2
p	323.	6.459	11.70	25.48	35.06	41.63	52.60	61.52	69.40	76.44	80.09	82.11	85.86	PRES 3
	333.	12.34	21.58	44.94	60.70	71.29	88.54	102.4	114.7	125.4	131.0	134.1	136.7	PRES 4
	313.	22.29	37.99	76.24	100.9	117.1	142.8	163.5	182.2	193.1	206.6	211.2	215.2	PRES 5
	353.	39.28	64.04	124.4	161.4	184.9	221.7	251.6	279.3	302.5	315.2	322.0	328.1	PRES 6
	363.	62.85	103.7	195.6	248.9	281.9	332.7	274.5	414.8	448.1	466.7	476.8	486.1	PRES 7
	373.	99.09	161.6	296.5	370.7	415.6	484.4	541.0	598.5	645.9	672.8	687.6	701.5	PRES 8
	403.	316.2	502.0	845.6	1016.	1120.	1283.	1399.	1550.	1682.	1757.	1800.	1042.	PRES 9
	433.	789.1	1216.	1857.	2194.	2431.	2833.	3006.	3357.	3706.	3889.	3997.	4103.	PRES 10

i	T (°K)	j →												
↓	↓													
	303.	.1191	.2191	.4821	.6747	.8115	1.043	1.221	1.378	1.521	1.592	1.629	1.661	DPT 1
	313.	.2363	.4150	.8679	1.188	1.410	1.773	2.046	2.290	2.504	2.612	2.667	2.714	DPT 2
$(\frac{\partial p}{\partial T})_M$	323.	.4377	.7445	1.495	1.997	2.331	2.861	3.267	3.632	3.941	4.103	4.185	4.256	DPT 3
	333.	.7629	1.270	2.463	3.207	3.682	4.413	4.993	5.526	5.963	6.201	6.324	6.434	DPT 4
	343.	1.260	2.064	3.882	4.933	5.574	6.542	7.339	8.098	8.710	9.056	9.239	9.408	DPT 5
	353.	1.981	3.211	5.860	7.281	8.116	9.361	10.41	11.48	12.33	12.83	13.10	13.35	DPT 6
	363.	2.984	4.793	8.488	10.34	11.40	12.98	14.32	15.78	16.97	17.67	18.07	18.45	DPT 7
	373.	4.324	6.888	11.82	14.15	15.48	17.51	19.14	21.13	22.78	23.76	24.32	24.87	DPT 8
	403.	10.81	16.72	25.61	29.81	32.63	37.39	39.58	44.13	48.56	50.94	52.38	53.80	DPT 9
	433.	21.40	31.57	41.62	48.86	55.46	67.77	68.93	78.15	89.00	94.06	97.07	100.0	DPT 10

i	T (°K)	j →												
↓	↓													
	303.	5.205	4.267	2.393	1.830	1.786	2.376	3.677	5.401	7.498	8.807	9.681	10.51	DMP 1
	313.	3.062	2.427	1.250	.9198	.9294	1.401	2.249	3.335	4.603	5.368	5.844	6.284	DMP 2
$(\frac{\partial M}{\partial p})_T$	323.	1.849	1.417	.6747	.4954	.5324	.8832	1.436	2.123	2.896	3.354	3.626	3.871	DMP 3
	333.	1.147	.8479	.3764	.2880	.3327	.5845	.9474	1.389	1.866	2.150	2.316	2.462	DMP 4
	343.	.7253	.5178	.2196	.1931	.2254	.4007	.6381	.9267	1.227	1.409	1.513	1.607	DMP 5
	353.	.4674	.3228	.1357	.1262	.1617	.2820	.4379	.6293	.8237	.9434	1.011	1.075	DMP 6
	363.	.3055	.2050	.08964	.09306	.1211	.2029	.3054	.4343	.5628	.6436	.6899	.7345	DMP 7
	373.	.2025	.1331	.06336	.07166	.09276	.1486	.2159	.3039	.3914	.4471	.4796	.5113	DMP 8
	403.	.06435	.04287	.02995	.03642	.04458	.06375	.08216	.1121	.1437	.1639	.1763	.1890	DMP 9
	433.	.02606	.01916	.01657	.01880	.02185	.02983	.03436	.04552	.05933	.06759	.07283	.07824	DMP 10

APPENDIX H

BIBLIOGRAPHY

1. Buettner, K., "Effects of Extreme Heat and Cold on Human Skin. III", J. of Applied Physiology, 5, 207 (1952).

2. Butler, C. P., Martin, S. B. and Lai, W., "Thermal Radiation Damage to Cellulosic Materials. Part II - Ignition of Alpha Cellulose by Square Wave Exposure", Technical Report No. TR-135, U. S. Naval Radiological Defense Laboratory, San Francisco, California, 1956.

3. Chen, N. Y., and Jensen, W. P., "Skin Simulants with Depth Magnification", Technical Report No. 5 from Fuels Research Laboratory, MIT, Contract NOnr - 1841(00), March 15, 1957.

4. Chen, N. Y., and Jensen, W. P., "Heat Transfer to Skin Through Thermally Irradiated Dry Cloth", Technical Report No. 6 from Fuels Research Laboratory, MIT, Contract NOnr - 1841(37), July 8, 1959.

5. Chen, N. Y., "Transient Heat and Moisture Transfer to Skin Through Thermally Irradiated Cloth", Technical Report No. 7 from Fuels Research Laboratory, MIT, Contracts NOnr - 1841(37) and No. DA 19-129-QM-454, January 12, 1959.

6. de Lhery, G. P., Derksen, W. and Monahan, T. I., "Research Report on the Spectral Reflectance and Transmittance of Standard Fabrics for Thermal Radiation Effects Studies", Lab. Project 5046-3, Part 91, Final Report, Naval Material Laboratory, New York Naval Shipyard, Brooklyn 1, New York, (1956).

7. Dietz: Leipzig Monatsch [illegible]ile (1912); quoted in "International Critical Tables", Vol. II, p. 237, McGraw-Hill Book Co., Inc., New York, (1927).

8. Eckert, E. R. G., "Introduction to the Transfer of Heat and Mass", p. 160, McGraw-Hill Book Co., Inc., New York, (195 .

9. Gardon, R., "Temperature Attained in Wood Exposed to High Intensity Thermal Radiation", Technical Report No. 3, DIC Project 6797, Fuels Research Laboratory, MIT, Cambridge, Massachusetts, (1953).

10. Gardon, R., "Temperature Attained in Wood Exposed to High Intensity Thermal Radiation, Appendix II, The MIT Solar Furnace", DIC Project 6797, Fuels Research Laboratory, MIT, Cambridge, Massachusetts, (1953).

11. Gardon, R., "A Segmented-Mirror Solar Furnace for High Intensity Thermal Radiation Studies", Rev. Sci. Instruments, 25, No. 5, p. 459, May 1954.

12. Ho Leong, E., and Williams, M. E., "Surface Temperatures in a Two-Layer Air-Spaced Slab System Irradiated from One Side", Technical Report No. 4, DIC Project No. 6797, Fuels Research Laboratory, MIT, Cambridge, Massachusetts, 1956.

13. Klei, H. E., "A Study of Unsteady State Natural Convection for a Vertical Plate", B. S. Thesis, Department of Chemical Engineering, MIT, June 1957.

14. McAdams, W. H., "Heat Transmission," Chapter III, 3rd Edition, McGraw-Hill Book Co., Inc., New York, 1954.

15. Moritz, A. R., and Henriques, F. C., Jr., "Studies of Thermal Injury. II. The Relative Importance of Time and Surface Temperature in the Causation of Cutaneous Burns", Am. J. Path., 23, 695, (1947).

16. Moritz, A. R., "Studies of Thermal Injury, III. The Pathology and Pathogenesis of Cutaneous Burns. An Experimental Study", Am. J. Path. 23, 915 (1947).

17. Moritz, A. R., Henriques, F. C., Jr., Dutra, F. R., and Weisiger, J. R., "Studies of Thermal Injury, IV. An Exploration of Casualty-Producing Attributes of Conflagrations; Local and Systemic Effects of General Cutaneous Exposure to Excessive Circumambient (Air) and Circumradiant Heat of Varying Duration and Intensity", Arch. Path., 43, 466 (1947).

18. Richtmyer, R. D., "Difference Methods for Initial-Value Problems", Interscience Publishers, New York, 1957.

19. Schmidt, E., "Föppls Festschrift", Springer, Berlin, 1924.

20. Schmidt, E., "Forsch. Gebiete Ingenieurw., 13, 177, (1942).

21. Siegel, R., "Transient Free Convection from a Vertical Flat Plate", Trans. A. S. M. E., 80, 347 (1958).

22. Urquhart, A. R., and Williams, A. M., J. Tex. Inst., 15, T559, (1924).

23. Ratter, J. F. Jr., "Transient Effects of a Time Varying Thermal Pulse," AFSWP Report TOI 58-7, March 1958.